CRANFIELD UNIVERSITY

XUE LONGXIAN

ACTUATION TECHNOLOGY FOR FLIGHT CONTROL SYSTEM ON CIVIL AIRCRAFT

SCHOOL OF ENGINEERING

MSc by Research THESIS

CRANFIELD UNIVERSITY

SCHOOL OF ENGINEERING

MSc by Research THESIS

Academic Year 2008-2009

XUE LONGXIAN

Actuation Technology for Flight Control System on Civil Aircraft

Supervisor: Dr. C. P. Lawson
Prof. J. P. Fielding

January 2009

This thesis is submitted in fulfilment of the requirements for the degree of Master of Science

ABSTRACT

This report addresses the author's Group Design Project (GDP) and Individual Research Project (IRP). The IRP is discussed primarily herein, presenting the actuation technology for the Flight Control System (FCS) on civil aircraft.

Actuation technology is one of the key technologies for next generation More Electric Aircraft (MEA) and All Electric Aircraft (AEA); it is also an important input for the preliminary design of the Flying Crane, the aircraft designed in the author's GDP.

Information regarding actuation technologies is investigated firstly. After initial comparison and engineering consideration, Electrohydrostatic Actuation (EHA) and variable area actuation are selected for further research. The tail unit of the Flying Crane is selected as the case study flight control surfaces and is analysed for the requirements. Based on these requirements, an EHA system and a variable area actuation system powered by localised hydraulic systems are designed and sized in terms of power, mass and Thermal Management System (TMS), and thereafter the reliability of each system is estimated and the safety is analysed. These two systems are then compared in fuel penalty, safety, maintenance and installation, cost, risk and certification. A conventional Fly-By-Wire (FBW) actuation system is used as the reference case.

The results show that both the EHA system and the variable area actuation system are feasible for the FCS on civil aircraft. The EHA system is proved to be quite efficient in power consumption and mass reduction. However, the reliability of EHA needs to be improved and the TMS of this system may lead to an increase in aircraft drag. The variable area actuation system demonstrates that it can significantly reduce the system design point and system size; while the localised hydraulic system is not as efficient as a centralised hydraulic system. Finally, a variable area actuation system powered by the centralised hydraulic systems is suggested for the FCS on civil aircraft and the Flying Crane. A variable area actuation system powered by localised hydraulic systems is recommended as the first step towards MEA and AEA in the future.

ACKNOWLEDGEMENTS

I would like to express my sincere thanks to my supervisor Dr. Craig Lawson, for his advices, helps and continual supports during my IRP and GDP. I am also extremely grateful to my second supervisor Professor John Fielding, and Dr. Howard Smith, Dr Shijun Guo, Dr Phil Stocking and all the staffs involved AVIC I MSc Programme Project.

I really appreciate my sponsors, Chengdu Aircraft Design & Research Institute, AVIC I and China Scholarship Council. Without their supports, I have no chance studying in Cranfield.

Thanks to MR. Yang Weiping, the mentor of AVIC I Aircraft Group, and all the AVIC I aircraft group members, especially MR. Niu Liang, Chen Rong, Li Shitu, Liu Huping and so on, for their helps and friendships, for the good teamwork during the GDP.

I would like also to address my special thanks to my friend MR. Stuart Andrews for having been wonderful mates during my year in Cranfield, for his help and friendship.

Finally, the last words are for my dear wife Wu Guoping, for her love, encouragements, helps and supports during I study in Cranfield.

CONTENTS

LIST OF FIGURES

LIST OF TABLES

NOTATIONS

Acronyms

1D	one Dimensional
2D	two Dimensional
AAM	Average Aircraft Mass
AEA	All Electric Aircraft
APU	Auxiliary Power Unit
AUM	All Up Mass
AVIC I	China Aviation Industry Corporation I
BIT	Build-In-Test
CS	Certification Specification
DFM	Design Fuel Mass
EBHA	Electrical Back-up Hydraulic Actuator
EDP	Engine Drive Pump
EHA	Electrohydrostatic Actuator
ELAC	Elevator Aileron Computer
EMA	Electromechanical Actuator
EMP	Electric Motor Drive Pump
EPS	Electrical power System
FAA	Federal Aviation Administration
FAC	Flight Augmentation Computer
FAR	Federal Aviation Regulations
FAT	Fault Tree Analysis
FBW	Fly-By-Wire
FCPC	Flight Control Primary Computers
FCS	Flight Control System
FCSC	Flight Control Secondary Computers
FH	Flight Hour
FMEA	Failure Modes and Effects Analysis
GDP	Group Design Project

GTF	Geared Turbofan
IAP	Integrated Actuator Package
IRP	Individual Research Project
JSF	Joint Strike Fighter
MAC	Mean Aerodynamic Chord
MEA	More Electric Aircraft
MTBF	Mean Time between Failures
PBW	Power-By-Wire
PHM	Prognostic and Health Management System
PTU	Power Transfer Units
RAT	Ram Air Turbine
SAE	Society of Automotive Engineers
SEC	Spoiler Elevator Computer
T-O	Take-off
TMS	Thermal Management System

Symbols

a	Sonic velocity
A	Area or surface area
C_L	Lift coefficient
C_D	Drag coefficient
F	Force or load
g	Gravitational constant of acceleration, 9.81m/s²
L	Arm of force
m	Mass
M	Mach number
P	Power
R	Ratio
sfc	Thrust specific fuel consumption
S	Stroke of actuator

t	Time
T	Moment
V	Velocity
α	Angle
ρ	Density
η	Efficiency
$\dot{Q}$	Heat
ΔW_{FO}	Extra weight of fuel due to system
Δf_p	Rate of fuel used due to system power off-take
ΔW_A	System weight
ΔD	System direct drag increase

Units

ft	feet (length)
in	inch (length)
kg	kilogramme (mass)
kts	one nautical mile per hour (velocity)
lb	pound (mass)
m	meter (length)
N	Newton (force)
nm	nautical miles (length)
psi	pound per square inch (pressure)
s	second (time)
W	Watt (power)
°	degree (angle)
°C	degree Celsius (temperature)

1 Introduction

1.1 Introduction

This report addresses the author's Group Design Project (GDP) and Individual Research Project (IRP). The GDP is the conceptual design of a 130-seat civil aircraft, and the details of the author's work in the GDP are described in Appendix A. The main body of this report is focused on the author's IRP, which presents the actuation technology for flight control systems (FCS) on civil aircraft.

A brief introduction to the background of the project is given below, which highlights the motivation of the project. It is followed by an overview of the project itself.

1.2 Background

1.2.1 More Electric Aircraft and All Electric Aircraft

Currently, engines are always the primary main power source on an aircraft. However, there are several secondary power systems, including mechanical, hydraulic, pneumatic and electric. Every secondary system has its own power generator, distribution, control and management components which constitute an integral and complex system. The use of multiple secondary power systems increases the complexity of the engine, reduces the engine efficiency and consumes more fuel. It also increases the cost of aircraft, reduces the performance and the reliability. Therefore, it is always attractive to try to simplify the current secondary power systems configuration, from which the concept of All Electric Aircraft (AEA) has developed.

In AEA, the hydraulic, pneumatic and mechanic power systems are replaced by an electrical power system. Therefore, all secondary power is distributed using the electrical system. All the users, including flight control actuation, landing gear extension and retraction, air conditioning and anti-icing, use the electrical power. A

More Electric Aircraft (MEA) is the intergradation of the conventional aircraft and the AEA, where electrical power is used to replace only parts of the secondary power systems. For instance, electric actuation is applied rather than the hydraulic actuation in flight control systems.

One of the key technologies for the MEA and AEA is electric actuation technology, which is still under development and still requires much work to reach maturity. Only a few Electrohydrostatic Actuator (EHA) and Electrical Back-up Hydraulic Actuator (EBHA) systems have been used on production aircraft to date.

Moreover, if it is intended to replace the hydraulic system on an MEA/AEA aircraft, then it shall also be necessary to consider an alternative actuator system. The hydraulic system on current generation civil aircraft is primarily used to power the flight control actuation system, and an alternative actuator system must be developed for an MEA/AEA without such a hydraulic system.

As a result of this, it is clearly important to study the actuation technology and analyse the application of this in the context of FCSs.

1.2.2 Flying Crane

Flying Crane is the aircraft designed in the author's GDP, the China Aviation Industry Corporation I (AVIC I) student group. It is a three-year cooperative project between Cranfield University and AVIC I, with the aim of training three groups of AVIC I students through the complete design process of a 130-seat civil aircraft. The author is in the first group which is charged with the conceptual design of the aircraft.

After six months' work, the conceptual design of the Flying Crane was completed. The final configuration finalized after progressing through several stages of design and competition with three other configurations. The Flying Crane is a wide body civil aircraft with a single aisle. It can accommodate 128 passengers for business and

economy mixed classes, while 150 passengers for single economy class. The range of Flying Crane is 2,000nm, and the take-off mass is 64,582kg [1].

The choice of a suitable actuation technology for the Flying Crane is an important issue during the conceptual design phase, because this leads to the question of whether to design an MEA/AEA. In addition, for the preliminary design of the Flying Crane, the GDP of the next AVIC I student group, the intended actuation technology to be used is an important design input.

Ultimately, actuation technology is selected as the research field for the author's IRP.

1.3 Project Description

1.3.1 Project Scope

Flight control actuation technology is a wide research field, which covers early manpowered actuation, dated hydraulic power-boost actuation, advanced EHA and EBHA systems, as well as Fly-By-Wire (FBW) actuation, which is the most common actuation technology in current aircraft. Also included in this field are some other actuation technologies under development, such as Integrated Actuator Package (IAP) and Electromechanical Actuator (EMA). However, it would be impossible to study all these aspects in the limited time. Consequently, a general comparison in terms of efficiency, complexity, thermal performance and engineering consideration for application on the Flying Crane would be undertaken. As a result, EHA and variable area actuation, a kind of advanced FBW actuation, are preferred to be further studied. These details are discussed in Chapter 2.

However, EHA has never been used for the primary FCS on a civil aircraft. Variable area actuation has only been developed for a fighter aircraft demonstrator and has never been studied further. This project will therefore design two types of actuation system using these two technologies for the tail unit of Flying Crane; comparing them and analyse the suitability of these two systems for the FCSs on civil aircraft. The

conclusion of which system offers the best actuation solution for the civil aircraft is given at the end of the thesis.

1.3.2 Project Objectives

a) Review flight control actuation technologies

b) Analyse the requirements of the tail unit flight control surfaces of the Flying Crane

c) Design and size an electrohydrostatic actuation system for the Flying Crane tail unit

d) Design and size a variable area actuation system for the Flying Crane tail unit

e) Compare the actuation systems, give the conclusion and suggestions for FCSs on civil aircraft

1.3.3 Project Process

For the first stage of the research, it is necessary to conduct a literature review of actuation technologies to understand the technology level of the research field. Meanwhile, general comparison and engineering consideration for application on the Flying Crane are completed to narrow down the research subject, and further understand the knowledge gaps in this field. The Literature review is presented in Chapter 2.

Case study comparison is a useful method to further study the technologies in the narrowed down field. Flight control surfaces of the tail unit including elevators and rudder of the Flying Crane are selected as the case study FCS, and the requirements are analysed. The case study introduction and requirements analysis are described in Chapter 3 and 4.

After analysing the requirements, two types of actuation system using EHA and variable area actuation technology respectively are designed. For the EHA system, EHA

technology is well developed and has been used in many engineering applications, so it can be used directly. Initially it is necessary is to design the system architecture. The following work will focus on sizing the system according to requirements, and checking the system safety by analysis and simple calculations. The EHA system sizing is addressed in Chapter 5.

Similar to the EHA system, system architecture of the variable area actuation system is designed firstly; then the power sources system architecture and system pressure are analysed. Power design point analysis, the key point of variable area actuation system design, is completed according to the actuator performance requirement curves derived in the Requirements Analysis section. This is followed by the actuation system sizing and system safety analysis. The variable area actuation system design is presented in Chapter 6.

When the parameters of each actuation system are indentified, a comparison between these two systems is undertaken. Fuel penalty, safety, maintenance and installation, cost, risk and certification are considered. A conventional FBW actuation system is used as the reference case. The conclusion of which technology offers the most reasonable and most suitable actuation solution for FCSs on civil aircraft is given. Furthermore, the recommendations for future work are analysed. The comparison, discussion and conclusion are described in Chapter 7 and 8.

The flow chart of the whole project is illustrated in Figure 1-1.

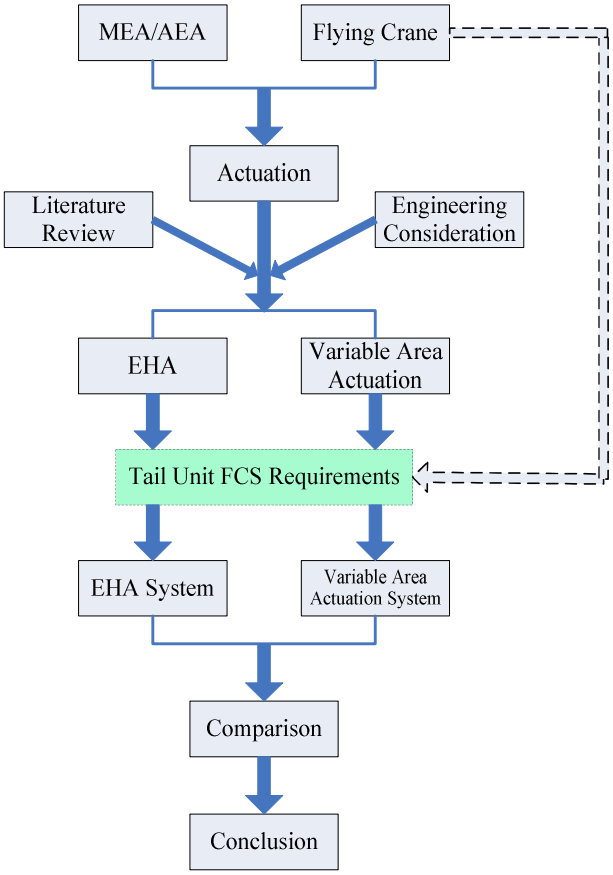

Figure 1-1 Project Process

1.3.4 Project Limitation

During this research project, the tail unit of the Flying Crane is selected as a case study. Since the Flying Crane is in the conceptual design phase and many parameters are not available, the requirements analysis mainly depends on simple calculation, comparison with similar aircraft and study of airworthiness regulations and related studies. In addition, some parameters of the components used in this project, for example, the failure rate of modern simplex EHA, are not available. Several professional companies have been contacted however, such as Parker Aerospace, Goodrich, Moog and EATON, though none were able to provide further information. Consequently, some parameters had to be based on assumption. Because of this, it is reminded that the reader should review the quantitative parts of this research with caution, and the methodology presented in this project is considered to be of greater value than the results obtained. It

is no doubt that the numerical results could be improved with the further design of the Flying Crane and more accurate information available.

Moreover, this research mainly focused on the flight control actuation system of elevators and rudder, which are only some elements of the complete primary flight control surfaces. The other components of the primary flight control surfaces, for example the ailerons, and the secondary flight control surfaces were not considered. However, the primary flight control surfaces are critical to the FCS because they work continuously and are concerned with the safety of aircraft. And the elevators and rudder, which are typical flight control surfaces in the primary FCS, consume more power. Therefore, it is expected that the actuation system designed for elevators and rudder could be suitably adapted to less demanding actuation functions, and the conclusion is suitable for the whole FCS on civil aircraft.

1.4 Summary

In this Chapter, the MEA/AEA and the Flying Crane were introduced, as well as the importance of studying the actuation technology for FCS on civil aircraft. The project scope was discussed and the work flow of research was described. In addition, the speculative nature of the research was highlighted to ensure the reader excises caution when interpreting the results. The findings of the literature review are addressed in Chapter 2 as the beginning of this project.

2 Literature Review

2.1 Introduction

This Chapter describes all the flight control actuation technologies except the manpower actuation, as well as the initial comparison and discussion among them, through which EHA and variable area actuation technologies are selected for further research.

2.2 Flight Control Actuation Technology Review

2.2.1 Overview

In terms of flight control actuation technologies, aircraft initially had very simple FCS, where the pilot was the producer of the forces required to move the control surfaces using mechanical means to transmit these forces, and this kind of system did not require secondary power system [2]. With the development of aircraft, the force requirements of flight control surfaces increased dramatically, the pilot could not cope with requirements any longer. Hydraulically powered and mechanically controlled actuators (hydraulic power-boost actuator) were introduced and used on aircraft. Then the hydraulically powered and electrically controlled actuators (FBW actuator) appeared and are used on most current aircraft to satisfy the increase of requirements of forces and control responses. In the FBW actuation technology, variable area actuation, a sub system technology, has ever been developed. Furthermore, with the introduction of the concept of MEA, electrically powered actuation technologies (Power-By-Wire), such as EHA and EBHA, have been developed and begun to be used on some new aircraft. Towards the future, EMA is under being studied currently and will be used on the AEA. In addition, IAP, another electrically powered actuation system, has also been developed.

2.2.2 Hydraulic Power-Boost Actuator

Hydraulic power-boost actuator is fully powered by the centralised hydraulic systems to provide the muscle for moving the control surfaces against the aerodynamic load, and it is controlled by the pilot's force to modulate the change in applied control power [2]. The pumps of centralised hydraulic systems are driven by the gear box of engine, electric motor or ram air turbine (RAT). The pilot's control force is transmitted by mechanical means; while the control valve within the actuator meters pressure to the ram in direct proportion to the pilot's input force.

The concept of hydraulic power-boost actuator is shown in Figure 2-1 [3].

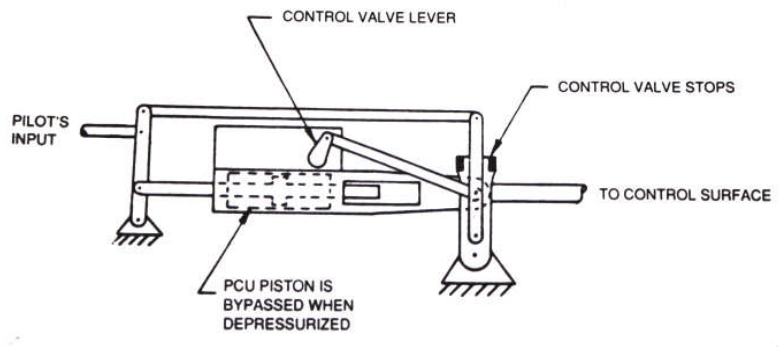

Figure 2-1 Hydraulic Power-Boost Actuator

Hydraulic power-boost actuator can produce huge force for the control surface; however, its control is irreversible [2]. This kind of actuators was used on the early aircraft.

2.2.3 Fly-By-Wire Actuator

FBW actuator is hydraulically powered by the centralised hydraulic systems and electrically controlled by the flight control computers. The control signals are produced based on the inputs of pilot and integrated with the air data, aircraft condition and the feedback of flight control surfaces. The servovalve receives control signals and drives the manifold which distributes the hydraulic flow to the ram to move the shaft.

The architecture of FBW actuator is illustrated in Figure 2-2 [4].

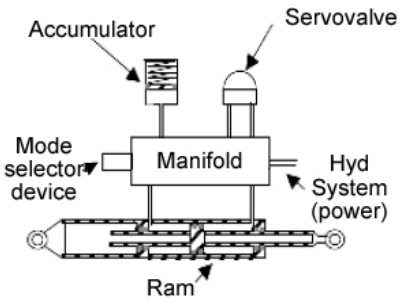

Figure 2-2 FBW Actuator

Compared with the hydraulic power-boost actuator, FBW actuator is also continuously powered by the centralised hydraulic systems and can produce huge force. However, its control is flexible, reversible and accurate due to the introduction of electrical control signals. This kind of actuators has been applied on most of the current aircraft.

2.2.4 Variable Area Actuator

Variable area actuator, one kind of FBW actuation, is also powered hydraulically and controlled electrically, but it has the additional function of piston area variable.

From the aerodynamic point of view, flight control surface always needs larger force and lower moving velocity in high speed flight; on the other hand, it needs smaller force and higher moving velocity in low speed flight [5]. Conventional constant piston area actuators must be designed based on the largest force requirement to decide the piston area, and integrated with the highest moving velocity requirement to calculate the flow requirement. Then hydraulic systems, the power sources of actuators, are sized according to this requirement. However, the largest force and the highest moving velocity are not happened at the same time. This makes the maximum using power much lower than the design power, as can be seen in Figure 2-3 (a) [4], which increases the mass and size of system, reduces the system efficiency. In the variable area actuator, there are two pistons within one ram, and the pistons' areas are different. In high speed condition, two pistons are in operation to fulfil the larger force requirement. In low speed condition, only the small area piston is in operation to meet the higher moving

velocity requirement without increasing the hydraulic flow requirement. The hydraulic system power design point can therefore be reduced by 50%, as illustrated in Figure 2-3 (b) [5]. To select the piston, a valve should be added and controlled by the signals from flight control computers. The other part of the variable area actuator is similar to those of the conventional FBW actuator. Although the variable area function makes the actuator more complex, at the same time, it reduces the design point and size of hydraulic systems significantly.

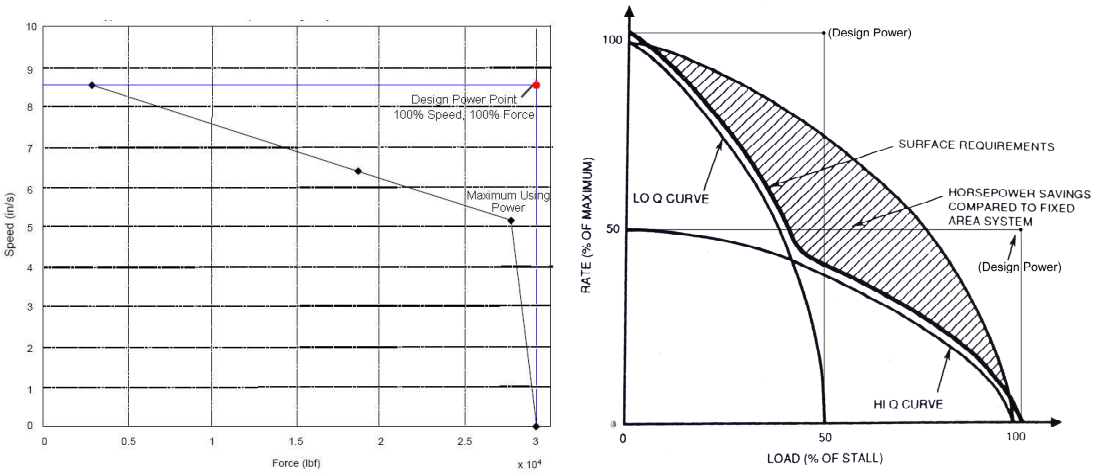

(a) (b)

Figure 2-3 FBW Actuator Power Sizing

An example of the variable area actuator is shown in Figure 2-4 [6].

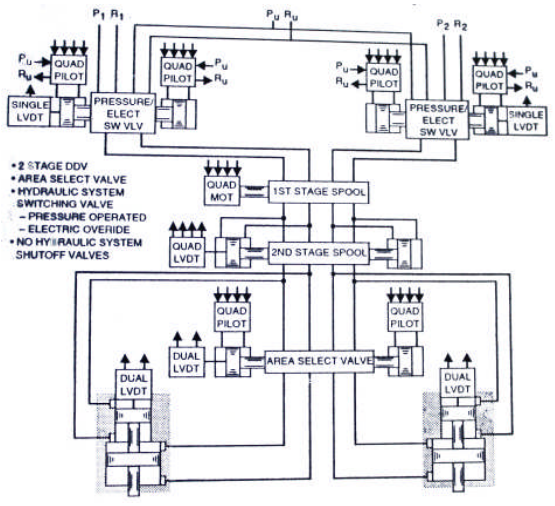

Figure 2-4 Variable Area Actuator

In contrast to the conventional FBW actuators, the variable area actuator reduces the power design point of centralised hydraulic systems, thus reduces the system mass and size and increases the efficiency of hydraulic system. This technology has ever been developed for the YF-23. However, due to the YF-23's failure in competition with the YF-22, the prototype of F-22, this technology has been abandoned and not been further developed ever since.

2.2.5 Integrated Actuator Package

Different from the hydraulic power-boost actuator and the FBW actuator (including the variable area actuator), IAP is both powered and controlled electrically. IAP can be regarded as a distributed conventional hydraulic system with actuators, which uses a constant speed electric motor to drive a variable displacement hydraulic pump, while the pump is integrated within a whole hydraulic circuit composed of components such as reservoir, accumulator and so on. The pump runs at constant speed, while the control signals from flight control computers vary the swash plate angle within the pump to change the displacement and direction of the hydraulic flow, therefore, control the ram actuation [7].

The concept of the IAP is shown in Figure 2-5 [7].

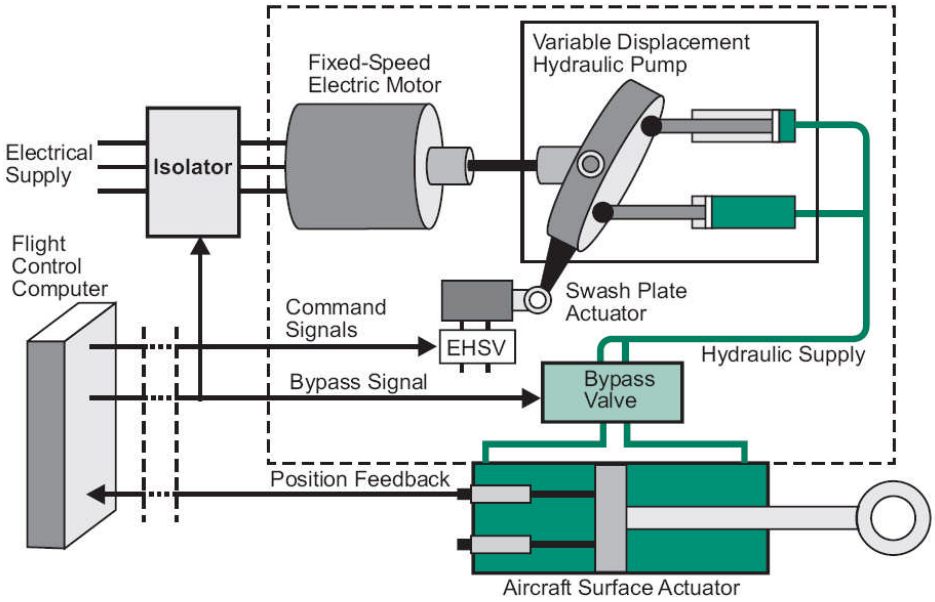

Figure 2-5 IAP Schematic

Similar to the FBW actuator, IAP works continuously to supply power to the hydraulic ram and is controlled electrically. However, as a Power-By-Wire (PBW) actuator, it does not rely on the centralised hydraulic systems. This kind of actuations has been developed and demonstrated.

2.2.6 Electrohydrostatic Actuator

Similar to IAP, EHA is also both powered and controlled electrically, and also likes a distributed hydraulic system with actuator. The difference between them is that EHA uses a variable speed electric motor to drive a fixed displacement hydraulic pump rather than a constant speed electric motor to drive a variable displacement hydraulic pump. EHA controls the ram actuation by changing the speed and direction of the electric motor according to the control signals.

The control layout of EHA is illustrated in Figure 2-6 [7].

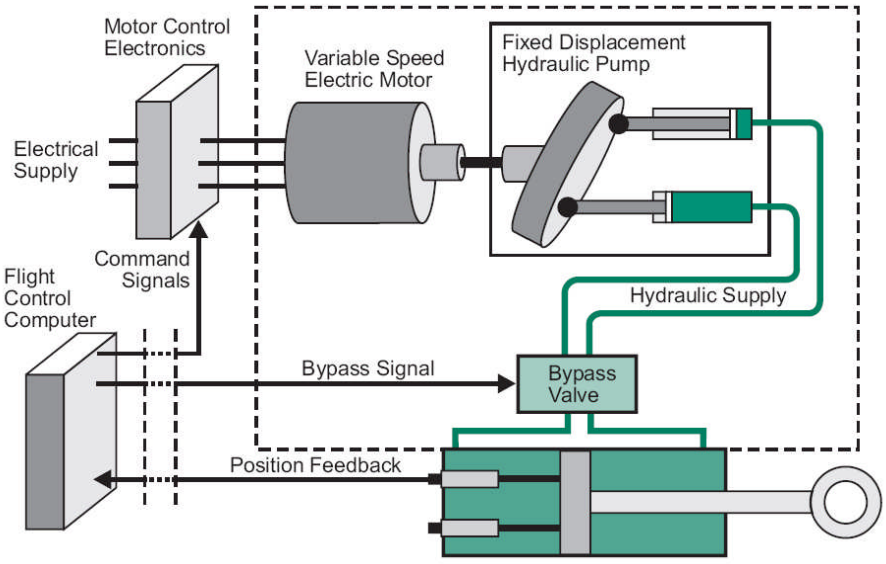

Figure 2-6 EHA Schematic

EHA controls the motor while IAP controls the pump. Although both of them supply power according to the requirements, the EHA is more efficient and consumes less power during standby operation, and it needs high power electric devices and has heat

issue. The EHA has been used on the primary FCS on the JSF (Joint Strike Fighter) F-35 and stand-by for the primary FCS on the Airbus A380.

2.2.7 Electrical Back-Up Hydraulic Actuator

Since most of the aircraft still require hydraulic power for heavy load such as landing gears extension and retraction, a hybrid actuator, EBHA, is introduced to take advantages of the combination of hydraulic power and electrical power [4]. As can be seen from its name, EBHA is the integration of the conventional FBW actuator and the EHA. It is powered by both hydraulic and electrical systems, while controlled by electrical system. In normal conditions, EBHA is powered by hydraulic systems as a FBW actuator. Once the hydraulic systems are out of order, it turns to the back-up channel and is powered by electrical systems as an EHA.

The relationship among the FBW actuator, the EHA and the EBHA are shown in Figure 2-7 [4].

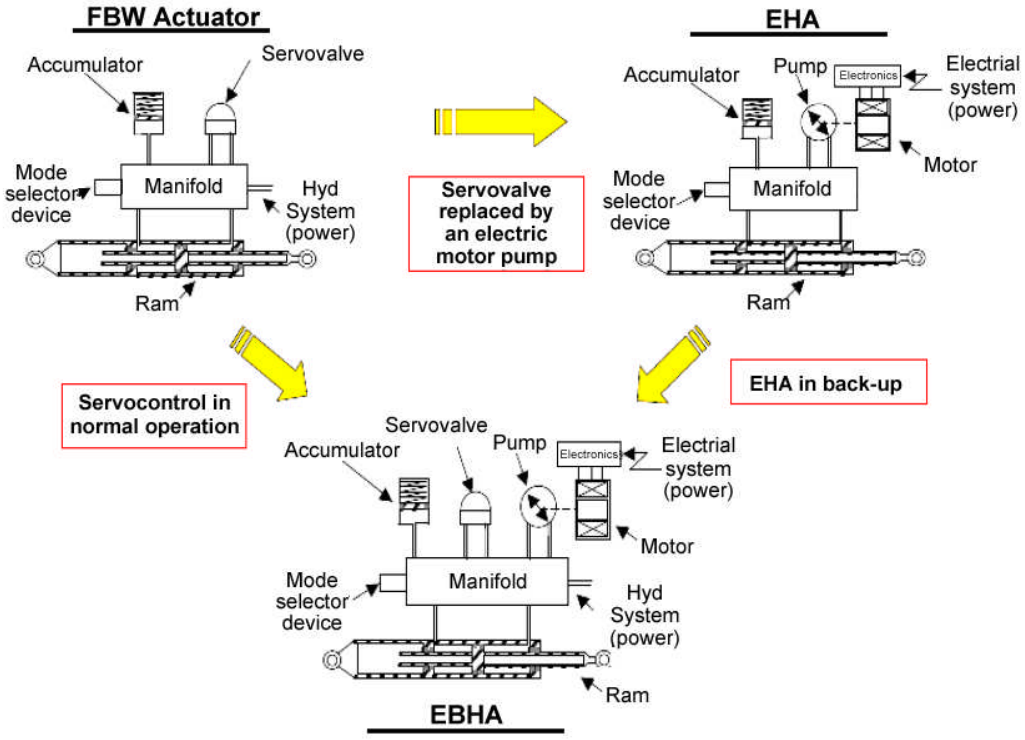

Figure 2-7 FBW Actuator, EHA and EBHA

Based on the same redundancy, the EBHA can reduce the mass of actuation system, and benefits from the phenomenon that hydraulic power and electrical power exist at the same time. However, this makes the actuator more complex and still relies on centralised hydraulic systems. To a certain extent, the EBHA can be regarded as the interim option between the FBW actuation and the PBW actuation. This kind of actuators is applied on the Airbus A380.

2.2.8 Electromechanical Actuator

Unlike the actuators described above, EMA does not contain any hydraulic components and does not use the hydraulic flow to drive the ram of actuator. It is a pure electric actuator which is both powered and controlled electrically. Similar to the EHA, another kind of PBW actuators, the EMA also uses a variable speed electric motor whose speed and direction are controlled by the signals from flight control computers. However, the EMA uses mechanical device to transmit the rotary power of motor to the piston so as to move the flight control surface.

The comparisons between the EMA and the EHA are illustrated in Figure 2-8 [4].

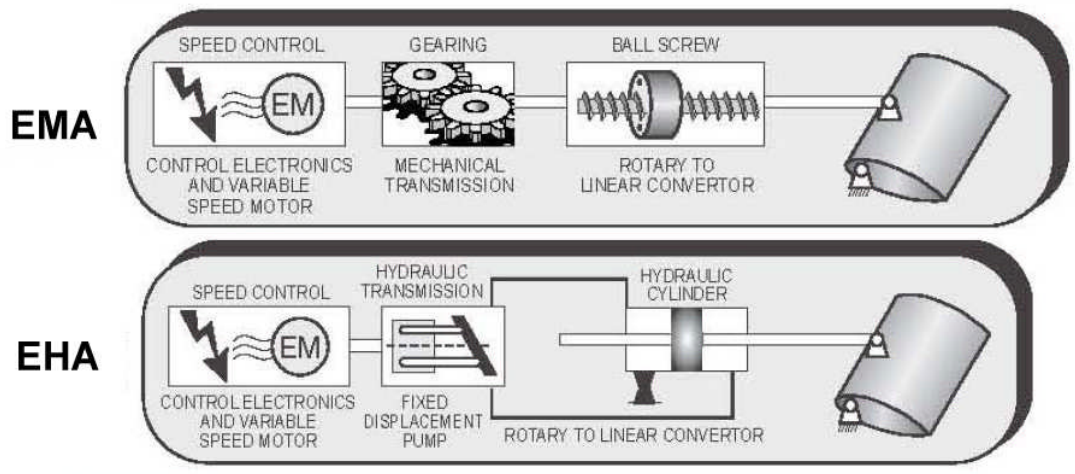

Figure 2-8 Architecture Comparison between EMA and EHA

Compared with the other actuation technologies, the EMA is an up-to-date technology and has not been used for flight control surfaces yet, and it still has some problems unsolved for example jam [8]. However, the EMA can fully replace hydraulic systems for flight control actuation systems and it will be an important technology for the AEA in the future.

2.3 Initial Comparison and Discussion

The general comparison and the major advantages and disadvantages of these actuation technologies are presented in Table 2-1.

Table 2-1 Initial Comparisons of Actuation Technology

Technology	Power	Control	Efficiency	Complexity	Thermal
Power -Boost	Centralised hydraulic	Mechanic	○	★	★
FBW	Centralised hydraulic	Low power electric	☆	☆	★
Variable Area	Centralised hydraulic	Low power electric	★	☆	★
IAP	High power electric	Low power electric	☆	☆	○
EHA	High power electric	Low/High power electric	★	☆	○
EBHA	Centralised hydraulic/ High power electric	Low/High power electric	☆	○	☆
EMA	High power electric	Low/High power electric	☆	○	○

Note: ★-good; ☆-normal; ○-bad.

In terms of thermal characteristic, both the power-boost actuator and the FBW actuator (including the variable area actuator) are powered by the centralised hydraulic systems. Continuous hydraulic flow takes the actuators' heat back to the heat exchangers, then transmits it to the heat sink. Therefore, the thermal characteristics of them are very well. For the IAP and the EHA, although both of them reintroduce hydraulic components and fluid, they are totally self-contained in the actuator assembly and have no interface to

the heat sink. They have some problems on thermal characteristics. In the research of Botten S.L. (*Flight Control Actuation Technology for Next-Generation All-Electric Aircraft*, 2000) [7], it was said that the thermal characteristics of IAP are better than that of the EHA because the electric motor of IAP is continuously running. However, as it is well-known to all, if the motor and pump keep working without control surfaces' power requirements, the electrical power it consumed converts to heat power. This will make the thermal characteristics even worse. Regarding the EBHA, normally it acts as a FBW actuator, thus it only has problems in back-up mode. In terms of the EMA, it produces more heat rejection than the hydraulic actuators, and it has no interface to transfer heat power [9]. The thermal characteristic of it is not good.

From the engineering application point of view, the power-boost actuator is low efficient and out of date; while the EMA is under development and far from application; the EBHA is just the interim option between the FBW and the PBW; while the performance of the IAP is quiet common. Considering from the integration of all aspects, EHA and FBW actuators are better solutions for the FCSs on civil aircraft. Furthermore, as a kind of PBW actuator, EHA is towards the future. From the risk and cost points of view, the FWB actuator is suitable for the aircraft to be designed in the near future. To make the aircraft more competitive, variable area technology should be applied on the FBW actuator.

However, EHA has never been used for the primary FCS on civil aircraft. Variable area actuation has only been developed for a prototype of fighter aircraft and has never been further studied. In addition, which actuation technology offers the best solution for FCSs on civil aircraft has not been studied. All these gaps will be tried to fulfil in this project.

2.4 Summary

This Chapter presented the information regarding actuation technologies on civil aircraft, and generally compared them. From initial comparison and engineering consideration, EHA and variable area actuation technologies were preferred to be further studied. And the knowledge gaps in this field were indentified.

3 Case Study Introduction

3.1 Introduction

Case study is a useful way to further analyse the actuation technologies. This Chapter presents the introduction of the case study of the project.

Flying Crane, the case study aircraft, is introduced firstly. This is followed by the introduction of the tail unit of the Flying Crane. At last, the flight control actuation system of the Airbus A320 is presented as a reference case.

3.2 Flying Crane

Flying Crane is the aircraft designed by the author's GDP as a next generation airliner to replace the current Boeing 737 and the Airbus A320. It is a medium to short haul, single-aisle, 130-seat jet liner with conventional configuration, and aiming to enter the market in 2020.

The Flying Crane has its unique features and advantages over the other aircraft in this category. Firstly, equipped with two Geared Turbofan (GTF) engines, it is expected to lower the fuel cost per seat mile greatly than current airliners. Secondly, the aircraft has the widest fuselage among the same class competitors which will greatly improve passengers' travel comfort and provide airlines more operational flexibility. At last, the design range of the Flying Crane is 2,000 nm, which makes the airliner more efficient in operation, particularly in Chinese domestic market [1].

Figure 3-1 illustrates one image of the Flying Crane [1].

Figure 3-1 Flying Crane

The main characteristics of the Flying Crane are presented in Table 3-1 [1, 10].

Table 3-1 Flying Crane Characteristics

Parameter	Data	Unit
Passenger Capacity	128 (mixed class)/ 150 (single class)	/
Range	2000	nm
Maximum Take-off Mass	64582	kg
Operational Empty Mass	37844	kg
Design Payload	12160	kg
Maximum Payload	17000	kg
Design Fuel Capacity	14978	kg
Maximum Fuel Capacity	17560	kg
Cruise Speed	0.78	M
Cruise Altitude	39000	ft
Service Ceiling	43000	ft
Fuel Tank Configuration	one centre tank, two inboard wing tanks and two outboard wing tanks	
Engine	Geared Turbofan (GTF) engine	

The reasons of choosing the Flying Crane as the case study aircraft are listed below. Firstly, the Flying Crane can represent the largest category aircraft requirement in the commercial aircraft market in the future. Based on the number of the Airbus A320 and the Boeing 737 currently in service and on order, the retirement of this category aircraft will be very huge in the next 20 years. Coupled with the rapid growth in air transport predicted for the foreseeable future, the requirement of this category aircraft is the most demanded [1]. Aiming to replace the A320 and the Boeing 737, the Flying Crane can represent the largest category aircraft requirement. Secondly, the parameters of the Flying Crane are easy to get. Different from the other aircraft such as the A320 and the Boeing 737, the Flying Crane is designed by the author's own group, and the parameters are charged by the author's group themselves. At last, taking the Flying Crane as the case study aircraft can benefit the next group of AVIC I student for their GDP. As a three-years cooperative project, the design of the Flying Crane will be continued by the next group of AVIC I student. Some suggestions, lessons and numerical results obtained in this research could be used in their GDP.

3.3 Tail Unit Flight Control Surfaces

The Flying Crane has been selected as the case study aircraft. However, it would be impossible to design actuation systems for all the flight control surfaces in the limited time. In addition, working for all the flight control surfaces means a lot of repeated work. As a result, the tail unit flight control surfaces are selected as the typical one, for which the actuation systems are designed.

The tail unit flight control surfaces are the most critical flight control surfaces in primary FCS, and primary FCS is more critical than secondary FCS for aircraft safety. In addition, as typical flight control surfaces, elevators and rudder always consume most of the actuation system power. It is expected that the tail unit flight control surfaces can represent the whole FCS on civil aircraft. Moreover, on a conventional aircraft, power sources, which are always located on the wing, are far from the tail unit. The connection

using pipes between power sources and tail unit flight control actuation systems causes maintenance and installation issues. It is expected this problem could be solved in this project. As a PBW system, the EHA system is powered by electrical power and does not have this problem. Regarding the variable area actuation system, localised hydraulic systems are good solutions for it.

The tail unit of the Flying Crane consists of single fin and low mounted tailplane. Conventional rudder and elevators are utilized for longitudinal and lateral trim and control with the trimming tailplane. The geometry parameters of the tail unit of the Flying Crane are presented in Table 3-2 [1].

Table 3-2 Flying Crane Tail Unit Parameters

Parameter	Tailplane	Fin	Unit
Reference Area	26.332	23.17	m^2
Span / Height	11.242	6.09	m
Aspect Ratio	4.8	1.6	/
Root Chord	3.66	5.765	m
Tip Chord	1.03	1.85	m
Leading Edge Swept Angle	35	41	°
1/4 Chord Swept Angle	30	35	°
Mean Aerodynamic Chord (MAC)	2.589	4.142	m
Setting Angle	-9 ~ 3	/	°
Wing Dihedral Angle	5	/	°
Control Surface Type	Round nose	Round nose	/
Control Surface Chord / Surface Chord	30	30	%
Control Surface Movement	±25	±20	°

3.4 Airbus A320 Flight Control Actuation System

As described in Section 3.2, the Airbus A320 and the Boeing 737 are the aircraft that the Flying Crane aims to replace, and the A320 is one of the most popular aircraft in current markets. Furthermore, the A320 is the first commercial aircraft using FBW actuation technology. The A320 is therefore selected as the reference of the case study aircraft.

The FCS and the related actuators on the A320 are illustrated in Figure 3-2 [11].

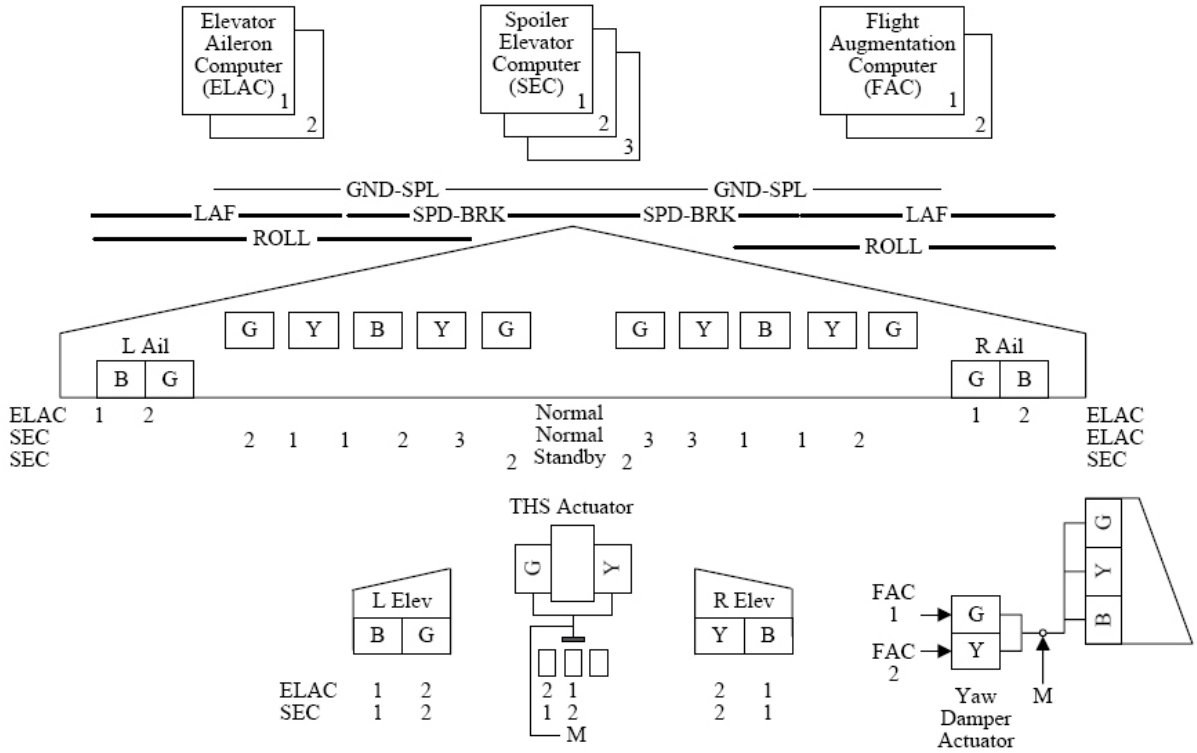

Figure 3-2 Airbus A320 Flight Control System

Figure 3-3 shows some actuators used on the A320 [12].

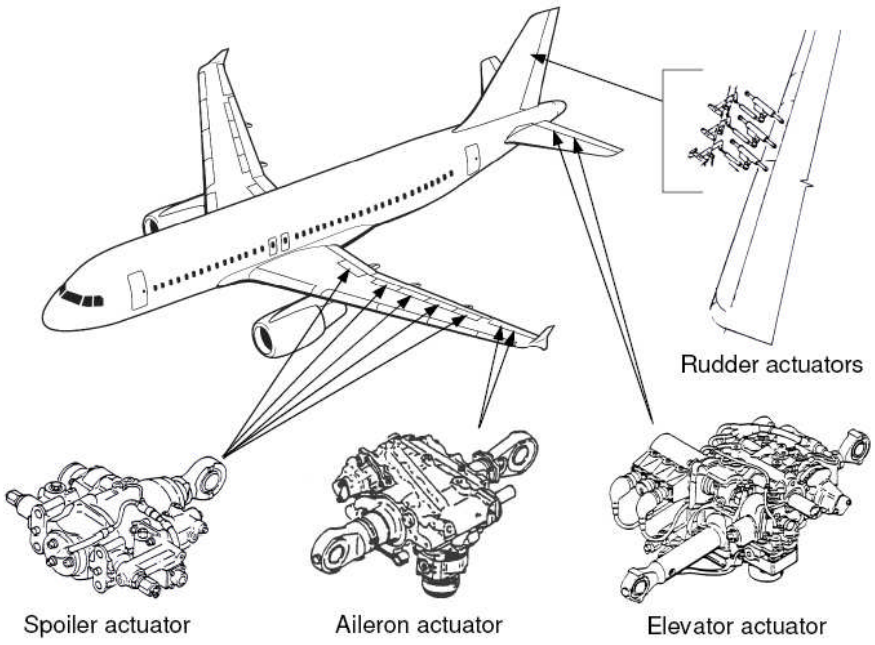

Figure 3-3 Airbus A320 Flight Control System Actuators

The three power sources for the FCS on the A320, green, yellow and blue hydraulic systems, are shown in Figure 3-4 [13].

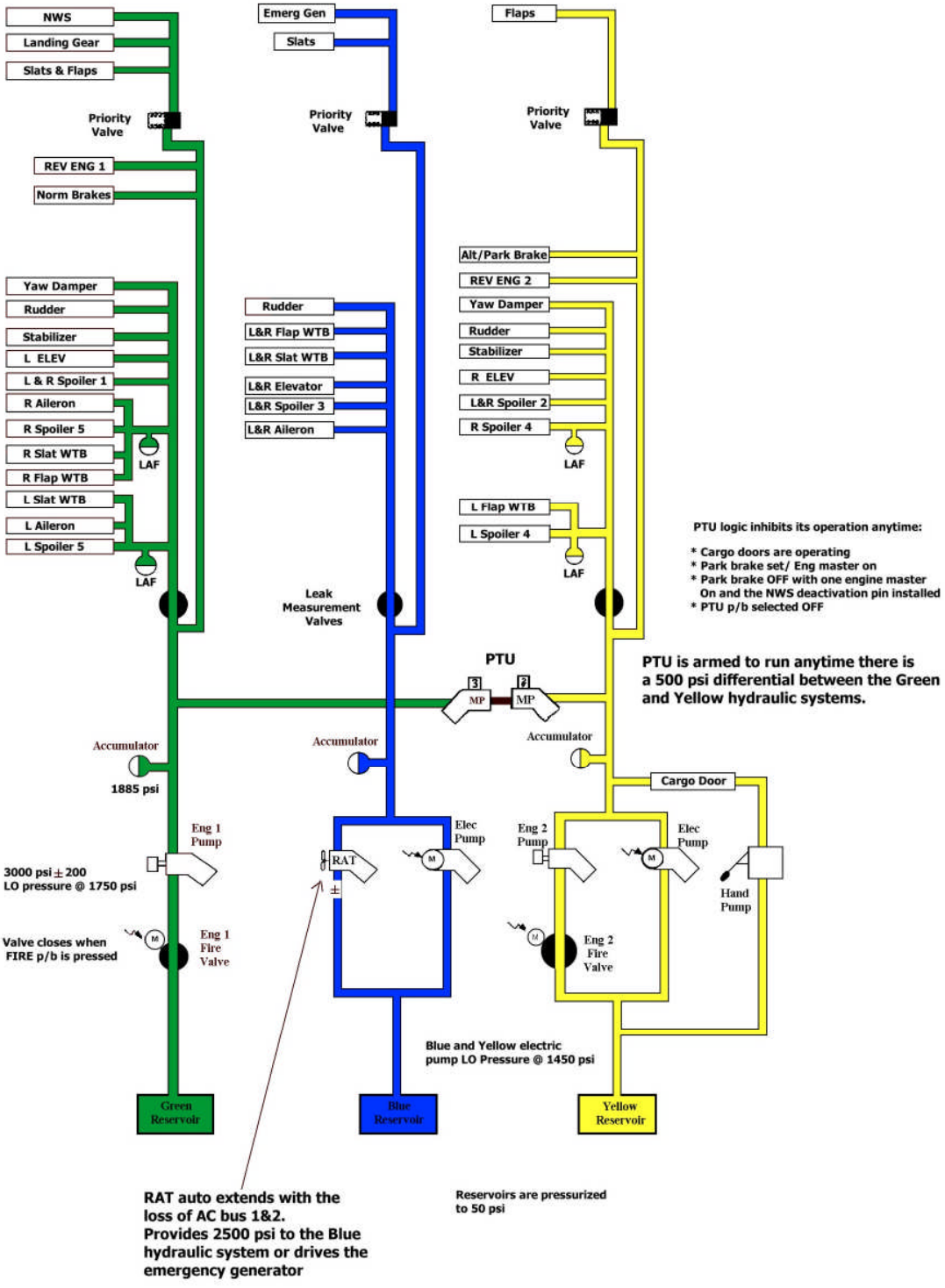

Figure 3-4 Airbus A320 Hydraulic Systems

The technical details of the actuators used for the tail unit of the A320 are presented in Table 3-3 [14].

Table 3-3 Airbus A320 Tail Unit Flight Control Surfaces and Actuators

	Elevator	**Rudder**
Purpose	Pitch control	Yaw control
Actuators	2 total 1 normal active 1 in damping mode	3 total 3 normally active (+2 yaw dampers)
Hydraulic System Failure Capability	Fail-Op / Fail-Safe	Fail-Op / Fail-Safe
Electrical system Failure Capability	Fail-Op / Fail-Op / Fail-Op / Fail-Safe	Fail-Op / Fail-Op
Maximum Control Surface Deflection	30°up 17°down	±25°at/blew 160kts ±3.5°at/above 380kts
Actuator Stroke	60 mm (2.4 in)	110 mm (4.3 in)
No Load Rate	60 mm/s (2.4 in/s)	110 mm/s (4.3 in/s)
Maximum Extend Force	27.7 kN (6230 lb)	44.3 kN (9960 lb)
Maximum Retract Force	27.7 kN (6230 lb)	44.3 kN (9960 lb)

3.5 Summary

This chapter introduced the case study of the project. The tail unit of the Flying Crane was selected as the case study since it can represent the complete FCS, as well as the Flying Crane can present the important category aircraft in the future. After that, the details of the flight control actuation system on the Airbus A320 which was selected as the reference of the case study were presented.

4 Requirement Analysis

4.1 Introduction

Before sizing or designing the actuation systems for the elevators and rudder of the Flying Crane, a set of requirements needs to be defined. Normally, the requirements can be divided into performance and safety.

In terms of performance, at the beginning, some load calculation formulae were chosen to be used as the main method. However, the Flying Crane is in conceptual design phase, a lot of parameters are not available. The calculation results would be meaningless when they were based on too many assumptions. After the discussion with Dr Lawson, to draw a comparison with the similar aircraft, the Airbus A320, is suggested as the main method. Meanwhile, some simple load calculation formulae are used as the assistances of comparison.

Similar to the performance, safety is also analysed by comparing with other civil aircraft associated with the studies of airworthiness regulations and some related researches.

4.2 Performance Analysis

The performance criteria of an actuation system typically include stall load, maximum rate capability (no load rate), frequency response, dynamic stiffness and failure transients [15]. However, some case studies (N. Bataille, 2006; D. Trosen, 1996; M. Aten, 2004) [16, 17, 18] proved that power, which is decided by stall load and no load rate, is adopted as the main design drive of an actuation system. For the EHA system, it can be sized according to the power requirement, but for the variable area actuation system, actuator performance curves as in Figure 2-3 (a) are necessary. Since power can be regarded as the function of stall load and no load rate [9], which has been included in the actuator performance curves, the work that needs to be done is to analyse the actuator performance curves. According to the performance curve in Figure 2-3 (a) [4]

and similar curves from researches of Montero Yanez [19] and J. Pointon [9], the key point of analysing performance curve is to calculate the stall load and no load rate.

4.2.1 Stall Load Estimation

Usually, take-off weight ratio is taken to estimate the power requirement of a new aircraft by comparing with the similar aircraft in case studies, it seems reasonable that to estimate stall load using weight ratio also. However, after the communication with MR. Ding Yaxiu, the load engineer in AVIC I group, another load calculation method using a simple load calculation formula is suggested:

$$F = \frac{1}{2} \times \rho \times V^2 \times c_L{}^{\alpha} \times \alpha \times A$$

Where F is aerodynamic load on flight control surface, ρ is the density of atmosphere, V is the speed of aircraft, C_L is the lift coefficient, α is the attack angle, A is the area of flight control surface.

Since the Flying Crane is similar to the Airbus A320, ρ , V , C_L and α of it are assumed to be same with those of the A320 in this case study. Therefore, from the above equation, it can be seen that for the similar aircraft, the aerodynamic load of flight control surface depends on the control surface area. As a result, the geometric ratio (2D) is selected to estimate the load rather than the weight ratio.

The aerodynamic load on control surface can be estimated by the area ratio (2D). However, in order to transfer the aerodynamic load to actuator force, the equation below is required:

$$T = F_s \times L_s = F_a \times L_a$$

Where T is moment, F_s is the aerodynamic load on flight control surface, L_s is the arm of aerodynamic load, F_a is the force of actuator, L_a is the arm of actuator force.

The arm of actuator force of the A320 can be calculated based on the stroke of actuator and the deflection of control surface. Since the installation of actuator always depends on the structure (geometry), geometry ratio (1D) is selected to estimate the arm of the actuator force of Flying Crane.

Based on the methods described above, the stall load of elevators and rudder of the Flying Crane is estimated. The results are illustrated in Table 4-1. The details of the estimation are presented in Appendix B.

Table 4-1 Airbus A320 and Flying Crane Elevators and Rudder

		A320	Flying Crane	Unit	Ratio		
					1D	2D	Reference
General							
	T-O Weight	73500	64582	kg			0.88
Elevator							
	Area	15.5	13.2	m²	0.92	0.85	0.85
	Deflection(up)	30	25	°			0.83
	Deflection(down)	17	25	°			1.47
	Actuator Stroke	60	58.6	mm			0.98
	Stall Load	27.7	23.5	kN			0.85
	Arm	75.3	69.4	mm			0.92
	Moment	2085.0	1632.3	N·m			0.78
Rudder							
	Area	21.5	23.2	m²	1.04	1.08	1.08
	Deflection(up)	25	20	°			0.8
	Deflection(down)	25	20	°			0.8
	Actuator Stroke	110	92.4	mm			0.84
	Stall Load	44.3	47.7	kN			1.08
	Arm	130.2	135.2	mm			1.04
	Moment	5768.0	6452.9	N·m			1.12

4.2.2 No Load Rate Estimation

The no load rates of elevators and rudder of the A320 are 60mm/s and 110mm/s respectively. Compared with the stroke of the relevant actuators, 60mm and 110mm for elevators and rudder separately, it is interesting to find that both the elevators and rudder can finish their maximum travel in one second under no load condition. After the discussion with MR. Kong Honghua, the flight control engineer of AVIC I group, 1s is suggested as the minimum time of actuation. As a result, the maximum rate (no load rate) of elevators and rudder of the Flying Crane is calculated as 58.6mm/s and 92.4mm/s respectively.

Referring to the similar trend of actuator performance curves with researches of J. Charriar [4], Montero Yanez [19] and J. Pointon [9], the elevator actuator performance curve and rudder actuator performance curve of the Flying Crane are made, as shown in Figure 4-1 and Figure 4-2.

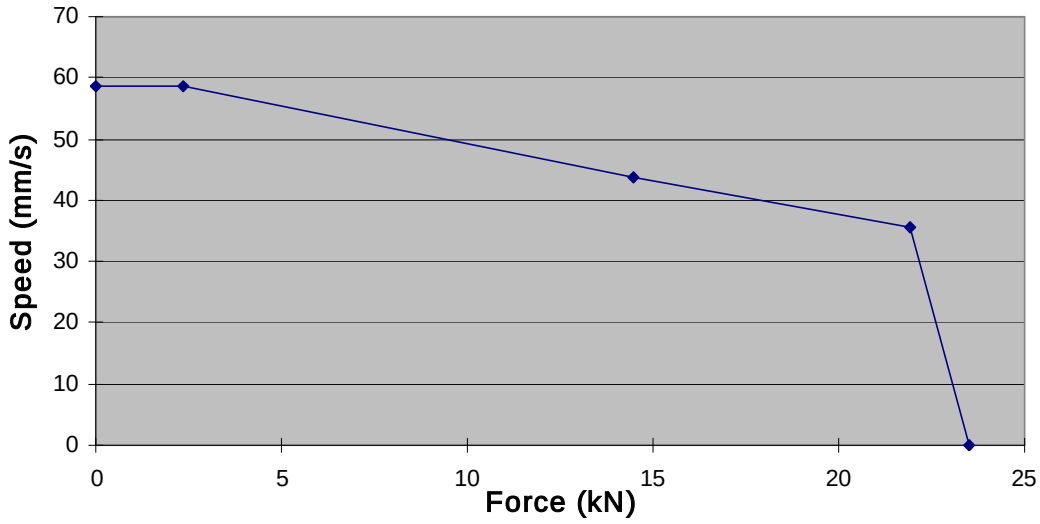

Figure 4-1 Flying Crane Elevator Actuator Performance Curve

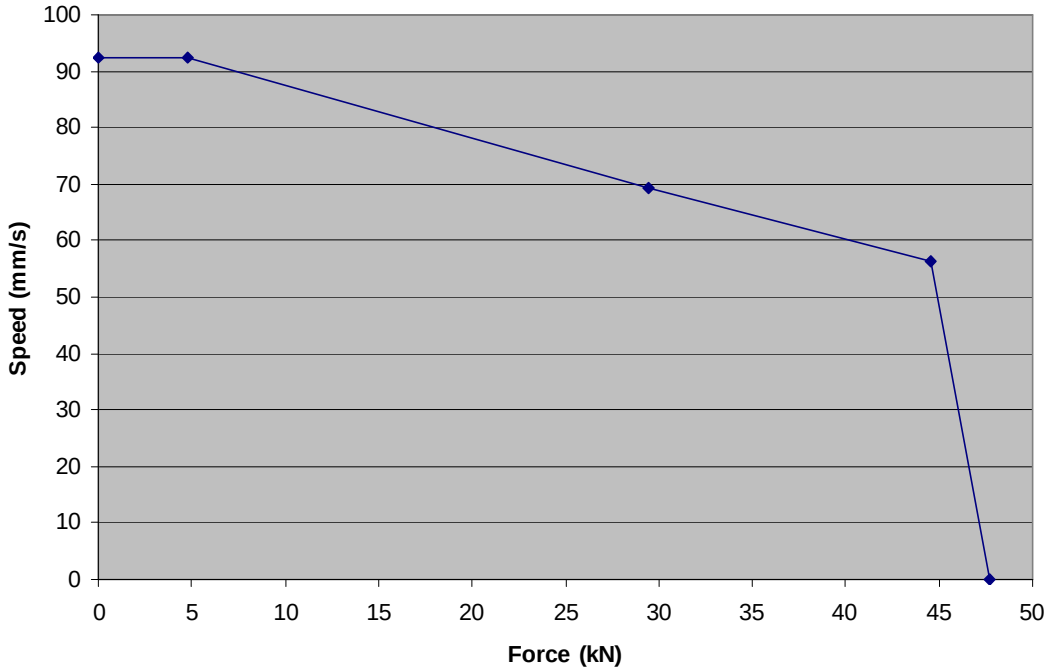

Figure 4-2 Flying Crane Rudder Actuator Performance Curve

From Figure 4-1 and Figure 4-2, the peak power of elevators and rudder of the Flying Crane is estimated as 781.7W and 2501.9W respectively (See Appendix B).

4.3 Safety Analysis

Ven den Bossche [20] stated that safety consideration is the primary drive of the architecture of flight control system, including number of actuators per control surface, number and distribution of power sources, and flight control computers. Since this study is focused on actuation system, the number of actuators per control surface and the number and distribution of power sources are the main issues to be considered as safety requirements.

According to the current airworthiness regulations, failures or combinations of failures resulting in the loss of aircraft should be extremely improbable. This means the failure rate should not exceed a probability of 10^{-9} per flight hour [21, 22].

Since the complete loss of power sources which supply power to the flight control actuation systems would result in the loss of aircraft control, especially the power sources for primary flight control actuation system; power sources for flight control actuation system should be several redundant. Based on the current level of reliability of secondary power sources, three independent sources are required to make the loss of flight control actuation system extremely improbable [20]. For the control loops, usually two independent loops are employed [15].

Most of up-to-date aircraft have three independent hydraulic systems as the power sources of flight control actuation system, two independent electrical systems as the control loops power, such as the Airbus A320 (Figure 3-2) and the A340 (Figure 4-3) [20]. This is the most popular configuration of power sources for FBW flight control actuation system applied on current aircraft, which is called '3H/2E' architecture.

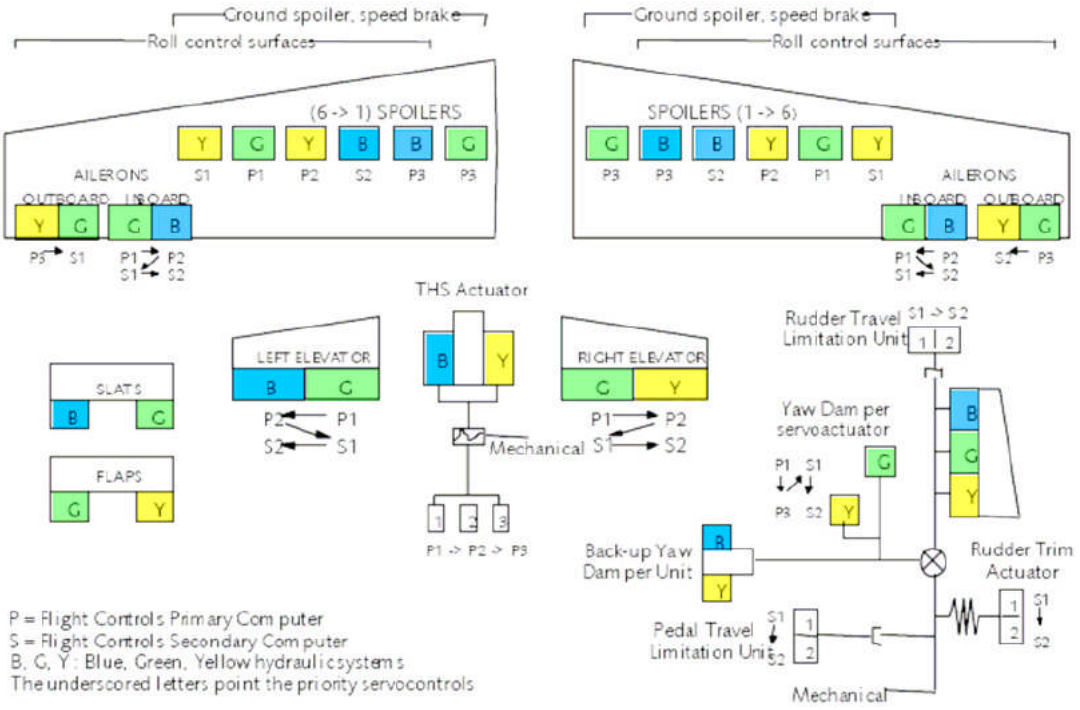

Figure 4-3 Airbus A340 Power Source and Actuator Distribution

In terms of the MEA, for example, the Airbus A380, it has two hydraulic sources and two electric sources, which is identified as '2H/2E' architecture, as shown in Figure 4-4 [23]. In the MEA, there are also three independent power sources (two hydraulic and

one electric) and two control power sources (two electric). The difference between the MEA and the conventional aircraft is that one electrical system is used to replace one hydraulic system by EHAs in the MEA. It means that electrical system acts as the actuation power source and control loops power at the same time. However, from safety point of view, both the configurations of '3H/2E' and '2H/2E' have three power sources and two control loops power.

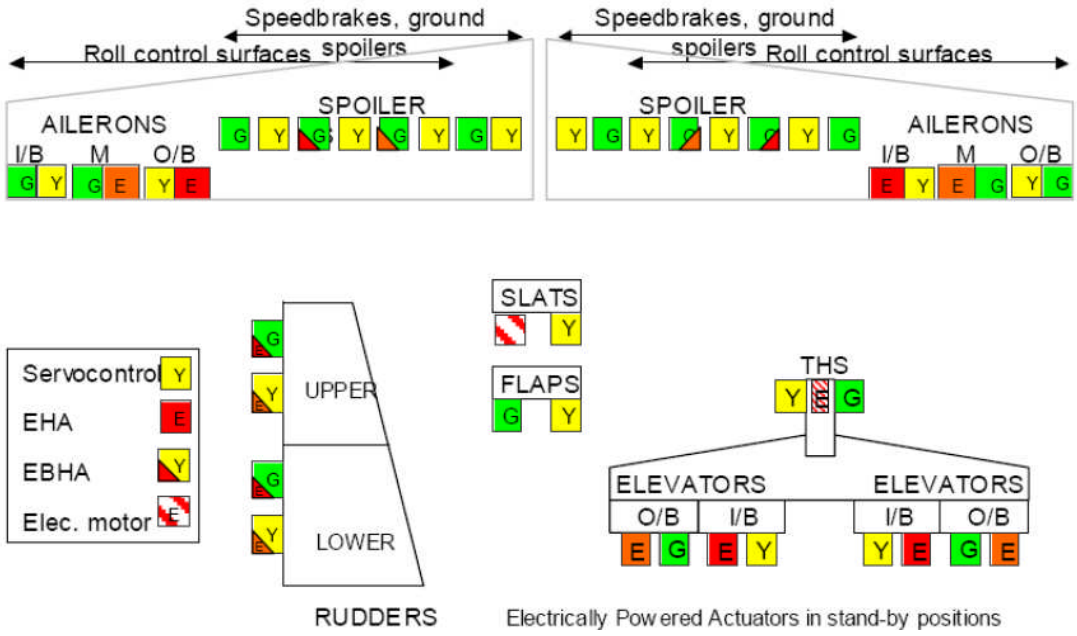

Figure 4-4 Airbus A380 Power Source and Actuator Distribution

For the number of actuators per control surface, it can be analysed by comparing with the current aircraft. From the actuator distribution of the A320 (Figure 3-2), the A340 (Figure 4-3) and the A380 (Figure 4-4), a general conclusion can be drawn as below:

- Elevator: four actuators powered by three power sources, while two actuators on each side powered by different power source. On each side, one actuator in normally active, the other in stand-by/damping mode;
- Ruder: three actuators powered by three power sources, all in normally active.
- All the actuators except EBHA are simplex, and each actuator is powered by one power source.

4.4 Summary

This chapter has discussed the requirements for flight control actuation system. Based on the comparison with the similar aircraft, simple calculations were completed to estimate the performance requirements. Actuator performance requirement curves were drawn according to the literature recommendations and limits used in similar studies. And the safety requirements were analysed by comparing with the similar aircraft associated with the studies of regulations and related researches.

The design requirements of the flight control actuation system for the Flying Crane tail unit are summarized in Table 4-2.

Table 4-2 Summary of Requirements

Surface	Actuator				System architecture	
	Stall load [kN]	**No load rate** [mm/s]	**Stroke** [mm]	**Peak power** [W]	**Power sources**	**Actuator number**
Elevator	23.5	58.6	58.6	781.7	2	2
Rudder	47.7	92.4	92.4	2501.9	3	3

5 Electrohydrostatic Actuation System Sizing

5.1 Introduction

As discussed in Chapter 2, EHA is an attractive option for the actuation system on civil aircraft in the near future, because it has high efficiency and does not rely on the centralised hydraulic systems. This chapter presents the preliminary design of the EHA system for the tail unit of the Flying Crane, which is based on the requirements analysed in Chapter 4.

The first step in sizing an EHA system is system architecture design, and then the power, mass and thermal management of it is estimated. This is followed by the safety analysis. A general summary is given at the end of this Chapter.

5.2 System Architecture

According to the analysis in Chapter 4, safety is the main drive for the architecture design of flight control actuation systems, which includes the following two aspects. In terms of power sources and control loops, based on the current technology level and its developing trend, three independent power sources and two independent control loops are required for the flight control actuation system to make the system safe. For the actuator number per control surface, three actuators for rudder and two actuators for each elevator are necessary because of the components reliability.

After having chosen the number of power sources and actuators, actuator distribution needs to be analysed. Taking the Airbus A320 as the reference (Figure 3-2), for the elevators, each side has two actuators powered by two centralised hydraulic systems. One system (Green or Yellow) is generated by an engine drive pump (EDP), the other system (Blue) is generated by an electric motor drive pump (EMP). The solo EMP hydraulic system is used on both sides, while the two EDP hydraulic systems (powered by different engines) are used on each side separately. Regarding rudder, it has three

actuators, which are powered by the three independent centralised hydraulic systems respectively. The actuation system architecture of the A320 is described in Table 5-1.

Table 5-1 A320 Tail Unit Actuation System Architecture

Control Surface	Actuator	Power Source	Mode
Elevator			
	Left outboard	Blue hydraulic system	Stand-By/Damping
	Left inboard	Green hydraulic system	Active
	Right inboard	Yellow hydraulic system	Active
	Right outboard	Blue hydraulic system	Stand-By/Damping
Rudder			
	Upper	Green hydraulic system	Active
	Centre	Yellow hydraulic system	Active
	Lower	Blue hydraulic system	Active

Since the Flying Crane is similar to the A320, the similar tail unit actuation system architecture is selected for the tail unit of the Flying Crane. In terms of power sources, there are four independent electrical systems powered by two engines and Auxiliary Power Unit (APU) on the Flying Crane [Personal conversion with Fu Lei, electrical system engineer of AVIC I GDP, Cranfield, 30th October 2008]. We name the systems powered by the left engine the system 1 and 2, while the system 3 and 4 for the systems powered by the right engine. The system 1 is used to replace the green hydraulic system, and the system 3 is used to replace the yellow hydraulic system, while the system 2 is chosen to replace the blue hydraulic system, although the system 4 has the same opportunity. For the actuators, EHAs are used to replace the FBW actuators directly. Concerning control loops, they are low voltage power which is in different channel with power sources. Furthermore, control loops and power sources have no direct relationship. Any of these four systems can be used. As a result, the system 2 and 4 are selected.

The draft of the EHA system architecture for the tail unit of the Flying Crane is illustrated in Figure 5-1.

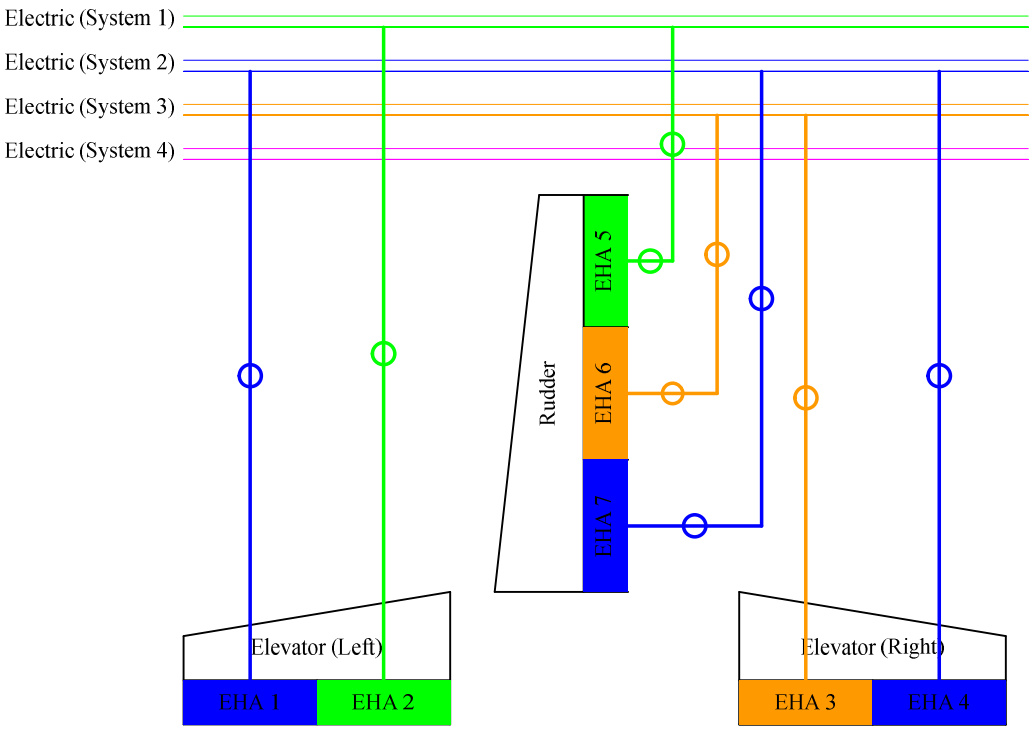

Figure 5-1 Draft of EHA System Architecture

In this EHA system architecture, there are two issues that should be noticed. Firstly, this system architecture does not fully take advantages of all the four electrical power sources existing in the aircraft, only three of them are used. Secondly, the left elevator is connected with the electrical system 1 and 2, and both of them are powered by the left engine. It means that in 'left engine out' failure mode, the left elevator will be out of control. If the electrical system 4 is used to replace the blue hydraulic system, the right elevator will face the same situation. Based on logic that ensures each primary flight control surface has a source of power to one actuator in the event of a total failure of one engine [8], the power source of the outboard actuator in the left elevator (EHA 1) is switched from the electrical system 2 to the system 4. Now, each surface is powered by at least two electrical systems from different engines, and all the four electrical systems are used. The finial allocation from the electrical systems to the tail unit actuators of the Flying Crane is shown in Figure 5-2.

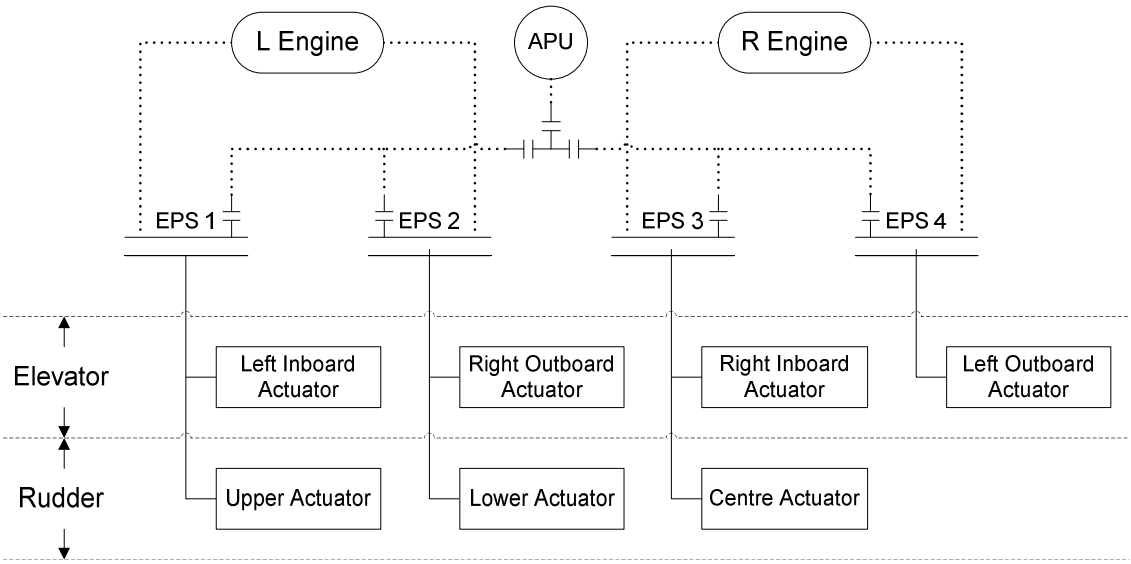

Figure 5-2 Electrical system to EHA Allocation

In this EHA system, all the three EHAs for the rudder are active in normal condition. The inboard EHAs of each elevator are active in normal condition, while the outboard two are in Stand-by/Damping mode. In addition, like the FBW actuators, all the EHAs are simplex actuators.

5.3 Power Estimation

5.3.1 Design Power Estimation

For the design point of EHA, it is always sized by the peak power requirement. In Chapter 4, the peak power of elevators and rudder for the Flying Crane have been analysed (See Table 4-2). Considering from sensitivity, a +10% error is required to adjust the power requirement as the actuator power design point [16]. Then the design power point of each actuator is:

$$P_{dp-elevator} = 1.1 \times P_{p-elevator} = 1.1 \times 781.7 = 861.0W$$

$$P_{dp-rudder} = 1.1 \times P_{p-rudder} = 1.1 \times 2501.9 = 2754.8W$$

Where P_{dp} is design power, P_p is peak power.

From a flight control point of view, elevators and rudder always act simultaneously, especially when the aircraft recovers from manoeuvre. Considering actuator mode (active or stand-by), the design power of the EHA system can be estimated as the sum of the design power of elevators and rudder. The sizing is illustrated in Table 5-2.

Table 5-2 EHA System Power

Power source	**Actuator**	**Mode**	**Power** (W)	**Total** (W)
Electrical system 1	Left inboard elevator	Active	861.0	3615.8
	Upper rudder	Active	2754.8	
Electrical system 2	Right outboard elevator	Stand-by	0/861.0	2754.8
	Lower rudder	Active	2754.8	
Electrical system 3	Right inboard elevator	Active	861.0	3615.8
	Centre rudder	Active	2754.8	
Electrical system 4	Left outboard elevator	Stand-by	0/861.0	0
Total	/	/	/	9986.4

5.3.2 Average Power Estimation

It is extremely difficult to determine the usage of aircraft control surfaces with accuracy, because it is influenced by many variable factors, such as the atmospheric turbulence and the specific missions. Several studies, including those of Bland [24] and Schneider [25], have used a simplified actuator duty cycle refereed to as the ‘80/20 Rule’. It assumes a typical actuator duty cycle as being maximum power for 20 percent of the time, with the remaining time spent at 20 percent of maximum power, as shown by the square wave pattern in Figure 5-3 [25].

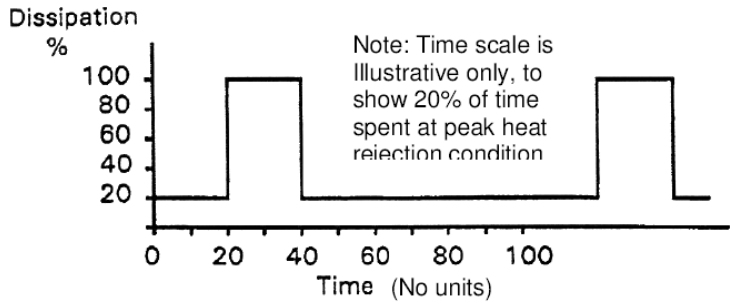

Figure 5-3 Actuator Duty Cycle Based on '80/20 Rule'

The duty cycle of '80/20 Rule' has been proved by Schneider that it gives an acceptable approximation to real actuator [25]. It is therefore selected to estimate the average power in this case study. Thus the average power of the EHA system is:

$$P_{a-EHA} = 0.2 \times P_{dp-EHA} + 0.8 \times 0.2 \times P_{dp-EHA} = 3595.2W$$

5.3.3 Power Consumption Estimation

After gaining the power of the EHA system, power consumption needs to be estimated. In terms of the EHA system efficiency, Bataille used 90% in his study of *Electrically Powered Control Surface Actuation* [16]. However, according to the current technology level, the two major components of EHA, hydraulic pump has an efficiency of 80%~85% [26]; advanced electric motor has an efficiency about 90% [27]. Since there is no pipe in the EHA, neglecting the loss of other components and taking the average as the efficiency of pump, the efficiency of whole EHA is estimated as 74%. Then the maximum power consumption of the EHA system is:

$$P_{mcon-EHA} = P_{dp-EHA} / \eta_{EHA} = 9986.4 / 0.74 = 13449.9W$$

Since the EHA system works on demand, the average power consumption of the EHA system depends on the average power requirements. Therefore, the average power consumption of the EHA system is calculated:

$$P_{acon-EHA} = P_{a-EHA} / \eta_{EHA} = 3595.2 / 0.74 = 4842.0W$$

5.4 Mass Estimation

To estimate the mass of the EHA system, specific power (power/mass ratio) of current products is always used. Till now, EHAs are only used on engineering in two types of aircraft except demonstrators, the EHA developed by Parker Aerospace for the primary FCS of the JSF F-35 [28] and the EHA developed by Goodrich as the back up actuators of primary FCS of the Airbus A380 [29].

According to reference 16, the specific power of the EHA on the F-35 is 186.05 W/kg, while the specific power of the EHA on the A380 is unavailable. The author has contacted both Parker and Goodrich via email, and also other professional companies such as Moog and EATON. However, none of them were able to provide further information. As a result, the specific power of the EHA on the F-35 is taken as the reference in this study. The mass of each actuator intended to be used on the Flying Crane tail unite can therefore be estimated:

$$M_{elevator-EHA} = \frac{P_{elevator-dp-EHA}}{R_{pm-EHA}} = \frac{861}{186.05} = 4.6kg$$

$$M_{ruder-EHA} = \frac{P_{rudderr-dp-EHA}}{R_{pm-EHA}} = \frac{2754.8}{186.05} = 14.8kg$$

The total mass of the EHA system for the Flying Crane tail unit is 62.9kg.

5.5 Thermal Management

5.5.1 Heat Load Estimation

The rate of heat rejection of a device is the difference between the input power and the output power [9]:

$$\dot{Q} = P_{in} - P_{out} = \frac{P_{out}}{\eta} - P_{out} = P_{out}(\frac{1}{\eta} - 1)$$

As analysed in Section 5.3.3, the efficiency of EHA is estimated as 74%, then the heat rejections (peak) of each EHA is:

$$\text{Elevator: } \dot{Q}_{pE-EHA} = P_{pout-E-EHA}(\frac{1}{\eta_{EHA}} - 1) = 861 \times (\frac{1}{0.74} - 1) = 298.6W$$

$$\text{Rudder: } \dot{Q}_{pR-EHA} = P_{pout-R-EHA}(\frac{1}{\eta_{EHA}} - 1) = 2754.8 \times (\frac{1}{0.74} - 1) = 955.4W$$

The total heat rejection of the EHA system is 3463.4W.

An identical calculation can be carried out for the average heat rejection (nominal operating conditions), by starting with the average output power. The results are summarised in Table 5-3 including both the peak and average heat rejections.

Table 5-3 Heat Rejection of EHA System

Actuator	**Heat Rejection** (W)	
	Peak	Average
Elevator	298.6	107.5
Rudder	955.4	343.9
EHA System	3463.4	1246.8

5.5.2 Thermal Management System Sizing

To control the temperature of the EHA system, a thermal management system (TMS) is required. As described in Chapter 2, on a conventional aircraft, the heat exchangers in centralised hydraulic systems transfer the heat power to the fuel. However, EHA is a self contained actuator which is separated from the centralised hydraulic systems, and tail unit is far from the fuel tank which is located in the wing of a aircraft, so fuel heat exchanger is not practical in an EHA system. A related research, *Thermal Management of Eletromechanical Actuation on an All-Electric Aircraft* by J. M. Pointon, suggested that ram-air-cooled cold plates are the best solution for EMA [9]. Since EHA and EMA are both PBW actuators and self contained, and they have similar interfaces to the other systems, air-cooled cold plates are selected for each EHA to cool the actuator.

The main parameters of the air-cooled cold plate TMS designed by Pointon for the rudder using EMA are illustrated in Table 5-4 [9].

Table 5-4 Air-Cooled Cold Plate TMS Parameters

		Case 1	Case 2
Design Requirements	Peak Temperature (°C)	125	150
	Heat Rejection (W)	664	664
Cooling Air	Flow Rate (g/s)	539	539

It can be seen from this table, both of the two air-cooled cold plate TMS design cases have the same power/flow ratio (heat rejection / cooling air flow rate):

$$R_{pf} = \frac{\dot{Q}_{heat}}{Q_{coolingair}} = \frac{664}{53.9} = 12.3 W / g / s$$

For the EHA system of the Flying Crane tail unit, as introduced in Chapter 2, it includes hydraulic circuits and can be regarded as distributed hydraulic system. According to the hydraulic system standard SAE 5440 [30], the maximum operating temperature of Type II hydraulic system is 135°C, while the maximum peak temperature is 155°C. This is close to the requirements of the air-cooled cold plate TMS in Pointon's research. Thus the power/flow ratio of air-cooled cold plate TMS in Pointon's research can be used for sizing the TMS for the EHA system on the Flying Crane:

$$Q_{ca-e} = \frac{\dot{Q}_{heat-e}}{R_{pf}} = \frac{107.5}{12.3} = 8.7 g / s$$

$$Q_{ca-r} = \frac{\dot{Q}_{heat-r}}{R_{pf}} = \frac{343.9}{12.3} = 27.9 g / s$$

The total cooling air flow requirement of the EHA system is 101.2g/s.

5.6 Safety Analysis

5.6.1 Failure Analysis

Since power sources are important factors for the actuation system safety, the failure conditions of power sources should be analysed. Table 5-5 shows the failure of one or more electrical systems and how this affects the functionality of the EHA system.

Table 5-5 EHA System Power Source Failure Analysis

		Electric system failure													
Surface	Actuator	1	2	3	4	1&2	1&3	1&4	2&3	2&4	3&4	1,2&3	1,2&4	1,3&4	2,3&4
L Elevator	Outboard														
	Inboard														
R Elevator	Inboard														
	Outboard														
Rudder	Upper														
	Centre														
	Lower														
		Actuator full capability availaible							Actuator not available						

Case ‘1’ / ‘3’ represents the failure where the electrical system 1 / 3 is lost. In this condition, there is at least one actuator in each control surface are full capability available. The EHA system can ensure the aircraft control. Case ‘1&2’ / ‘3&4’ represents the failure where both the electrical system 1 and 2, or 3 and 4 are lost. In this condition, there is still at least one actuator in each control surface keeping full capability. The control of aircraft is available.

5.6.2 Reliability and Redundancy Analysis

In terms of reliability, a research from June 1990 to December 1992 predicted that the failure rate of the EHA designed in that project is 73.668×10^{-6} / FH. For the surface using two EHAs, the probability of loss of operation is 2.25×10^{-8} /FH [19]. This is higher than ‘Extremely Improbable’ (10^{-9} /FH). However, that research is nearly 16 years ago. After that, the technology of EHA and related systems has been developed a lot, especially with the engineering application of EHA on the F-35 and the A380. Another project, the group design project Caracal by University of Bristol, 2006,

showed that the failure rate of a control surface with two dual-redundant EHAs is 1.74×10^{-10}/FH [31]. It seems that using two dual-redundant EHAs for one control surface is good solution. However, in project Caracal, they used 5.34×10^{-4} as the failure rate of EHA, it is even higher than the failure rate of the EHA 16 years ago developed by the former project.

In fact, the reliability of the EHA system could be expected to be higher than that of the FBW actuation system without considering the influences of the power sources. The EHA system can be regarded as a localised hydraulic circuit, but it works on demand, not as the conventional hydraulic system working continuously. Therefore, the usage of the EHA system is lower than that of an equivalent hydraulic system. Meanwhile, the elimination of hydraulic pipes reduces the leakage in an EHA system compared with a hydraulic mean. Both of these factors increase the Mean Time between Failures (MTBF) of EHA system and make it more reliable.

Based on the limited available data and assuming the failure rate of EHA can reach the technology level to be no more than 2.20×10^{-5}/FH, the failure rates of the EHA system for the Flying Crane tail unit are estimated 1.00×10^{-9}/FH and 1.25×10^{-10}/FH for pitch control (elevators) and yaw control (rudder) respectively. This means that the chance of the Flying Crane EHA system being lost is ‘Extremely Improbable’. For details of the failure rate estimation, see Appendix C.

For the redundancy of the EHA system on the Flying Crane, the ‘4E’ architecture has four power sources. As described in Chapter 4, the conventional ‘3H/2E’ and ‘2H/2E’ system only have three power sources, while the other systems are used for control loops. Thus the EHA system is more redundant in power sources. Moreover, all electric distribution in the EHA system simplifies the power configuration. Since electrical power is good at being monitored and controlled, the Prognostic and Health Management System (PHM) can be realised easily. Then the EHA system can provide easier failure isolation and reconfiguration capability. This increases the redundancy of the EHA system.

5.7 Summary

This Chapter has designed an EHA system for the tail unit of the Flying Crane. According to the safety requirements, the EHA system architecture was designed. Then the power, mass and thermal management of this system were sized based on the performance requirements. At last, the failure condition, reliability and redundancy were analysed.

The power and reliability of the EHA system described in this Chapter meet the performance requirements and safety requirements of FAR/CS25, which suggests that the EHA system is suitable for actuating the tail unit of the Flying Crane.

During the EHA system reliability analysis, there is an important hypothesis that the EHA's failure rate is no more than 2.20×10^{-5}/FH. However, this parameter is not confirmed by the professional companies. This means that the EHA system has risks. It will be further discussed in Chapter 7.

6 Variable Area Actuation System Design

6.1 Introduction

As one kind of FBW actuation, the variable area actuation system offers lower technology risk than the EHA system. Meanwhile, the variable area function makes it more efficient than the conventional FBW actuation system. This Chapter describes the preliminary design of the variable area actuation system for the tail unit of the Flying Crane.

Similar to the EHA system, the variable area actuation system architecture is designed firstly, then the system architecture and pressure of power generation, localised hydraulic systems, are analysed. After that, power design point analysis, which is the key point of variable area actuation system design, is completed based on the actuator performance requirement curves. This is followed by the system sizing including power, mass and TMS estimation. At last, the safety of the variable area actuation system is analysed and a general summary is given.

6.2 System Architecture

The difference between the variable area actuator and the conventional FBW actuator is that the former has an additional function, piston area variable. Since this function is inherent in the actuator and realised by the actuator itself, from system point of view, variable area actuator can be regarded as conventional FBW actuator. Thus the actuation system architecture using variable area actuators should be similar to the actuation system using conventional FBW actuators.

Tail unit is far from the power generations of conventional centralised hydraulic systems which are located in the wing on a wing mounted engine aircraft, thus localised hydraulic systems are better solution for tail unit flight control actuation system. As a result, localised hydraulic systems are selected as the power sources for the variable area actuation system for the tail unit of the Flying Crane.

Since localised hydraulic system can be regarded as minimised centralised hydraulic system except the difference of pump drive power sources, it is selected to replace centralised hydraulic system directly. Similar aircraft, for example, the A320, has three independent centralised hydraulic systems. For the Green hydraulic system, centralised hydraulic system uses one EDP as the power generator, which is replaced by an EMP in the localised hydraulic systems. The electric motor is powered by the electrical system 1 which generated by the left engine. In terms of the Blue system, centralised hydraulic system uses one EMP as power generator and one RAT for backup under emergency condition. While on the Flying Crane, the emergency power has been included in electrical systems [Personal conversion with Fu Lei, electrical system engineer of AVIC I GDP, Cranfield, 14th November 2008], thus another EMP is used to replace the RAT. To fully take advantages of the four electrical power sources and to make the system more redundant, the localised blue hydraulic system is powered by two different power sources, the electrical system 2 and 4, which are generated by different engines. For the Yellow system, centralised hydraulic system uses one EDP, one EMP and one hand pump as power generators, and there is a Power Transfer Units (PTU) between the green system and the yellow system. Because hand pump is only for backup of the cargo door actuation, it is cancelled in the localised hydraulic system. Similar to the Green system, one EMP powered by the electrical system 3 which generated by the right engine is selected to replace the EDP, and PTU is still provided in the localised hydraulic systems between the green system and the yellow system. However, for the EMP in the centralised yellow system, whether it is necessary or not to add a second EMP in the localised hydraulic system is uncertain, it needs to be considered on the whole system level.

For the whole variable area actuation system, all the four power sources on the Flying Crane have been used, and the PTU existing between the green system and the yellow system makes the two systems to backup for each other. In addition, the EMPs in blue system can supply power to each section of the tail unit FCS. If a second EMP is added in the yellow system, it must be powered by one of the four electrical systems which have been used, and the function of it would be same with one of the four existing EMPs. Furthermore, three localised hydraulic systems with four EMPs are used. Compared with the conventional centralised hydraulic systems which include five

power generators, one EDP in green system, one EMD and one RAT in blue system, one EDP and one EMP in yellow system, there are one less power generators in the localised hydraulic systems. However, localised hydraulic systems are only responsible for the tail unit FCS, not like conventional centralised hydraulic systems take charge of the whole FCS. It is assumed that four EMPs are enough for the localised hydraulic systems on the tail unit. Based on these points, the second EMP in the yellow localised hydraulic system is unnecessary.

The architecture of the variable area actuation system for the Flying Crane tail unit is illustrated in Figure 6-1.

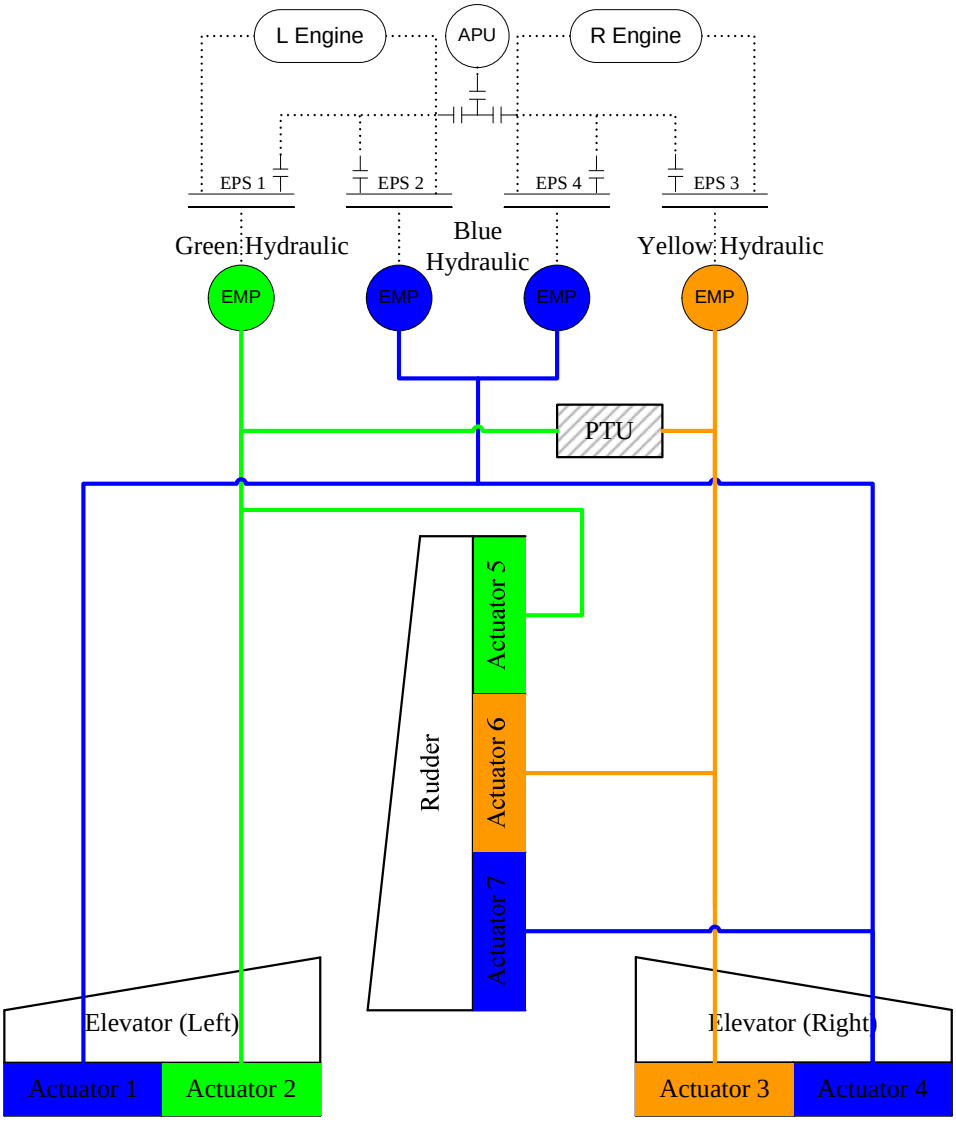

Figure 6-1 Variable Area Actuation System Architecture

Like the conventional FBW actuation system, all the actuators in the variable area system are simplex actuators and each of them is powered by one localised hydraulic system. Furthermore, all the three actuators for rudder are active in normal condition. The inboard actuators in each side of elevators are active in normal condition, while the outboard two are in Stand-by/Damping mode.

6.3 Power Generation Description

6.3.1 System Architecture

Localised hydraulic systems are the power generations of the variable area actuation system. As explained before, localised hydraulic systems can be regarded as minimised conventional centralised hydraulic systems. Based on the basic hydraulic system introduced in *Aircraft Hydraulic System* [32], hydraulic circuit design described in *Aircraft Systems* [11], and the analysis of hydraulic system of the A320 [12], the architecture of localised hydraulic system on the Flying Crane tail unit is designed. A typical one, green localised hydraulic system architecture, is illustrated in Figure 6-2.

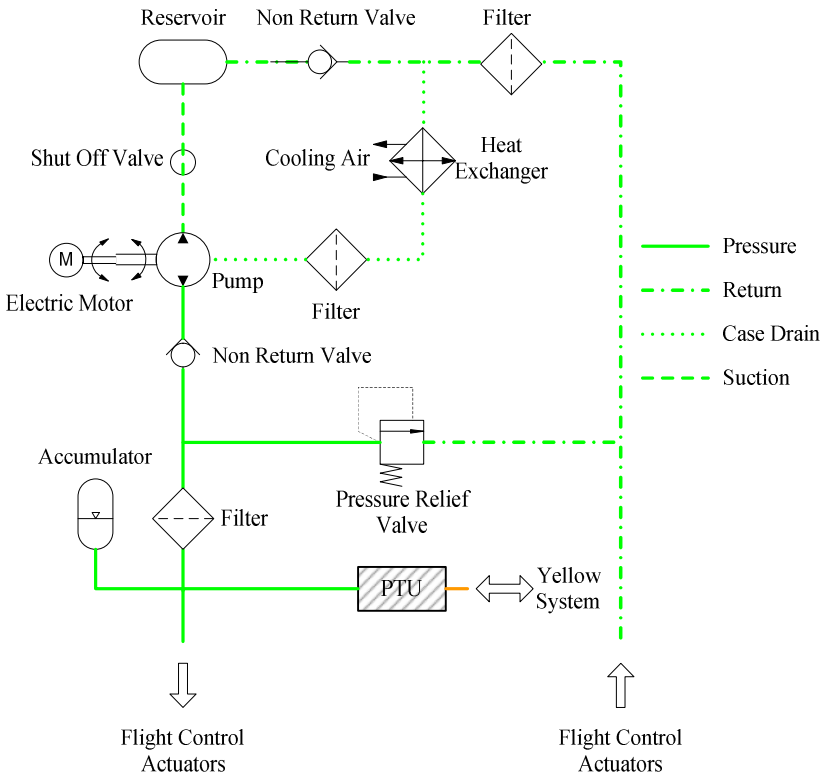

Figure 6-2 Green Localised Hydraulic System Architecture

It should be noticed that in Figure 6-2, the cool source of heat exchanger is cooling air. Because the heat sink is always fuel in conventional centralised hydraulic system. However, for the localised hydraulic systems on the tail unit, they are far from the fuel tanks which are always located on the wing. If the fuel is transferred from wing to the tail unit, pipes will increase the weight and bring on other issues, for instance, safety influence. As a result, cooling air is selected as the cool source to absorb the heat power of localised hydraulic systems. In addition, there is no heat issue of actuators themselves in the variable area actuation system, because hydraulic flow takes the heat power from actuators back the localised hydraulic systems and transfers it to cooling air. The TMS for the variable area actuation system will be described in Section 6.7.

Figure 6-2 presents the architecture of the green localised hydraulic system, while the yellow system is similar to the green system. For the blue system, it has two EMPs and no PTU with the other systems; except these, the architecture of the blue system is same with the green system and the yellow system.

6.3.2 System Pressure

In terms of hydraulic system pressure, high pressure can minimise the hydraulic system size and reduce the system mass. It is proved that when the pressure of a hydraulic system is increased from 3000psi to 5000psi, the volume of system can be reduced by 12.2%, while the mass can get a decrease of 28.3% [33]. Since every pound contributes to the fuel cost and impacts the bottom line for the airlines, high pressure is intended to be used on the localised hydraulic systems.

Since the 1970s, civil aircraft have been relegated to 3000psi hydraulic systems except Concord, which features a 4000psi system [34]. With the development of the Airbus A380 and the Boeing 787, 5000psi hydraulic systems have been realised on commercial aircraft. In military field, 5000psi hydraulic systems have been used on fighters for many years. However, 5000psi is still the highest hydraulic system pressure on aircraft of both civil and military field except some demonstrators.

Since the current material technology can not support 8000psi hydraulic system for engineering application, while 5000psi hydraulic system has been well developed, it is selected as the system pressure for localised hydraulic systems in the variable area actuation system.

6.4 Design Point Analysis

In the EHA, both fluid pressure and flow are variable, it makes the EHA working on demand, the design point of the EHA is therefore the maximum working point. For the FBW actuator, hydraulic system fluid flow is variable while fluid pressure is nearly constant, as described in Chapter 2, the design point is therefore the corner point. By variable area function, which means using large piston area in high speed flight and small piston area in low speed flight, the actuator performance curve can be divided into high speed flight curve (HI Q curve) and low speed flight curve (LO Q curve). The maximum power requirement of each curve is that curve's corner point; selecting the larger one as the design point of whole actuator, the actuator's design point can be reduced, because each of the two curves' corner points is smaller than the corner point of whole curve. To minimise the design point as small as possible, the best point is where the corner points of HI Q curve and LO Q curve are equal. This is the basic theory of the variable area actuator design point sizing.

Figure 6-3 illustrates the elevator performance requirement curve partition.

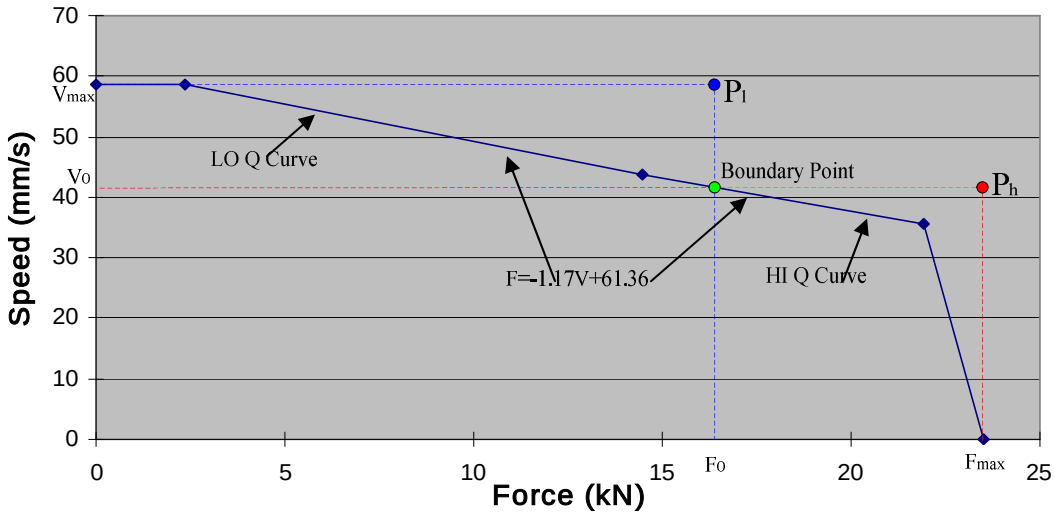

Figure 6-3 Variable Area Elevator Design Point Sizing

In Figure 6-3, the middle skew line can be described:

$$V = -1.17F + 61.36$$

Define F_0 as the force of the boundary point; the actuation speed can be expressed:

$$V_0 = -1.17F_0 + 61.36$$

Then the corner point of HI Q curve is:

$$P_h = F_{\max} \times V_0 = 23.5 \times (-1.17F_0 + 61.36) = -27.5F_0 + 1441.9$$

The corner point of LO Q curve is:

$$P_l = F_0 \times V_{\max} = F_0 \times 58.6 = 58.6F_0$$

Let P_h equal to P_l, the force of the boundary point can be calculated:

$$F_0 = \frac{1441.9}{(58.6 + 27.5)} = 16.7kN$$

Thus the design power of elevator is:

$$P_{d-e} = F_0 \times V_{\max} = 16.7 \times 58.6 = 980.7W$$

Similar to the elevators, the design power of the rudder is calculated, as a result of 3138.9W.

6.5 Power Estimation

6.5.1 Design Power Estimation

As described in Chapter 5, elevators and rudder always act simultaneously; therefore, the power requirements of each hydraulic system can be estimated as the sum of power requirements of each actuator it powered. Based on the variable area actuation system architecture illustrated in Figure 6-1 and the actuator mode (active or stand-by), the power requirement of each hydraulic system is estimated, as shown in Table 6-1.

Table 6-1 Hydraulic System Power

Power source	**Actuator**			**System Power** (W)	
	Name	Mode	Power(W)	Required	Designed
Green system	L inboard elevator	Active	980.7	4119.6	4531.6
	Upper rudder	Active	3138.9		
Blue system	R outboard elevator	Stand-by	0/980.7	3138.9	3452.8
	Lower rudder	Active	3138.9		
	L outboard elevator	Stand-by	0/980.7		
Yellow system	R inboard elevator	Active	980.7	4119.6	4531.6
	Centre rudder	Active	3138.9		
Total	/	/	/	11378.1	12515.9

Similar to the EHA system, a +10% error is taken into account as the sensitivity consideration of power requirement to adjust the design power of the hydraulic systems. Thus the design power of each system is:

$$P_{dp-G} = 1.1 \times P_{p-G} = 1.1 \times 4119.6 = 4531.6W$$

$$P_{dp-B} = 1.1 \times P_{p-B} = 1.1 \times 3138.9 = 3452.8W$$

$$P_{dp-Y} = 1.1 \times P_{p-Y} = 1.1 \times 4119.6 = 4531.6W$$

6.5.2 Average Power Estimation

For the average power of hydraulic system, since the hydraulic pump is variable displacement piston pump, and its displacement is supplied according to the load (power requirement), hydraulic system can also be regarded as working on demand system. According to 5.3.2, the duty cycle of actuator can be estimated by ‘80/20 Rule’. As the power sources of actuators, the average power of hydraulic systems can also be estimated by ‘80/20 Rule’:

$$P_{a-G} = 0.2 \times P_{dp-G} + 0.8 \times 0.2 \times P_{dp-G} = 1631.4W$$

$$P_{a-B} = 0.2 \times P_{dp-B} + 0.8 \times 0.2 \times P_{dp-B} = 1243.0W$$

$$P_{a-Y} = 0.2 \times P_{dp-Y} + 0.8 \times 0.2 \times P_{dp-Y} = 1631.4W$$

6.5.3 Power Consumption Estimation

To estimate the power consumption, system efficiency should be estimated firstly. According to the current technology level, the efficiencies of electric motor and hydraulic pump are 90% and 80%~85% respectively [26, 27]. Compared with the EHA system, there are a lot of hydraulic pipes in the variable area actuation system. Assuming the power loss in hydraulic pipes and components is 5% and taking the average as the efficiency of hydraulic pump, the efficiency of whole variable area actuation system can be estimated:

$$\eta_{VAA} = \eta_m \times \eta_{ahp} \times \eta_p = 0.9 \times \frac{0.8 + 0.85}{2} \times (1 - 0.05) = 70.5\%$$

Then the maximum power consumption of each hydraulic system is:

$$P_{mcon-G} = P_{dp-G} / \eta_{VAA} = 4531.6 / 0.705 = 6424.4W$$

$$P_{mcon-B} = P_{dp-B} / \eta_{VAA} = 3452.8 / 0.705 = 4894.9W$$

$$P_{mcon-Y} = P_{dp-Y} / \eta_{VAA} = 4531.6 / 0.705 = 6424.4W$$

Since the hydraulic systems can be regarded as working on demand system, the average power consumption of each hydraulic system is calculated based on the average system power:

$$P_{acon-G} = P_{a-G} / \eta_{VAA} = 1631.4 / 0.705 = 2312.8W$$

$$P_{acon-B} = P_{a-B} / \eta_{VAA} = 1243 / 0.705 = 1762.2W$$

$$P_{acon-Y} = P_{a-Y} / \eta_{VAA} = 1631.4 / 0.705 = 2312.8W$$

The total average power consumption of the variable area actuation system is therefore 6387.7W.

6.6 Mass Estimation

Similar to the EHA system, the mass of the variable area actuation system is estimated by specific power. The similar aircraft A320 is taken as the reference. According to Reference 16, the power of green, blue and yellow hydraulic system on the A320 is 61.22kW, 8kW and 61.22kW separately, the total mass of hydraulic systems is about 880kg. Then the specific power of hydraulic system is:

$$R_{PM} = \frac{P}{M} = \frac{(61.22 + 8 + 61.22) \times 10^3}{880} = 148.2 W / kg$$

However, on the A320, the hydraulic system pressure is 3000psi. According to the description in 6.3.2, the mass of a hydraulic system can be reduced by 28.3% when the system pressure is increased from 3000psi to 5000psi. Then the specific power of hydraulic system with 5000psi system pressure is:

$$R'_{PM} = \frac{R_{PM}}{1 - 0.283} = \frac{148.2}{0.717} = 206.7 W / kg$$

Thus the mass of each system can be calculated:

$$M_G = \frac{P_{dp-G}}{R'_{PM}} = \frac{4531.6}{206.7} = 21.9 kg$$

$$M_B = \frac{P_{dp-B}}{R'_{PM}} = \frac{3454.8}{206.7} = 16.7 kg$$

$$M_Y = \frac{P_{dp-Y}}{R'_{PM}} = \frac{4531.6}{206.7} = 21.9 kg$$

The total mass of variable area actuation is therefore 60.5kg.

6.7 Thermal Management

6.7.1 Heat Load Estimation

Since heat rejection of a system is the power loss between input and output, the heat load of each system can be calculated based on the power estimated in section 6.5. The results are shown in Table 6-2.

Table 6-2 Heat Rejection of Variable Area Actuation System

System	**Heat Rejection** (W)	
	Peak	**Average**
Green	1892.8	681.4
Blue	1442.3	519.3
Yellow	1892.8	681.4
Total	5227.8	1882.1

6.7.2 Thermal Management System Sizing

Neglecting the heat loss of radiation and convection by pipes and components, all the heat load is dispelled by heat exchanger. As introduced in section 6.3.1, cooling air has been selected as the cool source of TMS for variable area actuation system. In Chapter 5, the power/flow ratio of air-cooled cold plat TMS is estimated as 12.3W/g/s. Then the cooling air requirement of variable area actuation system can be estimated:

$$Q_{ca-G} = \frac{\dot{Q}_{heat-G}}{R_{pf}} = \frac{681.4}{12.3} = 55.3g/s$$

$$Q_{ca-B} = \frac{\dot{Q}_{heat-B}}{R_{pf}} = \frac{519.3}{12.3} = 42.1g/s$$

$$Q_{ca-Y} = \frac{\dot{Q}_{heat-Y}}{R_{pf}} = \frac{681.4}{12.3} = 55.3g/s$$

The total cooling air flow requirement of the variable area actuation system is 152.8g/s.

6.8 Safety Analysis

6.8.1 Failure Analysis

Table 6-3 illustrates the variable area actuation system functions affected by the failure of power sources, electrical systems.

Table 6-3 Variable Area Actuation System Power Source Failure Analysis

System /Surface	Subsystem /Actuator	Electric system failure													
		1	2	3	4	1&2	1&3	1&4	2&3	2&4	3&4	1,2&3	1,2&4	1,3&4	2,3&4
Hydraulic	Green														
	Blue														
	Yellow														
L Elevator	Outboard														
	Inboard														
R Elevator	Inboard														
	Outboard														
Rudder	Upper														
	Centre														
	Lower														
		Full capability availaible					Half capability availaible					Not available			

Case ‘1’ / ‘3’ represents the failure where the electrical system 1 / 3 is lost. In this condition, the respective localised hydraulic system is lost (green / yellow), but the symmetry system (yellow / green) supplies power via PTU to the actuators failed system powered. Thus all the actuators powered by the green and yellow system keep half capability. Case ‘1&2’ / ‘3&4’ represents the failure where both the electrical system 1 and 2, or 3 and 4 are lost. In this condition, the normal system of green and yellow supplies power to the users of both systems, the actuators are therefore half capability available, while blue system is powered by two EMPs, which keep actuators full capability. For the case ‘1&3’ / ‘2&4’ which represents that both the electrical system 1 and 3, or 2 and 4 are failure, the respective hydraulic system of green and yellow, or blue system is lost. In either of each condition, there is at least on actuator in each control surface is full capacity available. In three electrical systems failure condition, such as case ‘1&2&3’ or ’2&3&4’, each control surface still can be controlled (case ‘2&3&4’ only half capability available).

6.8.2 Reliability and Redundancy

Compared with the conventional FBW actuation system, the main differences in the variable area actuation system are that it uses localised hydraulic systems as power generations and the actuators are variable area actuators. For the localised hydraulic systems, as described in section 6.2 and 6.3, they are similar to the conventional centralised hydraulic systems. Furthermore, localised hydraulic systems only supply power to the actuators located on the tail unit, while centralised hydraulic systems power all the actuators of FCS and other utility actuation systems, such as landing gear extension and retraction and anti-skid brake system. Every actuation system's failure influences the reliability of the centralised hydraulic system it connects. From this point of view, the reliability of localised hydraulic system is higher than that of the centralised hydraulic system. In terms of variable area actuator which is still one kind of FBW actuator, the reliability of it should be on the same level with the conventional FBW actuators. For the other parts of the variable area actuation, it is same with those of the conventional FBW actuation. From these points analysed above, the reliability of the variable area actuation system should be no lower than that of the conventional FBW actuation system.

More accurate reliability assessments of the variable area actuation system are achieved using dependency block diagrams. The results show the failure rates of pitch control (elevators) and yaw control (rudder) are 3.51×10^{-10} /FH and 1.25×10^{-10} /FH respectively. Both of them are smaller than the 'Extremely Improbable' (10^{-9} /FH), which means that the variable area actuation system designed for the Flying Crane tail unit can satisfy the safety requirements of FAR/CS25. For details of the reliability estimation, see Appendix D.

In terms of the redundancy, the variable area actuation system has '4E' power sources, which is same with the EHA system. And three localised hydraulic systems are employed as the power generations. Compared with the '3H/2E' architecture of the conventional FBW actuation, there are also three channels power are provided in the variable area actuation system. In addition, the actuator numbers of the variable area

actuation system are same with that of the conventional FBW actuation. Therefore, from view of power sources and actuator numbers, the redundancy of variable area actuation system is same with the convention FBW actuation system. Moreover, similar to the EHA system, the all electric distribution of power sources provides easier failure isolation and reconfiguration capability. This increases the redundancy of the variable area actuation system.

6.9 Summary

This chapter has discussed the variable area actuation system design for the tail unit on the Flying Crane. System architecture was designed by comparing with the conventional FBW actuation system, then the localised hydraulic system architecture and pressure are analysed. After that, the design points of variable area actuators are sized based on the performance requirement curves, followed by the system sizing including power, mass and TMS. At last, the safety issues in terms of power sources failure condition, reliability and redundancy were analysed.

The performance and safety of the variable area actuation system described in this Chapter show that the system is feasible for actuating the flight control surfaces on the Flying Crane tail unit.

7 Comparison and Discussion

7.1 Introduction

Chapter 5 and 6 described the designs of the EHA system and the variable area actuation system, and it was suggested that both of them are technically feasible for the application on the Flying Crane tail unit. This Chapter serves to assess and compare these two actuation systems, and discusses the advantages and disadvantages of each system.

As a reference for the comparison and discussion, a conventional FBW actuation system is sized firstly. Then the EHA system and the variable area actuation system are compared and discussed from a broader perspective including fuel penalty, safety, maintenance and installation, cost, risk and certification. A summary is given at the end of the Chapter.

7.2 Parameters and Reference

As discussed in Chapter 2, FBW actuation technology is the most popular actuation technology on the current aircraft, while EHA and variable area actuation technology are better solutions towards the future. In order to compare the EHA system and the variable area actuation system, conventional FBW actuation system is taken as a reference.

Based on the requirements analysed in Chapter 4, a conventional FBW actuation system powered by centralised hydraulic systems is sized, as presented in Appendix E.

Table 7-1 shows the parameters of the EHA system, the variable area actuation system and the conventional FBW actuation system.

Table 7-1 System Parameters

	Average power consumption (W)	**System mass** (kg)	**Cooling air requirement** (g/s)
EHA	4842.0	62.9	101.2
Variable area actuation	6387.7	60.5	152.8
FBW Actuation	8969.3	85.0	0

It should be noticed that the conventional FBW actuation system is powered by centralised hydraulic systems, where fuel is used as the heat sink for thermal management. As a result, the cooling air requirement of conventional FBW actuation system is zero.

7.3 System Fuel Penalty

The existing airframe systems on the aircraft are for specific functions, as the EHA system and the variable area actuation system are designed for actuating the flight control surfaces. However, airframe systems have a very significant effect on the overall aircraft performance. To realise the respective system functions and requirements, systems cause penalties in aircraft fuel consumption directly, due to the following three factors [35]:

a. System power off-take requirements (shaft power and/or bleed);
b. System weight;
c. System resultant direct aircraft drag increases.

The system fuel penalties can be regarded as the systems costs on the aircraft level in terms of system power, mass and drag. Based on the methods introduced by Reference 35, the fuel penalties of the EHA system, the variable area actuation system and the conventional FBW actuation system are calculated. The results are presented in Table 7-2 (see Appendix F for details).

Table 7-2 System Fuel Penalty

	Power penalty	Mass penalty	Drag penalty	Total
EHA	15.4	92.0	59.2	166.6
Variable area actuation	20.3	88.5	89.3	198.1
FBW actuation	19.9	124.4	0	144.3

Unit: N

The fuel penalties constitution for each system is shown in Figure 7-1.

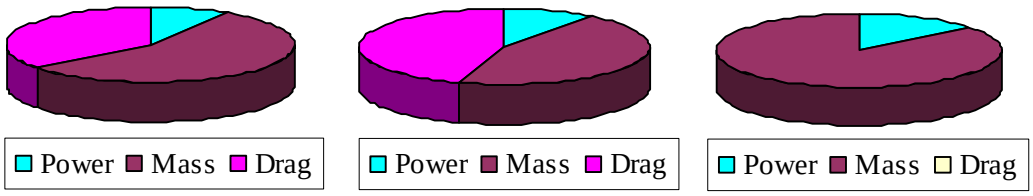

(a) (b) (c)

Figure 7-1 System Fuel Penalties Constitution

Pie chart (a) presents the fuel penalties constitution for the EHA system. The mass penalty occupies the largest percentage, followed by the drag penalty, while the power penalty takes the smallest percentage. It can be seen that in the EHA system, the most important influence factors of system fuel penalties are mass and drag, while the influence of power off-take is small.

Pie chart (b) illustrates the fuel penalties constitution for the variable area actuation system. Similar to the EHA system, the mass penalty takes the largest percentage; the power penalty occupies the smallest. The system fuel penalties of the variable area actuation system are mainly caused by mass and drag.

The fuel penalties constitution for the conventional FBW actuation system is presented by pie chart (c). The mass penalty also occupies the largest percentage, and the power penalty takes a small piece, while the drag penalty is zero because the conventional

FBW actuation system does not need cooling air and there is no aircraft drag increase. The main fuel penalty of this system is caused by mass.

In terms of the fuel penalties difference among different systems, it is surprising to find that the fuel penalty of the variable area actuation system powered by localised hydraulic systems is the largest, followed by the EHA system, while the fuel penalty of conventional FBW actuation system is the smallest. The reason is that cooling air is required to cool both of the EHA system and the variable area actuation system, which increases the direct aircraft drag and causes drag penalty.

The power off-take penalties of all these three systems are quite close, and the EHA system is slightly smaller than the other two systems, because the EHA system is a totally working on demand system, this leads to less power consumption. Comparing the variable area actuation system with the conventional FBW actuation system, results show that although the former's power consumption is lower than the latter's, the power off-take penalty of it is larger. The reason of this phenomenon is that localised hydraulic systems, the power sources of the variable area actuation system, are powered by the electrical systems, and there is power loss due to the efficiency of electrical system. While centralised hydraulic systems, the power sources of the FBW actuation system, take shaft power directly from engines. The power transfer means in the EHA system and the variable area actuation system is from shaft power to electrical power, and to hydraulic power, then to actuator mechanic power. It is from shaft power to hydraulic power, then to actuator mechanic power in the conventional FBW actuation system. The additional power conversion in the EHA system and the variable area actuation system increases the power off-take penalties.

On the mass penalty, the conventional FBW actuation system is the largest, while the EHA system and the variable area actuation system are much smaller. For the EHA system, the working on demand factor reduces its power design point, thus reduces the system mass. Regarding the variable area actuation system, it is mainly due to two aspects, one is that the variable area function reduces the power design point of system;

the other is that the 5000 psi system pressure of hydraulic system increases the system power/mass ratio.

For the drag penalty, there is no drag penalty in the conventional FBW actuation system because it does not need cooling air. However, the drag penalty of the variable area actuation system is larger than that of the EHA system, because the system efficiencies in both systems are close, but in power design point, the former system is larger than the latter.

The differences of fuel penalties among these three systems are illustrated in Figure 7-2.

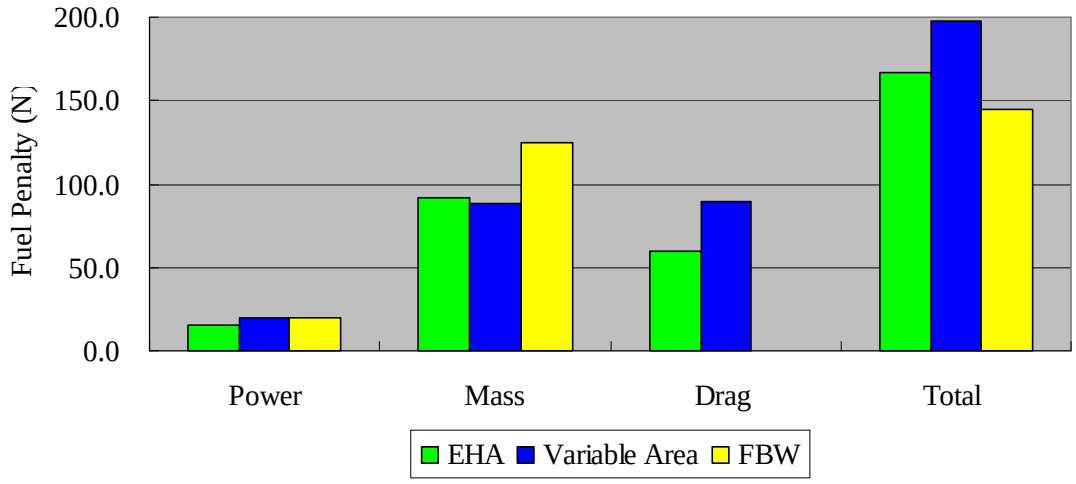

Figure 7-2 Comparison of System Fuel Penalties

From the analysis and discussions above we can see, in terms of the power consumption and system mass, the EHA system is quite efficient due to the working on demand factor in it. However, the cooling air requirement in EHA system results in an increase of both aircraft drag and system fuel penalty. Similar to the EHA system, the variable area actuation system is also efficient in system mass reduction due to the variable area factor; while the cooling air requirement causes drag penalty increase. Therefore, from fuel penalty reduction point of view, the main drawback of the EHA system and the variable area actuation system is the cooling air requirement.

If we match different actuation systems with different power sources, the fuel penalties are changed, as shown in Table 7-3.

Table 7-3 System Fuel Penalty with Different Match

	EPS	Localised hydraulic	Centralised hydraulic
EHA	166.6	/	/
Variable area actuation	/	198.1	102.7
FBW actuation	/	278.2	144.3

Unit: N

In Table 7-3, the variable area actuation system powered by centralised hydraulic systems takes the smallest fuel penalty among all the different matches. Compared with the FBW actuation system, there is 28.8% fuel penalty reduction in the variable area actuation system.

If the TMS for the EHA system and localised hydraulic system can be solved without drag increase, the fuel penalties of each system are also changed, as presented in Table 7-4.

Table 7-4 System Fuel Penalty without Drag

	EPS	Localised hydraulic	Centralised hydraulic
EHA	107.4	/	/
Variable area actuation	/	108.8	102.7
FBW actuation	/	152.8	144.3

Unit: N

It can be seen from Table 7-4 that the fuel penalties of the EHA system and the variable area actuation system are quite close, and it can be reduced a lot if there is no aircraft drag increases caused by system thermal management.

Generally speaking, the variable area actuation system powered by centralised hydraulic systems is the best solution for FCSs on civil aircraft in terms of fuel penalties reduction. If the TMS can be solved without drag increase, both the EHA system and the variable area actuation system are also good solutions from this point of view.

7.4 Safety

Safety is affected by the power sources, system reliability and system characteristics.

The power sources failure analysis of the EHA system and the variable area system have been completed in Section 5.6.1 and 6.8.1, as shown in Table 5-1 and Table 6-3. In one electrical system failure condition, for the EHA system, there is at least one actuator is full capability available in each control surface. While for the variable area actuation system, all the actuators are available with some of them only in half capability. In two electrical systems failure condition, both actuation systems can provide control ability for each control surface. In three electrical systems failure condition, the EHA system loses at least one control surface, while for the variable area actuation system, all the control surfaces can be controlled with some of them are half capability available. From power sources failure influence point of view, the survivability of the variable area actuation system is higher than that of the EHA system.

In terms of reliability, which has been estimated in Appendix C and D, the failure rate of the EHA system is estimated as 1.00×10^{-9}/FH and 1.25×10^{-10}/FH for pitch control (elevators) and yaw control (rudder) respectively; while for variable area actuation system, it is separately estimated as 3.51×10^{-10}/FH and 1.25×10^{-10}/FH. It can be seen that the reliability of the variable area actuation system is higher than that of the EHA system. In addition, there is a hypothesis in the EHA system that the failure rate of EHA can reach the level to be no more than 2.20×10^{-5}/FH.

For system characteristics, all the three systems contain hydraulic fluid. However, the EHA system is self-contained which results in a very small hazard of fluid leakage. The

other two systems have pipes, but the localised hydraulic systems only have pipes in specific space, while pipes exit all over the aircraft in the centralised hydraulic systems, which leads to the higher leakage hazard. Furthermore, due to the electrical power distribution, the EHA system and the variable area actuation system can realise failure isolation and system reconfiguration easily. Hence the higher fault tolerances, which increase the systems' safety.

7.5 Maintenance and Installation

As one kind of PBW actuation system, the EHA system has a lot of advantages in maintenance. Firstly, the introduction of electric circuits removes the hydraulic system pipes, which always causes maintenance work due to hydraulic fluid leakage. And all the components are concentrated on one actuator package. As a result, the accesses requirements for maintenance work are reduced. Secondly, the PHM system is applied to the EHA system easily since electrical power can be easily monitored and managed. Through Build-In-Test (BIT) and fault diagnostic, system faults can be detected, and the potential failures can be predicted, then in-advanced maintenance is realised. By fault analysis and fault location, failure components can be accurately located, and the maintenance time is shortened. In addition, the expert system in PHM system has the ability to judge which kind of maintenance work is critical, and which kind can be delayed. As a result, the work schedule for maintenance is arranged [36]. At last, the scale of maintenance equipments and engineers is reduced due to the cancellation of hydraulic circuits.

The variable area actuation system has hydraulic circuits, which are localised and powered by electrical systems. This configuration is similar to the EHA system. Therefore, these two systems share some similar advantages. In addition, although they are still hydraulic circuits, the localised hydraulic systems exist in specific space rather than all over the aircraft in the centralised hydraulic systems. Hence the possibility of leakage and following maintenance work in the variable area actuation system is lower than that of the conventional FBW actuation system. Furthermore, the PHM system can also be introduced to the variable area actuation system to reduce maintenance work and

realise in-advanced maintenance. However, the localised hydraulic systems increase the amount of hydraulic circuits, which causes the increase of the maintenance work and the increase of the load of PHM system.

In terms of installation, the actuators of the conventional FBW actuation system are installed on the control surfaces, while most of the components of the centralised hydraulic systems are located near engines. The connection pipes between the power sources and actuators are always long ones, this causes some installation issues. For the variable area actuation system, the actuators are also located on the control surfaces, while the localised hydraulic systems are installed in the same area. Hence the much shorter hydraulic pipes are required. Although electrical lines are required to power the localised hydraulic systems, its installation is not as critical as that of the hydraulic pipes which must consider issues such as pulsation and leakage. Different from the systems analysed above, the EHA system totally cancels hydraulic pipes, and all its components are concentrated on one package. This leads to easy installation without pipes issues. However, the size of the whole EHA package is much greater than any conventional hydraulic components or FBW actuators, and installation of such a big package on the control surface is a big problem because the space near control surface is limited.

7.6 Cost

The cost of aircraft can be divided into two parts, i.e. product cost and operating cost. The former consists of in-house production and subcontractor cost which occupies 66% and in-house assembly cost which takes the remaining 34% [37]. From system level of view, in-house production and subcontractor cost is spent on outside production and purchased equipments, while in-house assembly cost is used for integrating the various major components and subassemblies into a complete aircraft ready to be delivered. The cost of outside production and purchased equipments always depends on technology difficulty, quantity and material. In these three aspects, the quantity of all the three actuation systems designed or sized in this case study are the same, and the material is similar. Regarding technology difficulties, the conventional FBW actuation system is

the most mature technology while the EHA system is the most advanced. As a result, the outside production and purchased equipments cost of the EHA system is the highest, followed by the variable area actuation system, while the conventional FBW actuation system is the lowest. The in-house assembly includes all minor assembly, half of installation and checkout and half of quality control from system level of view [37]. The quality control in all the three actuation systems is the same. Regarding installation, as discussed in Section7.5, the conventional FBW actuation system is the most complex system, followed by the variable area actuation system and the EHA system.

Different from the system product cost which only takes a small piece in the whole aircraft level [37], system operating cost produces huge influences on the operating cost of the whole aircraft, because systems bring on most of the maintenance work for the aircraft. The system operating cost can be analysed in the following aspects: fuel penalty, maintenance and life-cycle. Fuel means direct cost of airliners. System fuel penalties of all these three actuation systems were analysed in Section 7.3, which proved that the variable area actuation system powered by centralised hydraulic systems is the best one. Maintenance cost is one of the largest parts of cost for airliners. Reducing maintenance work means reducing requirements of support equipments and engineers, which leads to save money. The maintenance of these three actuation systems was discussed in Section 7.6, which proved that the EHA system is better than the other two systems. Life-cycle always depends on the reliability [38]. The more reliable a system is, the lower life-cycle cost the system has. From this point of view, the variable area actuation system and the conventional FBW actuation system are better than the EHA system.

7.7 Risk

The risks of developing a system are caused by uncertainties, which include statistical uncertainties due to limited data and limited knowledge and technology uncertainties. For the risk associated with a new system, it is based largely on the experience with similar systems and the technologies that are used to develop the new system [39].

For the three actuation systems developed in this case study, statistical uncertainties exist in all of them, because the design requirements of the three systems are analysed with uncertainties, as described in Chapter 4. In terms of technology uncertainties, the conventional FBW actuation system is mature and well developed, thus there is no technology uncertainty in it. Regarding the variable area actuation system, there are technology uncertainties. However, as a kind of FBW actuation, the variable area actuation system has plenty of experiences with the similar FBW actuation system. Therefore the technology uncertainties of the variable area actuation system are limited. For the EHA system, although it has been used on the F-35 and the A380, it is still under development. And there are a lot of unsolved problems, such as thermal management and reliability. In this case study, the failure rate of a simplex EHA is expected to be no more than 2.20×10^{-5}/FH, which is not confirmed. The technology uncertainties of the EHA system are serious, therefore the higher risk of the EHA system than the other two systems.

7.8 Certification

The process of certification for a civil aircraft is proved to be expensive, lengthy and inflexible, the cost is huge. Reference 40 suggests six basic rules for the Federal Aviation Administration (FAA) certification of electronic system, as shown below:

Rule 1: Know the Regulations (and Guidance)

Rule 2: Know the FAA organizations

Rule 3: Know the Industry Standards

Rule 4: Know the Issues

Rule 5: Plan for Certification in Advance

Rule 6: Maintain a Relationship with the FAA

It seems that these six basic rules are also applicable for the actuation systems. However, Rule 1, 2, 5 and 6 are not in the category of technology, so they are not taken into consideration in this case study.

In terms of Rule 3, standards are the media wherein industry and the airworthiness regulation organizations reach agreement on the safety issues related to systems and equipments [40]. As a mature system, the conventional FBW actuation system has complete standards. Although the variable area actuation system has unwell-known technology, it still belongs to FBW category and has a lot of standards as references. For the EHA system, both the technologies and standards are under development. Therefore from industry standards point of view, the conventional FBW actuation system is the best, followed by the variable area actuation system, while the EHA is the last one.

Regarding Rule 4, the issues of developing an airborne system or equipment include software, high intensity radiated field and lighting, and complexity [40]. For actuation systems, complexity is the main issue. As discussed in Chapter 2, the conventional FBW actuation system is better than the other two systems in terms of system complexity.

For the certification itself, reliability and redundancy are the key factors. It terms of those, the conventional FBW actuation system and the variable area actuation system are better than the EHA system.

In general, the conventional FBW actuation system is the easiest system to be certificated, followed by the variable area actuation system, while the EHA system is the hardest one.

7.9 Summary

This chapter has compared the EHA system with the variable area actuation system in system fuel penalty, safety, maintenance and installation, cost, risk and certification, with a conventional FBW actuation system as the reference. All aspects of each system were analysed and discussed. Table 7-5 summarizes the major advantages and disadvantages of each system.

Table 7-5 Comparison of Case Study Actuation Systems

	EHA	Variable area actuation	FBW actuation
Fuel penalty	☆	○	☆
Safety	○	★	★
Maintenance	★	☆	○
Installation	☆	☆	○
Cost	☆	☆	☆
Risk	○	☆	★
Certification	○	☆	★

Note: ★-good; ☆-normal; ○-bad.

However, the results are not as expected, especially one of the most important factors, the fuel penalty. The working on demand factor of the EHA system makes the system's power off-take penalty and the mass penalty very efficient. On the other hand, the drag penalty increases the total penalties due to cooling air requirement. This situation also happens on the variable area actuation system, its variable area function makes the system quite efficient in mass reduction, but the drag penalty goes the opposite way to the total fuel penalties.

Using mature technology, the conventional FBW actuation system has good characters on safety, risk and certification, bad characters on maintenance and installation, while its fuel penalty and cost are common. For the variable area actuation system, it is quite balanced in all aspects, except its fuel penalty is not good due to the drag issue caused by the localised hydraulic systems' thermal management. Regarding the EHA system, the maintenance of it is good because the PBW system is easy to realise PHM. However, as an under development technology, the EHA system has problems in terms of safety, risk and certification.

8 Conclusion

8.1 Conclusion

This project carried out the studies of actuation technology for the FCS on civil aircraft. An EHA system and a variable area actuation system were designed and sized for the tail unit of the Flying Crane. The results show that the two actuation technologies are both feasible for the FCS on civil aircraft.

The EHA system is quite efficient on power consumption and mass reduction due to the working on demand factor. It is also good at maintenance since the PHM system is easy to be realised. However, the thermal management of the system may result in an increase in aircraft drag; and the reliability of EHA needs to be improved to reduce the cost, risk and the difficulties to obtain certification.

For the variable area actuation system, the piston area variable function significantly reduces the system design point and size. This therefore leads to the reduction of system fuel penalty by 28.8% in this case study.

Localised hydraulic systems seem attractive for the tail unit of aircraft. However, an additional power conversion causes more power consumption, and the thermal management of the system may result in an aircraft drag increase.

Variable area actuation system powered by centralised hydraulic systems is deemed the best solution for the FCS on civil aircraft, and it is therefore suggested to be used on the Flying Crane. This actuation system takes advantages of both variable area actuators which can reduce the size of system and centralised hydraulic systems which do not cause aircraft drag increases. In addition, based on the current technology level, the safety, cost, risk and certification issues of variable area actuation systems powered by centralised hydraulic systems are more acceptable than those of the EHA system.

Towards the MEA and AEA in the future, variable area actuation system powered by localised hydraulic systems is suggested as the first step. This takes advantage of the FBW actuation, and moreover it is powered by the electrical systems instead of centralised hydraulic systems. With the development of EHA technology, the variable area actuation system would be replaced by the EHA systems directly, because both systems have the similar interfaces to other systems including power configurations and control means. Finally, EHA systems could be replaced by the EMAs when the EMA technology is mature enough.

Limited by the time and availability of data, some details, such as the influence of an accumulator which can reduce the design point of hydraulic system and the heat loss of radiation in sizing the TMS, were neglected. Many of the calculations were based on assumption and comparison with the similar aircraft. This means that the case study actuation system designs may not accurately represent the hardware that would be required for the case study aircraft. If more data was available and physical testing of the actuation system was possible, the numerical results could be improved. Furthermore, simulations will also be required to ultimately determine which system offers the best actuation solution for the case study aircraft.

8.2 Contributions

An EHA system was designed for the primary FCS on the case study aircraft. The results show that EHA is feasible for the FCS on civil aircraft, and is helpful to reduce the actuation system power consumption and system mass.

The variable area actuation technology demonstrated that it is suitable for the flight control actuation system on civil aircraft. It can significantly reduce the actuation system design point and system size. This technology is also feasible for the actuation system in other fields, such as engineering machinery and ships.

Localised hydraulic system had been proved not as efficient as centralised hydraulic system due to the additional power conversion and thermal management, but it is

valuable to be further studied since it can be regarded as the interim option between FBW actuation and PWB actuation.

Through comparison of actuation technologies, an actuation system solution for the FCS on the Flying Crane and civil aircraft was recommended. A suggested strategy for the actuation system for next generation MEA/ AEA was produced.

Ultimately, the gaps for future work, such as the reliability of EHA and the TMS for EHA system and localised hydraulic system, have been indentified.

8.3 Recommendations for Future Work

The work carried out in this project has demonstrated that the EHA system and the variable area actuation system are both feasible for FCS in civil aircraft applications. However, before the final recommendations are given, further studies are required to indentify the most appropriate actuation technology for FCS on civil aircraft. Suggestions are described below of suitable areas of further study, as well as how improvement could be made to the work done in this project.

Firstly, the accuracy of the case study work can be improved if more data became available. For example, the requirement can be checked and validated with the Flying Crane's further development, especially after the preliminary design.

Secondly, further work is required to study methods of improving the reliability of EHA. This could lead to the reduction of EHA system cost and risk, increase the system safety, and make system certification easier to obtain.

Thirdly, it is attractive to study the TMS for EHA and localised hydraulic systems. Although there have been some TMS concepts for PBW actuation systems, most of them need cooling air, which causes an increase in aircraft drag and hence higher fuel consumption. It is expected that some other kinds of TMS with more efficiency in fuel penalties could be developed.

Fourthly, the application of piston area variable in EHA would be an interesting study. Variable area actuation technology has been proved to be quite efficient in system design point and system size reduction, while EHA is efficient in power consumption. It is expected that the integration of these two technologies can take advantage of both of them, and the performance and efficiency of EHA could therefore be further improved.

Fifthly, simulations of EHA systems and variable area actuation systems will be useful to compare the performance of the two systems and determine which system offers the better solution for the case study aircraft.

Finally, an investigation into control laws for variable area actuation is also needed to enable a complete actuation system control loops. The work should include the study of the relationship between flight condition and control surface actuation loads, and developing the control laws for piston area changes.

REFERENCES

1. AVIC I MSc Programme Aircraft Group. (2008), *Flying Crane Specification (Group Design Project report)*, Cranfield University, Cranfield, UK.

2. RUBERTUS, D. P., HUNTER, L. D. and CECERE, G. J. (1984), "*Electromechanical actuation technology for the all-electric aircraft*", vol. AES-20, pp. 243-249.

3. Raymond, E.T. and Chenoweth, C.C., (1993), *Aircraft flight control actuation system design* [Book], Warrendale, PA: Society of Automotive Engineers, Inc.

4. Charrier, J. and Kulshreshtha, A. (2007), "*Electric Actuation For Flight & Engine Control System: Evolution, Current Trends & Future Challenges*", 45th AIAA Aerospace Sciences Meeting and Exhibit, vol. AIAA Paper 2007-1391.

5. VIETEN, K. W. (1992), "*High-performance fighter fly-by-wire flight control actuation system [for YF-23A prototype]*", AIAA, Aerospace Design Conference, Irvine, CA; UNITED STATES; 3-6 Feb. 1992, Vol. AIAA Paper 1992-1123, .

6. HAYRE, A., DULL, T. O. M. and MEYN, F. (1992), "*The ATF YF-23 Vehicle Management System*", AIAA, Aerospace Design Conference, Irvine, CA; UNITED STATES; 3-6 Feb. 1992, Vol. AIAA Paper 1992-1076, .

7. Botten, S. L., Whitley, C. R. and King, A. D. (2000), "*Flight Control Actuation Technology for Next-Generation All-Electric Aircraft* ", Technology Review Journal-Millennium Issue·Fall/Winter 2000, pp. 55-68.

8. Dodds, G. M. (2004), "*MEA-TIMES SYSTEM ARCHITECTURE*", Royal Aeronautical Society (RAeS), More-Electric Aircraft Conference, 27-28 Apr. 2004, Hamilton Place, London, United Kingdom, .

9. Pointon, J. M., (2007), *Thermal Management of Electromechanical Actuation on an All-Electric Aircraft(MSc thesis)*, Cranfield University, Cranfield, UK.

10. Xue Longxian (2008), *Conceptual Design of a 130-Seat Civil Airliner Flying Crane- Mass Estimation, Centre of Gravity Calculation and Systems Analysis (GDP Report)*. Cranfield University, Cranfield, UK.

11. Moir, I. and Seabridge, A., (2008), *Aircraft systems - Mechanical, electrical, and avionics subsystems integration*, 3rd ed., in UNITED KINGDOM, Chichester, United Kingdom and New York: John Wiley & Sons Ltd.

12. ATG Ltd. (19--), *Airbus A320 Training Notes: Vol. 1*, Aeronautical Training Group (ATG) Ltd.

13. Great Lakes Airline Pictures Website (2008), available at: http://pictures.readytocopy.com/displayimage.php?pid=857&fullsize=1 (accessed 17 November 2008)

14. SAE International (2001), *Description of Actuation Systems for Aircraft with Fly-By-Wire Flight Control Systems*, Aeronautical Information Report AIR4253, Society of Automotive Engineers (SAE), Warrendale, PA, USA 51

15. Ravenscroft, S. (1999), "*Actuation systems*", In *FLIGHT CONTROL SYSTEMS-practical issues in design and implementation* (Ed. Roger W. Pratt), United Kingdom: The Institute of Electrical Engineers.

16. Bataille, N. (2006), *Electrically Powered Control Surface Actuation (MSc thesis)*, Cranfield University, Cranfield, UK.

17. Trosen, D. W. and Cannon, B. J. (1996), "*Electric actuation and control system*", IECEC 96; Proceedings of the 31st Intersociety Energy Conversion Engineering Conference, Washington, DC; UNITED STATES; 11-16 Aug. 1996, Piscataway, NJ: Institute of Electrical and Electronics Engineers, .

18. Aten, M., Whitley, C., Towers, G., Wheeler, P., Clare, J., Bradley, K., (2004), "*Dynamic performance of a matrix converter driven electro-mechanical actuator for an aircraft rudder*", Power Electronics, Machines and Drives, 2004. (PEMD 2004). Second International Conference on (Conf. Publ. No. 498) Volume 1, 31 March-2 April 2004 Page(s):326 - 331 Vol.1.

19. Montero Yanez, J. S. (1996), "*All electric aircraft flight control actuation (ELAC)*", In *Advanced in Onboard System Technology* (Ed. A. Del Core), in UNITED KINGDOM, Chichester, United Kingdom and New York: John Wiley & Sons.

20. Van den Bossche, D. (2004), "*More Electric Control Surface Actuation: A Standard for the Next Generation of Transport Aircraft*", Royal Aeronautical Society (RAeS), More-Electric Aircraft Conference, 27-28 Apr. 2004, Hamilton Place, London, United Kingdom, .

21. European Aviation Safety Agency (2005/06), *Certification Specifications For Large Aeroplanes*, CS-25, European Aviation Safety Agency (EASA)

22. Federal Aviation Administration, *Federal Aviation Regulation*, FAR, Federal Aviation Administration (FAA), Washington.

23. Xavier Le tron (2007), *A380 Flight Controls Overview* (presentation notes), 27th September 2007, Hamburg University of Applied Sciences, Hamburg, German.

24. Bland, T. J. and Funke, K. D. (1992), "*Advanced Cooling for High Power Electric Actuators*", SAE, Aerospace Atlantic Conference, Dayton, OH; USA; 7-10 Apr. 1992, SAE 921022, Society of Automotive Engineers (SAE), Warrendale, PA, USA

25. Schneider, M. G., Thomson, S. M., Bland, T. J. and Yerkes, K. L. (1994), *Test Results of Reflux-Cooled Electromechanical Actuator*, SAE 942176, Society of Automotive Engineers (SAE), Warrendale, PA, USA

26. Eaton Corporation Website (2008), available at: http://www.aerospace.eaton.com (accessed 6 November 2008)

27. GE Aviation Systems Website (2008), available at: http://www.geaviationsystems.com (accessed 8 November 2008)

28. Parker Aerospace Website (2008). available at: http://www.parker.com (accessed 10 November 2008)

29. Goodrich Corporation Website (2008), available at: http://www.goodrich.com (accessed 12 November 2008)

30. SAE International (2002), *Hydraulic Systems, Aircraft, Design and Installation, Requirements for*, SAE-AS5440, Society of Automotive Engineers (SAE), Warrendale, PA, USA 51

31. Edward Pomfrett, Jason Yon. (2006), *CARACAL Systems-Section 2 (Group Design Project report)*, University of Bristol, Bristol, UK.

32. NEESE, W. (1991), *Aircraft Hydraulic Systems* (3rd revised and enlarged edition) [Book], Krieger, Malabar FL.

33. Wang Zhanlin, etc. (2004), *Aircraft High Pressure Hydraulic Power Systems* [Book], BeiJingHangKongHangTianDaXueChuBanShe, Beijing, China.

34. Heney, P. J.(2002), *A380 pushes 5000 psi into realm of the common man*, Hydraulics & Pneumatics, December 2002.

35. Lawson, C. P., *Analysis of the Fuel Penalties of Airframe Systems (lecture notes)*, AVD 0503, Cranfield University, Cranfield, UK.

36. Brown, E. R., McCollom, N. N., Moore, E. E., Hess, A. (2007), *"Prognostics and Health Management- A Data-Driven Approach to Supporting the F-35 Lighting II"*, New York: Institute of Electrical and Electronics Engineers, Inc., .

37. BELTRAMO, M. N., TRAPP, D. L., KIMOTO, B. W., MARSH, D. P. and Science Applications, Inc., Los Angeles, CA. Economic Analysis Div (1977), *Parametric study of transport aircraft systems cost and weight*, NASA-CR-151970; Pagination 288P.

38. Harrison, L. H. and Saraceni, P. J.,Jr (1994), *"Certification issues for complex digital hardware"*, AIAA/IEEE Digital Avionics Systems Conference, 13th, Phoenix, AZ, Proceedings; UNITED STATES; Oct. 30-Nov. 3 1994, New York:

Institute of Electrical and Electronics Engineers, Inc., .

39. Pettit, C. L. and Veley, D. E. (2003), *"Risk Allocation Issues for Systems Engineering of Airframes"*; Uncertainty Modelling and Analysis, IEEE 2003. ISUMA 2003. Fourth International Symposium on 24-24 Sept. 2003 Page(s):232 – 240.

40. Keller, F. L. (1992), *"Basic electronic systems certification [for airborne applications]*", IEEE/AIAA Digital Avionics Systems Conference, 11th, Seattle, WA, Proceedings; UNITED STATES; 5-8 Oct. 1992, New York: Institute of Electrical and Electronics Engineers, Inc., .

41. Maydew, M. (2002), *Advanced Actuation Systems for the More Electric Aircraft (PhD thesis)*, Cranfield University, Cranfield, UK

42. Sadeghi, T and Motamed, F. (1992), *"Evaluation and Comparison of Triple and Quadruple Flight Control Architecture"*, Aerospace and Electronic Systems Magazine, IEEE. Volume 7, Issue 3, Part 1, March 1992 Page(s):20 - 31.

43. Lawson, C. P., *Calculation of the Fuel Penalties of Airframe Systems (lecture notes)*, AVD 0504, Cranfield University, Cranfield, UK.

44. Aerospaceweb Website (2008), *Atmosphere Data*, available at: http://www.aerospaceweb.org/design/scripts/atmosphere (accessed 5 December 2008)

BIBLIOGRAPHY

1. Atallah, K., Caparrelli, F., Bingham, C.M. etc.(1999), "*Comparison of electrical drive technologies for aircraft flight control surface actuation*" Electrical Machines and Drives, 1999. Ninth International Conference on (Conf. Publ. No. 468), 1-3 Sept. 1999, pp. 159-163.

2. BAKER, R., PITTS, F. E. L. I. X. L.,eds and National Aeronautics and Space Administration. Langley Research Center, Hampton, VA. (1992), "*Fly-By-Light/Power-By-Wire Requirements and Technology Workshop*", vol. NASA-CP-10108; NAS 1.55:10108.

3. Bauer, C., Lagadec, K., Bes, C. and Mongeau, M. (2007), "*Flight Control System Architecture Optimization for Fly-By-Wire Airliners*", vol. 30, no. 4, pp. 1023-1029.

4. Belcastro, C. M. and Belcastro, C. M. (2001), "*Application of failure detection, identification, and accommodation methods for improved aircraft safety*", 2001 American Control Conference, Arlington, VA; UNITED STATES; 25-27 June 2001, Piscataway, NJ: Institute of Electrical and Electronics Engineers, .

5. Biteus, J., Cedersund, G., Frisk, E. (2004) *Improving Airplane Safety by Incorporating Diagnosis into Existing Safety Practice* (report), Linkopings University, Linkoping, Sweden.

6. Bjorn, J., Johan, A., Petter, K. (2001) *Thermal Modelling of an Electro-Hydrostatic Actuation System,* Recent Advantages in Aerospace Hydraulics, Jun 13-15, 2001, Toulouse, France.

7. BONNICE, W. and BAKER, W. (1988), *Intelligent fault diagnosis and failure management of flight control actuation systems* (Final Report, May 1986 - Mar. 1988), NASA-CR-177481; NAS 1.26:177481; CSDL-R-2055.

8. Briere, D. (1997), "*Airbus electrical flight control systems*", Nouvelle Revue d'Aeronautique et d'Astronautique, , no. 2, pp. 50-56.

9. Churn, P. M., Maxwell, C. J., Schofield, N., Howe, D. and Powell, D. J. (1998), "*Electro-hydraulic actuation of primary flight control surfaces*", All Electric Aircraft (Digest No. 1998/260), IEE Colloquium on17 June 1998, pp. 3/1-3/5.

10. Couaillac, F. (2007). *Environment Control Systems for the All-Electric Aircraft*. Cranfield University, Cranfield.

11. Croke, S. and Herrenschmidt, J. (1994), "*More electric initiative - Power-By-Wire actuation alternatives*", NAECON 94; Proceedings of the IEEE 1994 National Aerospace and Electronics Conference, Dayton, OH, Vol. 2; UNITED STATES; 23-27 May 1994, New York: Institute of Electrical and Electronics Engineers, Inc., .

12. Crowder, R. and Maxwell, C. (1997), "*Simulation of a Prototype Electrically Powered Integrated Actuator for Civil Aircraft*", Proceedings of the Institute of Mechanical Engineers (IMechE), vol. 211, pp. 381-394

13. Cutts, S. J. (2002), "*A collaborative approach to the More Electric Aircraft*", Power Electronics, Machines and Drives, 2002. International Conference on (Conf. Publ. No. 487), 4-7 June 2002, pp. 223-228.

14. Faleiro, L. (2005), "*Beyond the More Electric Aircraft*", Aerospace America, vol. 43, no. 9, pp. 35-40.

15. Felix, M. and Routex, J. (2007), "*A Copper Bird for Aircraft Equipment Systems Integration and Electrical Network Characterization*", 45th AIAA Aerospace Sciences Meeting and Exhibit, vol. AIAA Paper 2007-1392.

16. Fenny, C. A. and Schultz, D. P. (2005), "*Design & Development of the Ba 609 Civil Tiltrotor Hydraulic System Architecture*", AHS International 60th Annual Forum: New Frontiers in Vertical Flight Proceedings, .

17. Ferreira, C., Ng, E. and Radun, A. (2002), "*Power electronics and conditioning for electric actuation - Phase I*", vol. AIAA Paper 2002-0723.

18. Fronista, G. L. and Bradbury, G. (1997), "*An electromechanical actuator for a transport aircraft spoiler surface*", IECEC-97; Proceedings of the 32nd Intersociety Energy Conversion Engineering Conference, Honolulu, HI, Vol. 1 - Aerospace power systems and technologies; UNITED STATES; July 27-Aug. 1 1997, New York: American Institute of Chemical Engineers, .

19. Field, L. (2005), *Airplane Digital Distributed Fly-By-Wire Flight Control Systems Architectures: Reasons for Migratory Patterns of Computational Functionality*, for SAE 549: Systems Architecting

20. Gern, F. H., Inman, D. J. and Kapania, R. K. (2002), "*Computation of actuation power requirements for smart wings with morphing airfoils*", vol. AIAA Paper 2002-1629.

21. HAMMOND, M. and SHARKEY, J. O. H. N.,comps (1993), "*Electrical Actuation Technology Bridging*", vol. NASA-CP-3213; M-720; NAS 1.55:3213.

22. HANSEN, I. and KENNEY, B. (1993), "*Specification and testing for power by wire aircraft*", UNITED STATES, Vol. NASA-TM-106232; E-7951; NAS 1.15:106232, .

23. Hockley, C. J. and Appleton, D. P. (1997), "*Setting the requirements for the Royal Air Force's next generation aircraft*", IEEE Annual Reliability and Maintainability Symposium, Philadelphia, PA, Proceedings; UNITED STATES; 13-16 Jan. 1997, Piscataway, NJ: Institute of Electrical and Electronics Engineers, Inc., .

24. HOFFMAN, A. C., HANSEN, I. G., BEACH, R. F., PLENCNER, R. M., DENGLER, R. P., JEFFERIES, K. S., FRYE, R. J. and National Aeronautics and Space Administration. Lewis Research Center, Cleveland, OH (1985), *Advanced secondary power system for transport aircraft*, NASA-TP-2463; E-2434; NAS 1.60:2463; Pagination 38P.

25. Jackson, D. G., Owens, D. G., Cronin, D. J. and Severson, J. A. (2001), "*Certification and integration aspects of a primary ice detection system*", vol. AIAA Paper 2001-0398.

26. Jahns, T. M. and Van Nocker, R. C. (1990), "*High-performance EHA controls using an interior permanent magnet motor*", IEEE Transactions on Aerospace and Electronic Systems, vol. 26, no. 3, pp. 534-542.

27. Janker, P., Claeyssen, F., Grohmann, B. etc.(2008) "*New Actuators for Aircraft and Space Applications*", 11th International Conference on New Actuators, Bremen, Germany, 9-11 June, pp346-354, ACTUATOR 2008.

28. Jones, R. I. (1999), *"The More Electric Aircraft: The Past and The Future?"*, Proceedings of the IEE Colloquium on Electric Machines and Systems for the More Electric Aircraft, 9 Nov 1999, Ref. no. 1999/180, The Institution of Electrical Engineers (IEE), Savoy Place, London, UK

29. JORGE MANUEL RIBERA BODI, (2002), *Conceptual Cost Estimating for Aircraft Systems. Feasibility Study.(MSc thesis)*, Cranfield University, Cranfield, UK.

30. Lawson, C. P., *Advanced & Possible Future Airframe Systems*(lecture notes), Cranfield University, Cranfield, UK.

31. Lawson, C. P., *Flight Control Power Systems* (lecture notes), Cranfield University, Cranfield, UK.

32. LISCHKE, M. and MEYER, K. (1992), "*TEAMS - Technical expert aircraft maintenance system*", NAECON 92; Proceedings of the IEEE 1992 National Aerospace and Electronics Conference, Dayton, OH; UNITED STATES; 18-22 May 1992, New York, Institute of Electrical and Electronics Engineers, Inc., .

33. Mackey, R. (2001), "*Generalized cross-signal anomaly detection on aircraft hydraulic system*", 2001 IEEE Aerospace Conference, Big Sky, MT; UNITED STATES; 10-17 Mar. 2001, Piscataway, NJ: IEEE, .

34. Matsui, G. (2006) *Local backup hydraulic actuator for aircraft control systems* (invention), Seed Intellectual Property law Group PLLC- Seattle, WA. USA.

35. Moir, I. (1998), "*The All-Electric Aircraft - Major Challenges*", Proceedings of the IEE Colloquium on All-Electric Aircraft, 17 June 1998, Ref. no. 1998/260, The

Institution of Electrical Engineers (IEE), Savoy Place, London, UK

36. Moir, I. and Seabridge, A. G. (2004), *Design and development of aircraft systems : An Introduction*, , Bur St Edmunds :$Professional Engineering Publications.

37. Pachter, M., Houpis, C. H., Kang, K.(1997) "*Modelling and Control of an Electro-Hydrostatic Actuator*", International Journal of Robust and Nonlinear Control, VOL. 7, 591-608 (1997).

38. Richard, E. and Quigley, Jr. (1993), "*More Electric Aircraft* ", IEEE, pp. 906-911., New York: Institute of Electrical and Electronics Engineers, Inc., .

39. ROTH, M., TAYLOR, L. and HANSEN, I. (1996), "*Status of Electrical Actuator Applications*", UNITED STATES, Vol. NASA-TM-107319; NAS 1.15:107319; E-10416; NIPS-96-97732, .

40. Scholz, D. (2002), *Aircraft Systems- Reliability, Mass, Power and Cost*, European Workshop on Aircraft Design Education (2002), pp. 33-37, Hamburg, Germany.

41. SHARMA, T. and ZILBERMAN, B. (1990), "*Reliability analysis of redundant aircraft systems with possible latent failures*", 1990 Annual Reliability and Maintainability Symposium, Los Angeles, CA; UNITED STATES; 23-25 Jan. 1990, New York, Institute of Electrical and Electronics Engineers, Inc., .

42. SIMSIC, C. (1991), "*Electric actuation system duty cycles (in fly-by-wire /power-by-wire control)*", NAECON 91; Proceedings of the IEEE National Aerospace and Electronics Conference, Dayton, OH; UNITED STATES; 20-24 May 1991, New York, Institute of Electrical and Electronics Engineers, Inc., .

43. SUNDBERG, G. (1990), "*Civil air transport: A fresh look at power-by-wire and fly-by-light*", UNITED STATES, Vol. NASA-TM-102574; E-5402; NAS 1.15:102574, .

44. Vieten, K. W., Snyder, J. D. and Clark, R. P. "*Redundancy management concepts for advanced actuation systems*", 1993 AIAA/AHS/ASEE Aerospace Design Conference; Irvine, CA; Feb. 16-19, 1993, Vol. AIAA Paper 1993-1168, American Institute of Aeronautics and Astronautics, Inc, Reston, VA, 20191-4344, United States, .

45. Weimer, J. (2002), "*Power electronics in the more electric aircraft*", AIAA Aerospace Sciences Meeting & Exhibit, 40th, Reno, NV; UNITED STATES; 14-17 Jan. 2002, Vol. AIAA Paper 2002-0727, Reston, VA: American Institute of Aeronautics and Astronautics, Inc., .

46. Weimer, J. A. (1993), "*Electrical power technology for the More Electric Aircraft*", AIAA/IEEE Digital Avionics Systems Conference, 12th, Fort Worth, TX, Proceedings; UNITED STATES; 25-28 Oct. 1993, New York: Institute of Electrical and Electronics Engineers, Inc., .

47. Yao, Y., Zhao, W., Ergun, O. and Johnson, E. (2005), "*Aircraft Scheduling with Maintenance and Crew Consideration*", AIAA 5th Aviation, Technology, Integration, and Operations Conference (ATIO); Arlington, VA; USA; 26-28 Sept. 2005, Vol. AIAA Paper 2005-7416, American Institute of Aeronautics and Astronautics, 1801 Alexander Bell Drive, Suite 500, Reston, VA, 20191-4344, USA, [URL:http://www.aiaa.org], .

48. Zavala, E. (1997), "*Fiber optic experience with the smart actuation system on the F-18 systems research aircraft*", AIAA/IEEE Digital Avionics Systems Conference (DASC), 16th, Irvine, CA, Proceedings. Vol. 2; UNITED STATES; 26-30 Oct. 1997, Piscataway, NJ: Institute of Electrical and Electronics Engineers, Inc., .

LIST OF APPENDICES

Appendix A – Group Design Project Report

Conceptual Design of a 130-Seat Civil Airliner Flying Crane

- Mass Estimation, Centre of Gravity Calculation, Fuel Tank Design and Systems Analysis

EXECUTIVE SUMMARY

This report addresses the author's individual work in the group design project, which is the conceptual design of a 130-seat civil airliner named the Flying Crane.

The report covers the whole process of the conceptual design of the Flying Crane. During the first stage, the current 80 to 150 seats aircraft were surveyed. This report mainly focuses on the manufacturers, technology and family issues of the Airbus A320 family. In the second stage, it presents the performance requirements. After that, the whole team was divided into four sub-teams charged with four configurations design respectively. This report relates the cabin layout and cross-section design of the single aisle conventional configuration. Based on the primary conceptual design of each configuration, the performance assessment was completed and presented in this report. After the assessments, two configurations were selected. In the following stage, this report addresses the mass estimation, breakdown and centre of gravity calculation of the single aisle configuration. The two configurations were then assessed again, and the final configuration was chosen. Finally, the centre of gravity calculation, fuel tank layout and airframe systems requirement analysis of the Flying Crane was presented.

Keywords:
Conceptual Design, Performance, Cabin Layout, Mass Estimation, Breakdown, Centre of Gravity, Fuel Tank, System Requirements.

CONTENTS

TABLE OF FIGURES

TABLE OF TABLES

NOTATIONS

APS	Auxiliary Power System
APU	Auxiliary Power Unit
AVIC I	China Aviation Industry Corporation I
CG	Centre of Gravity
CRT	Cathode Ray Tube
EADS	European Aeronautic Defence and Space Company
ECS	Environment Control System
FAR	Federal Aviation Regulations
FCS	Flight Control System
GTF	Geared Turbofan
JAA	Joint Aviation Authorities
LCD	Liquid Crystal Display
L/D	Lift Drag Ratio
M	Mach Number
MAC	Mean Aerodynamic Chord
PBW	Power-By-Wire
PHM	Prognostic and Health Management System
sfc	Specific Fuel Consumption
T-O	Take-off

I Introduction

I.1 Project Description

This project is a 130-seat civil aircraft conceptual design and acts as the AVIC I students' group design project. There are totally 24 members in the group, the author is responsible for a part of the group project work, and this report relates the individual work the author did in it.

I.2 Flying Crane

Flying Crane is the aircraft designed by the AVIC I group. The final configuration of the aircraft comes into being after experiencing several stages' design and competing with the other three configurations. It is a wide body civil aircraft with single aisle. It can accommodate 128 passengers for business and economy mixed classes, while 150 passengers for single economy class. The range of the Flying Crane is 2,000nm, and the take-off mass is 64,582kg.

The Flying Crane has its unique features and advantages over the other aircraft in this category. It is expected to be more efficient in fuel consumption by equipped with two GTF engines. In addition, the aircraft has wide fuselage which will greatly improve passengers' travel comfort and provide airlines with more operational flexibility. At last, the design range of the Flying Crane makes the airliner more efficient in operation, particularly in Chinese domestic market.

I.3 Design Stages

The conceptual design of the Flying Crane mainly has three phases that are divided into six stages. The derivation requirements phase includes market survey and requirements analysis. The conceptual design and evaluation phase includes primary conceptual

design, configuration assessments and concept further develop. The last phase is the consolation and review.

In the first stage, the group was divided into six sub-teams to survey the current 80-150 seats aircraft on general characteristics, manufacturers, aerodynamic/static stability characteristics, geometric design characteristics, performance characteristics and operators. A whole database with all the parameters of the six aspects was established at the end of this stage. The author worked for the manufacturers survey sub-team.

In the second stage, the group was divided into six sub-teams again to analyse the design drivers and general requirements, performance requirements, data/model validation and matching, family issue and design constrains, market and strategic aims respectively. After this stage, the general requirements of every aspect of the aircraft to be designed were gained. In this stage, the author worked as the coordinator of the performance requirements sub-team.

After the market survey and requirements analysis in and the first two stages, the group started to design their own aircraft. Four configurations, single aisle conventional configuration, twin aisles configuration, long range configuration and upper wing mounted engine configuration, were studied by four sub-teams separately. All configurations' passenger capacity is 150 for single economy class and 128 for business and economy mixed classes. The range for those configurations is 2,000nm except the long range one which is 3,200nm. After six weeks' work, the general parameters of each configuration were given, including geometric parameters, aerodynamic parameters, mass, cabin layout, fuel performance and so on. The author was responsibility for the cabin layout and cross-section design in the single aisle conventional configuration sub-team.

In order to evaluate the design of the four configurations, the whole group was divided into five sub-teams to assess each aspect of each design, including performance, family, markets, strategic and cost. Each sub-team selected the parameters they need and distributed the weighting factor of each parameter, then set the assess criteria and gave

the score of each parameter. Integrated with the weighting factor, score of each aspect was got. The total score was gained by the same way. After twice assessments and updates, the single aisle conventional configuration and twin aisles configuration became the winners and were selected to be further developed. In this stage, the author worked as the coordinator of the performance assessment sub-team.

In the fourth stage, the four sub-teams combined into two sub-teams and worked to develop the concept of the configurations selected. Some detailed work were finished in this stage, such as the landing gear arrangement, detailed centre of gravity range, static margin and the basic structure layout. In the end of this stage, the evaluations were done again. As a result, the combination of the two configurations became the final configuration of the Flying Crane, which used the wide body of the twin aisles configuration and single aisle of the single aisle conventional configuration. The author was in charge of the mass estimation, breakdown and centre of gravity calculation in the single aisle conventional configuration sub-team.

In the last stage, the whole group worked on the final configuration. There were eight sub-teams worked on eight specific aspects of the Flying Crane respectively. The parameters were checked again and much more detailed specifications were completed during this stage. As a result, the specifications of the Flying Crane were given and final reports were completed. The author was the coordinator of the structure, powerplant and airframe system sub-team and took charge of the centre of gravity check, fuel tank layout and airframe system requirements analysis.

II Manufacturers Survey

II.1 Task

At the beginning of the aircraft design, market survey is required.

The task of manufacturers survey sub-team is: Comprehensive survey of manufacturers that produce civil transport aircraft in the 80-150 passenger category. The review should include what aircraft do they produce and how they fit into their 'family' structures, the collaboration with other companies when those aircraft been produced and what is the market share. In addition, the history of these aircrafts should be surveyed, including the time those aircrafts lunched, updates/stretches and so on. Moreover, the technologies used in manufacture processes, materials, systems, avionics should be included.

In the manufacturers survey sub-team, the author took charge of the survey of the Airbus' 80-150 passenger aircraft, the A320 family.

II.2 Introduction

The Airbus A320 family is short to medium range commercial passenger airliners manufactured by the Airbus in collaboration with the CFM international (engine), Pratt & Whitney (engine), Liebherr/ABG-Semca (air conditioning), Hamilton Sundstrand/Nord-Micro (pressurization), Hamilton Sundstrand (primary electrical system) and Honeywell (APS).

The Airbus A320 family includes four series, the original mid-sized A320, the slightly smaller A319, the significantly smaller A318 and the slightly larger A321. The passenger capacity of the A320 family ranges from 107 to 220, which is 107 (2-class)/117 (1-class), 124 (2-class)/145 (1-class), 150 (2-class)/180 (1-class) and 185 (2-class)/220 (1-class) for

the A318, A319, A320 and A321 respectively. The A318, A319 and A320 are in 80 to 150 passenger category.

The Airbus A320 family is the best-selling airliner family after the Boeing 737 family. Until 31st Mar 2008, the deliveries of the A318, A319 and A320 are 56, 1,064 and 1,881 separately; the orders of these three series are 93, 1,603 and 3,735 respectively.

II.3 Development

In the early of the 1980s, the global requirement of airliners in 80 to 150 passenger category to replace the Boeing 727 and the early variants of the Boeing 737 increased quickly. Targeted at this demand, the Airbus launched its plan to develop a same size, improved operating economics and various passenger capacities aircraft, the A320, on 23 Mar 1984. Unlike the first product of Airbus, the A300, was funded by EADS (European Aeronautic Defence and Space Company), the A320 was operated by the Airbus itself.

The initial version of the A320 (A320-100) took its first flight with two CFMI CFM56-5 engines on 22 Feb 1987 and got the certification on 26 Feb 1988. The first delivery of it was on 28 Mar 1988. The A320-100 was produced only 21 and replaced by the A320-200, which features wingtip fences, wing centre-section fuel tank increased fuel capacity over the A320-100 for increased range and higher maximum Take-off mass. The A320-200 were powered by two CFMI CFM56-5s engines or two IAE V2500 engines (first flown 28 July 1988), which received the certification of JAA on 8 November 1988 and 20 April 1989 respectively. The A320-200 began its delivery on 18 May 1989 and has been sold 1,860, while the order of it was unfinished, it is 1,854 up to 31st Mar 2008.

Based on the original mid-sized A320 with 150 (2-class)/180 (1-class) passenger capacity, the Airbus launched program to develop a short-fuselage A320, the A319, for the requirement of various passenger capacities on 10 June 1993. The A319-100 with virtually the same fuel capacity as the A320-200 made its first flight with two CFMI CFM56-5A engines on 29 August 1995 and received certification on 10 Apr 1996. The

first delivery of the A319 was on 25 April 1996, and then it changed engines with two IAE V2524. Another version of the A319 is the A319CJ, which is a Airbus Corporate Jetliner announced at 1997 Paris Air Show and can carry up to 40 passengers. Based on the A319CJ, the Airbus also developed the A319LR and the A319 Executive. Unlike the A319-100 with 124 (2-class)/145 (1-class) passenger capacity, all of the A319CJ, A319LR and A319 Executive are 40 seats level airliners.

The smallest aircraft in the Airbus family, the A318, also as known as the "Mini-Airbus" with 107 (2-class)/117 (1-class) passenger capacity, is the short-bodied version of the A319. The program was launched on 26 April 1999 with orders, commitments and options for 109 aircraft. The A318 made maiden flight powered by two Pratt & Whitney PW6000 engines on 15 January 2002. Due to the delays in PW6000 program, the A318 has ever re-engined with CFM56-5B/Ps. The first delivery of the A318 was on 22 July 2003. Like the A319, the A318 also developed business jet, the A318 Elite, which is only 14 to 18 passenger capacity. However, during the A318 program, it ran into several problems. One was the decline demands for new aircraft after the September 11, 2001 attacks. Another one was the new Pratt & Whitney turbofan engines, which burned more fuel than expected: by the time CFMI had a more efficient engine ready for market. Many A318 customers had already backed out, which had selected the Pratt & Whitney engines, and amended its A318 orders, opting instead for the A319 or A320 aircraft.

Another member of the Airbus A320 family is the A321, the wide-bodied version of the A320, which is the largest aircraft in A320 family with 185 (2-class)/220 (1-class) passenger capacity and is out of the category being surveyed.

II.4 Technologies

As a successful airliner family, the Airbus A320 family introduced many advanced technologies and created a lot of precedents in civil aircraft field.

In terms of geometrical shape, the A320 adopt advanced-technology wings with 25° sweepback at quarter-chord, 5° 6' 36" dihedral plus experience from the A310 and significant commonality with other Airbus aircraft where cost-effective, and 6° tailplane dihedral.

Concerning airframe and systems, the A320 is the first subsonic commercial aircraft introducing the centralised maintenance system and using composites for major primary structures. The former system constantly gathers the status information and detects the failures concerning engines, as well as other key systems such as flight controls, hydraulics and avionics; then sends it to display on the cockpit displays to the pilots. Another technology first applied on a civil airliner is the fully digital fly-by-wire flight control system. The fully glass cockpit rather than the hybrid versions and the centre-of-gravity control using fuel technology are also characters of the A320. Recently, the Airbus started installing LCD (liquid crystal display) units in the flight deck of its new A318, A319, A320, and A321 instead of the original CRT (cathode ray tube) displays. This technology reduces the mass and produces less heat.

In manufacture processes, the latest member of the A320 family, A318, introduced Laser welding (rather than riveting) used on lower fuselage to reduce costs and mass. It is the first time that this technology was used on airliner.

II.5 Summary

This chapter presented the manufacturers survey of the Airbus A320 family. The Airbus A320 family occupies a large percentage in the 80 to 150 passenger category's aircraft markets, and it has several successful design characters.

In terms of family structure, the A320 family selected a reasonable design point as the baseline. The passenger capacity can be increased or reduced based on lengthening or shortening the body of the baseline without changing the wings and tail, this saved the design cost of whole family significantly. Considering the technologies, the advanced

technologies used on the A320 family increased its competitive ability, especially the fly-by-wire technology. Beside this, the other technologies, such as the centralised maintenance system and composite material for major primary structures, have great influence on the development of the A320 family. At last, from the development of the A320 family, we can also find that it is very important to cooperate with the other specialist companies.

Generally speaking, as a successful family in 80 to 150 passenger category, the Airbus A320 family takes advantage of its wide range of passenger capacity, logical family structure, advanced technologies and cooperation with the other companies. It is important to consider the selection of design point, the family structure, the use of advanced technologies and the cooperation when designing a new aircraft.

III Performance Requirements

III.1 Task

After the market survey, the requirements of the aircraft to be designed are analysed.

The task of the performance requirements sub-team is: Based on the requirements investigated by the other teams, the performance requirements should be analysed. It should include passenger capacity, range, field performance, cruise speed, engine type and so on.

In this stage, the author worked as the coordinator of the performance requirements sub-team and was responsibility for the passenger capacity and range requirement analysis.

III.2 Study Strategy

To analyse the passenger capacity and range requirements, it is important to understand the target of the aircraft. As a civil aircraft, the target is to win the markets; hence, the analysis should be based on the market requirements firstly.

To win the markets, the competitors should be considered. If the aircraft to be designed is similar to the current aircraft, it is very useful to learn the advantages of competitors, and also to avoid the lessons.

At last, from the survey of manufacturers, family structure is an important issue for the design of civil aircraft, the family structure should be considered and the passenger capacity and range should be selected on a reasonable design point.

Generally speaking, the passenger capacity and range requirements analysis should be based on the market requirements, the competitors and the family structure. Besides this, the matching of the passenger capacity and range should be considered.

III.3 Passenger Capacity Requirement

Market requirements indicate that in the next 20 years, there are totally 29,400 civil aircraft needed globally, 12,500 of them are those current aircraft to be retired, and 16,900 of them are the new requirement. In the requirement, 74% is 100 to 200 seats single aisle aircraft. In addition, the main target market of the aircraft to be designed is the domestic market of China. Based on the analysis of the market requirement sub-team, 79% of the China market requirements is the 100 to 200 seats single aisle aircraft. For the future market related passenger capacity, 100 to 200 seats market is a huge market and is selected as the passenger capacity requirement.

In terms of the passenger capacity of the competitors, the Airbus A320 is 107 to 185, while the Boeing 737 is 115 to 160, so that 100 to 200 passenger capacity is reasonable to compete with the Airbus and Boeing.

Concerning family structure, the design point of the passenger capacity influences the development versions. If the design point is too high, there is not too much space to develop the bigger version; it is the same condition for the low design point to develop the smaller version. As a result, 130 seats is selected as the design point for the 100 seats to 200 seats range.

III.4 Range Requirement

Based on the analysis of the market requirements sub-team, the length of the top ten busiest airliner routes of China are 400nm to 1,100nm. The longest distance from north China to south China is 1,840nm, and the longest one from east China to west China is

1,770nm. From this point of view, design payload range 2,000nm can fully satisfy the domestic and inter-regional routs demands.

Concerning the competitors, in 80-150 passenger category aircraft, the two successful series, the Airbus A320 family various from 1,500nm to 2,700nm, the Boeing 737 family various from 1,900nm to 3,200nm. Therefore, the design range of 2,000nm is reasonable for 80-150 passenger category aircraft.

Similar to the passenger capacity issue, the range influences the development versions. If the range is too long, it is not efficient to develop the shorten version. If it is too short, it will cost too much to develop lengthen version. Considering the design point of passenger capacity is only 130 seats, 2,000nm is selected for the baseline.

III.5 Summary

The performance requirements for the aircraft to be designed was analysed in this Chapter. From market requirements, competitors and family structure, the passenger capacity and range are suggested of 130 seats and 2,000nm as the baseline.

IV Cabin Layout

IV.1 Task

After the market survey and derivation of requirements, the general requirements of the aircraft to be designed have been gained. The passenger capacity is 150 for single economy class and 128 for economy and business mixed classes, range is 2,000nm, ceiling is 12,000m, cruise speed is 0.78M, take-off distance is 1,900m and landing distance is 1,800m.

In this stage, the whole group is divided into four sub-teams named different colours to develop the concepts of four different configurations respectively based on the same requirements. The Blue team works for the single aisle conventional configuration, the Red team works for the twin aisles configuration, the Yellow team works for the long range configuration (3,200nm) and the Gold team works for the upper wing mounted engine configuration. Each team should develop the general characteristics including the mass, geometry, aerodynamic, cabin layout and so on.

The author worked in the blue team and was in charge of the cabin layout of the single aisle conventional configuration aircraft.

IV.2 Cabin Design

The aircraft to be designed is single aisle conventional configuration, the passenger capacity is 150 for single economy class and 128 for economy and business mixed classes. According to aircraft design convention, 128 seats for mixed classes is the design point. Therefore, the payload and the cabin sizing are based on 128 seats.

IV.2.1 Cross-section

The first step is to decide the number of seats to be placed abreast. According to airworthiness regulation FAR 25.817, the number of seats on each side of the aisle should be no more than three. The similar single aisle aircraft, both the A319 and the Boeing 737-700 are 3-3 abreast. As a result, 3-3 abreast is selected for the economy class seat arrangement, and 2-2 abreast is selected for the business class.

Concerning the seat width, there is no regulations about this item. However, the wider seats, the more passenger comfortable. 18 inch and 21 inch are used for the economy class and the business class respectively on the A319, while it is 17 inch and 21 inch on Boeing 737-700. Permission by the cost, 20 inch for the economy class and 25 inch for the business class are selected.

For the aisle, airworthiness regulation gives the minimum width is 380mm (15inch), while it is 19 inch on the A319 and 20 inch on the Boeing 737-700. According to Torenbeek's *Synthesis of Subsonic Airplane Design*, 20 inch (50.8cm) is selected as the width and 2.2m as the aisle height.

The thickness of the furnishing and structure of fuselage is about 0.15m, while the distance between seat and cabin wall is from 25mm to 50mm (according to Torenbeek's *Synthesis of Subsonic Airplane Design*). Then the width of the fuselage can be calculated:

$$B_{fuselage} = B_{seat} \times N_{row} + B_{aisle} + 2 \times (T_{structure} + D_{seat-wall}) = 3.95m$$

FAR 25.817 regulates all passengers must be able to move their heads freely without touching the cabin walls, this requires a free space with radius of at least 0.20 to 0.25m measure from the eyes, then the cabin wall can be drawn. In order to take the container LD3, the cross-section needs to be built up from two segments with different radii. As a result, the height can be estimated as 4.47m.

The cross-section of the aircraft is illustrated in Figure IV-1.

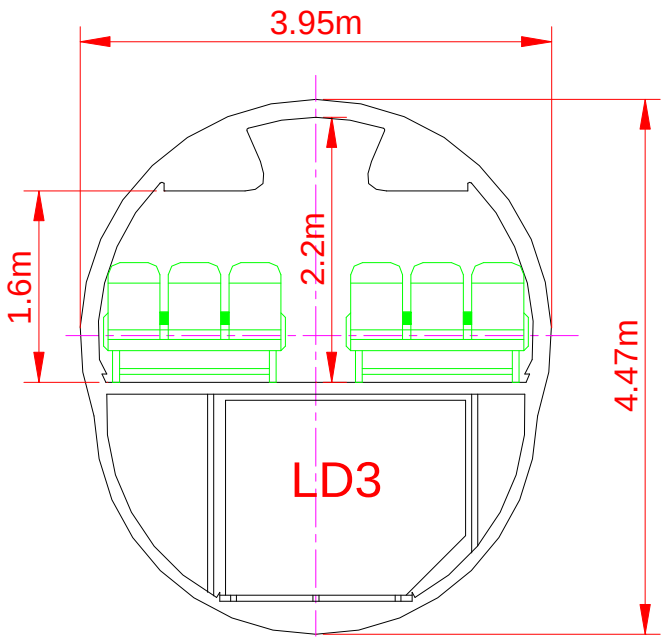

Figure IV-1 Cross-section

IV.2.2 Seats Location and Cabin Dimensions

After designed the cross-section, the plane arrangement of seats should be decided. The first step is to select the seat pitch. The airworthiness regulations only regulate the minimum between the backrest of two rows is 26 inch, while the backrest of each seat is about three inch. As a result, 29 inch is taken as the minimum seat pitch. To win the markets, comfortable is a big issue to be considered. From this point of view, compared with the A319's 31 inch for economy seat and the Boeing 737-700's 31 inch for economy seat, 32 inch is selected for economy class seat pitch, while 40 inch for business class.

The passenger doors are confirmed according to the airworthiness regulations, which include six doors, two in the front of the fuselage, two in the rear of the fuselage, the last two in the centre of aircraft and upper wings.

The furnishing is also designed based on the regulations. There are three attendants, two galleys and three lavatories, one in the front and the other two in the rear.

Since the seats have been arranged, the lavatories, galleys, passenger doors and space near the doors have been accounted for, the forward and rearward of the cabin can be fixed. The cabin length is:

$$L_{cabin} = R_{bu\sin ess} \times P_{bu\sin ess} + R_{economy} \times P_{economy} + L_{furnishing} + \Delta = 21.912m$$

While Δ is the error of the pitch.

Taking the forward length of fuselage as 15% of total fuselage, rearward length as 22%, the total length of fuselage can be calculated as 34.77m.

The mixed classes cabin layout, which includes 16 business seats and 112 economy seats, is shown in Figure Ⅳ-2.

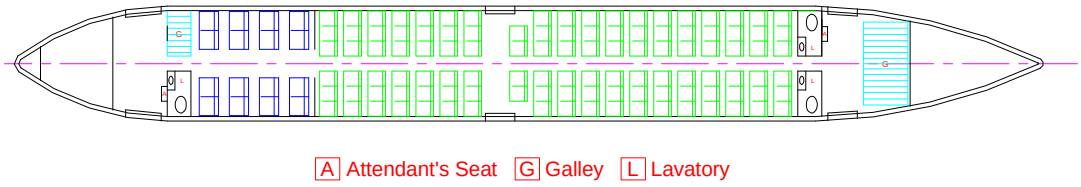

Figure IV-2 Mixed Classes Cabin Layout

The single class cabin layout, which includes 148 economy seats, is illustrated in Figure Ⅳ-3.

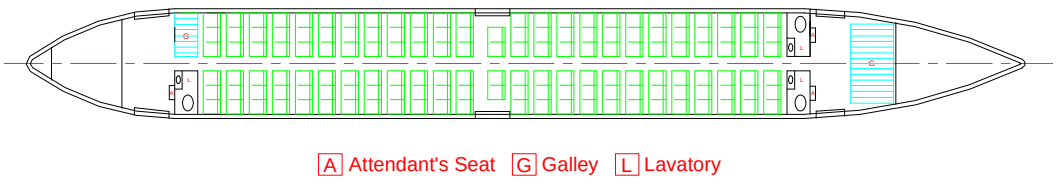

Figure IV-3 Single Class Cabin Layout

The parameters of cabin is presented in Table Ⅳ-1.

Table IV-1 Cabin Parameters

	Mixed Classes		Single Class
	Business	**Economy**	**Economy**
Seats	16	112	148
Seat Pitch (inch)	40	32	31.5
Seat Width (inch)	25	20	20
Aisle Width (inch)	38	20	20

V Performance Assessment

V.1 Task

After the primary design of the concepts of four different configurations, the concepts need to be evaluated.

The task of the performance assessment sub-team is: Review the work and the report produced in the second stage by the performance requirements sub-team. From the work and any additional issues that have subsequently arisen, propose a sufficient number of performance characteristics that the aircraft can be measured against. Allocate a weighting factor for each of the parameters that signifies how important any individual parameters is to the project as a whole, assess the performance of the four configurations developed in the last stage. The result should be forwarded to the 'assessment matrix'.

As the coordinator of the performance assessment sub-team, the author organized the work of this sub-team and did the primary assessment of performance, then the other team members further developed it to the final performance assessment.

V.2 Parameters Selection and Weighting Factor Allocation

To measure the performance of the configuration, the first step is choosing the performance parameters. According to the description of the aircraft's performance in *Jane's All The World's Aircraft*, combined with the definition of performance in Roskam's *Airplane Design*, Raymer's *Aircraft Design* and Torenbeek's *Synthesis of Subsonic Airplane Design*, the performance parameters selected to be measured include: range, passenger capacity, take-off length, landing length, cruise speed, ceiling and climb rate.

There are totally eight performance parameters selected to be measured. To allocate the weighting factor of each parameter, all the team members gave the order of the parameters based on its importance for the whole performance they considered. The most important one gets the eight, the second gets the seven…, the least important one gets the one, then combine them together and take one as the total, the weighting factor of each parameter can be gained, as shown in Table V-1.

Table V-1 Weighting Factor Allocation

	Team member 1	Team member 2	Team member 3	Total	Weighting Factor
Range	7	6	8	21	0.19
Seat	6	7	6	19	0.18
Payload	8	8	7	23	0.21
T-O Length	3	1	5	9	0.08
Landing Length	4	2	4	10	0.09
Cruise Speed	5	4	2	11	0.10
Ceiling	1	3	1	5	0.05
Climb rate	2	5	3	10	0.09
Total	36	36	36	108	1

V.3 Assessment Criteria Set Up

After the parameters selection and weighting factor allocation, the assessment criteria is set up.

For the development of the criteria for each parameter, the first idea is based the market. Taking the similar aircraft, 80-150 seats aircraft, as a whole, the market share rate of each aircraft can be regarded as a coefficient. Using the parameters of each aircraft multiplies its coefficients, and putting all the results together, the results can be regarded as the criteria. Comparing with the criteria, the score of the parameter of the designing aircraft can be gained. However, the market share rate always not depends on the performance, using this method to set up the criteria is not suitable. The second idea is whether consider the relation between each two parameters, for

example the passenger capacity and payload. However, each parameter of aircraft has the relationship with the other parameters. Therefore, the assessment matrix will be very huge and complex considering relations. In addition, the relation can be balanced by gaining different score in different parameters with each parameter assessed separately. The assessment criteria should be set up by individual parameters.

For the individual parameter assessment criteria, 100 is taken as the score for the best one. Comparing the parameters of the other aircraft with the best one, the score of the aircraft can be calculated. In order to compare with the current aircraft, the Airbus A319 and the Boeing 737-700 are considered together with the four configurations when setting up the assessment criteria. For example, considering range, the longest is the best, so the Boeing 737-700 whose range is 3,260nm gets the range score 100, the range score of the A319 whose range is 1,900nm can be calculated:

$$S_{R-A319} = \frac{R_{A319}}{R_{737-700}} \times S_{R-737-700} = \frac{1900}{3260} \times 100 = 58.3$$

The range scores of the other aircraft can also be calculated by the same way, and the other parameters' score can be gained by the same method.

V.4 Assessment Result

According to the performance assessment criteria developed in Section 5.3, each of the performance parameters gets a score. Combined with the weighting factors, the score of each configuration is got, as presented in Table V-2.

It can be seen from Table V-2, the Boeing 737-700 has the highest score in these six aircraft in terms of performance. For the four configurations designed, the Yellow team gets the highest score followed by the Golden team, while the Red team is the worst. However, this is only the primary performance assessment. During the next step, the performance parameters selection is optimized, and the measure criteria is adjusted. This part of work can be seen in the GDP report of another team member, MR. Zhang Zhigang's *Conceptual Design of a 130-Seat Civil Airliner Flying Crane-Geometrical Investigation, Evaluation Criteria, Weight and Performance Estimation*.

Table V-2 Performance Assessment Result

	Range		Seat		Payload		T-O Length		Landing Length		Cruise Speed		Ceiling		Climb Rate		Total Score
Blue	2000	61.3	128	100.0	12160	69.9	1900	91.8	1800	75.0	0.78	99.4	12000	96.0	2500	90.7	**82.0**
Golden	2000	61.3	128	100.0	12160	69.9	1900	91.8	1800	75.0	0.78	99.4	12000	96.0	2756	100.0	**82.8**
Red	2000	61.3	128	100.0	12160	69.9	1900	91.8	1800	75.0	0.78	99.4	12000	96.0	2300	83.5	**81.3**
Yellow	3200	98.2	128	100.0	12160	69.9	1900	91.8	1800	75.0	0.78	99.4	12000	96.0	2600	94.3	**89.5**
Airbus A319	1900	58.3	124	96.9	17390	100.0	1750	99.7	1350	100.0	0.78	99.4	12000	96.0	/	92.1	**90.3**
Boeing 737-700	3260	100.0	128	100.0	11610	66.8	1744	100.0	1418	95.2	0.785	100.0	12500	100.0	/	92.1	**91.7**
Factor	0.19		0.18		0.21		0.08		0.09		0.10		0.05		0.09		

Note: Lack of the parameters of climb rate of the A319 and the Boeing 737-700, the scores of climb rate for these two aircraft take the average of the other four configurations.

VI Mass Estimation and Centre of Gravity Calculation

VI.1 Task

After twice assessments, the Blue team's single aisle conventional configuration and the Red team's twin aisles configuration became the winners and went to the next stage.

In this stage, the Blue team and the Yellow team combined to the Jade team. The task of Jade team is: to further develop the concept of the single aisle conventional configuration. Areas that might not have been explored need to be developed further, including parameters should be checked, landing gear arrangement meets all requirements, centre of gravity range must be detailed, the wing should be correctly positioned to give a feasible static margin at all flight conditions, and so on.

As a member in the Jade team, the author was in charge of the mass estimation, breakdown and centre of gravity calculation.

VI.2 Mass Estimation

VI.2.1 Model Establishment

To estimate the gross mass of the aircraft, the estimation model should be established firstly. The Roskam method was selected as the theory for the estimation model during the first step.

Roskam method is based on the fuel consumption. According to Roskam's *Airplane Design*, the finishing mass to beginning mass ratio (the change is fuel consumption) of each phase is selected as conventional, which is shown in Table 6-1. The other parameters needed for the Roskam method such as the cruise status, lift drag ratio and fuel consumption of cruise and loiter, fuel consumption of fly to alternate and descend

status, are given by the performance sub-team. The cruise status is 12,000m altitude and 0.78 M speed, the loiter time is 45min, the range of fly to alternate and descend is 200nm, while the speed is 250kts. The lift drag ratio and fuel consumption of those three phases are shown in Table VI-1.

Table VI-1 Weight Estimation Parameters

Phase	Mass ratio	L/D	sfc (lbs/lbs/hr)
Engine Start and Warm up	0.99		
Taxi	0.99		
Take-off	0.995		
Climb	0.98		
Cruise	0.877	17	0.5
Loiter	0.982	19	0.46
Descent	0.99		
Fly to alternate and descend	0.948	12	0.8
Landing, Taxi, Shutdown	0.992		

VI.2.2 Model Adjustment

Before using the Roskam mass estimation model, the accuracy of it must be checked, the similar aircraft, A319, was chosen to do it.

The finishing/ beginning mass ratio is chosen as the same with in Table 6-1. The sfc is confirmed according to the engine it used, the lift drag ratio is calculated based on the public parameters, the other parameters such as cruise status is got from the official website of Airbus.

Using the Roskam Model, the take-off mass of the A319 is calculated as 66,050kg. Compared with the real data, 64,400kg, there is 2.5% error. It is regarded that the mass estimation model is accurate to guess the gross mass.

VI.2.3 Gross Mass Estimation

Put the parameters of the current designing aircraft into the estimation model, the gross mass is got, as presented in Table VI-2.

Table VI-2 Gross Mass

	Mass (kg)	Percentage
Take-off	57293	
Empty	31765	55.5%
Fuel	13368	23.3%
Payload	12160	21.2%

VI.2.4 Mass Check

In order to check the gross mass calculated by the Roskam model, another method, Torenbeek method, was used. The Torenbeek method uses the quite different way to estimate the gross mass of aircraft. It depends on the geometric parameters of the aircraft and calculates the ratio, then uses the diagram to check it.

Same with the Roskam method, the A319 was chosen to check the accuracy of the Torenbeek method firstly, and the result is reasonable. Then the current designing aircraft is checked by the same way, the result shows that the gross mass calculated by the Roskam method is acceptable.

VI.3 Mass Breakdown and Update

After the confirmation of the gross mass, the mass is broken down to each part, including structure and systems, using the Cranfield methods.

VI.3.1 Structure Components

Since the design range of the aircraft is 2,000nm, which can be regarded as short range, the following calculations are abided by this notion.

For typical jet transporters, the empirical equation to calculate the mass of wing based on the take-off mass is:

$$W_w = 0.03 \times W_{to}^{1.1} = 5140.8kg$$

The mass of fuselage for short range aircraft is:

$$W_f = 0.014 \times W_{to}^{1.18} = 5763.5kg$$

The mass of tail unit based on the take-off mass is:

$$W_t = 0.14 \times W_{to}^{0.83} = 1245.5kg$$

The mass of undercarriage for aircraft has 2 units of undercarriage is:

$$W_u = 0.038 \times W_{to} = 2177kg$$

Mass relevant to powerplant calculation based on powerplant mass is:

$$W_p \times 2 = 4200kg$$

$$W_{pr} = 0.03 \times W_p \times 2 + 0.17 \times W_p \times 2 = 840kg$$

Therefore, the total mass of structural components is:

$$W_{sc} = W_w + W_f + W_t + W_u + W_{pr} = 15166.8kg$$

VI.3.2 Powerplant, Systems and Equipments

The dry mass of each engine is guessed of 2,100kg by another sub-team. The empirical factor of turbofan engines installation is 1.3, therefore, the mass of powerplant including installation based on the dry mass is:

$$W_{pi} = 1.3 \times W_p \times 2 = 5460kg$$

The empirical equation to calculate the mass of fuel system based on the take-off mass is:

$$W_{fs} = 0.05 \times W_{to}^{0.8} = 320.2kg$$

The mass of powered flight control system is:

$$W_{fcs} = 0.11 \times W_{to}^{0.8} = 704.5kg$$

The mass of hydraulic system with powered controls is:

$$W_{hs} = 3.2 \times W_{to}^{0.5} = 766kg$$

The mass of electrical power system is:

$$W_{eps} = 0.75 \times W_{to}^{0.67} = 1156.1kg$$

The mass of accessory drives is:

$$W_{ad} = 0.003 \times W_{to} = 171.9kg$$

Since the passenger capacity of the aircraft is 130, which can be regarded as small airliner. The minimum mass of auxiliary power units for small airliner is about 200kg. Then the mass of the auxiliary power units is guessed:

$$W_{apu} = 350kg$$

The mass of environment control system based on the take-off mass is:

$$W_{ecs} = 0.035 \times W_{to}^{0.88} + 0.16 \times W_{to}^{0.7} = 881.1kg$$

Except domestic operations, the aircraft can also intend for international operations, thus the mass of instruments and automatic controls is guessed about 170kg, and the mass of radio, radar and navigation equipment is 160kg.

The mass of fire precautions and tank protection based on the take-off mass is:

$$W_{fp} = 0.003 \times W_{to} = 171.9kg$$

The mass of external paint based on the wing area is:

$$W_{ep} = 0.5 \times S_w = 49kg$$

For the mass of furnishings, the total furnishing allowance for airliners should be 45 kg per passenger, thus the total mass of furnishing is:

$$W_{fur} = 45 \times 128 = 5760kg$$

Then the total mass of powerplant, systems and equipments is:

$$W_{pse} = W_{pi} + W_{fs} + W_{fcs} + W_{hs} + W_{eps} + W_{ad} + W_{apu} + W_{ecs} + W_{fp} + W_{ep} + W_{fur} = 16360.7kg$$

VI.3.3 Mass Update

From the mass breakdown, the new empty mass is got:

$$W'_{emp} = W_{sc} + W_{pse} + W_{crew} = 31527.7kg$$

In this formula, the W_{crew} is regarded as two pilots and four assistants, and the mass of each of them is 95 kg including the baggage. The new empty mass, 31,527.7 kg, which is different with the initial gross empty mass 31,765kg, hence the gross mass should be updated to reduce the error. The basic calculation model, Roskam method, is based on the fuel consumption, so that the fuel percentage, which is 23.3%, should be fixed,; the payload, 12,160kg, is also fixed. From the formula:

$$W_{to} = W_{emp} + W_{fuel} + W_{payload}$$

The relation between Wt-o and Wemp is got. In Section 6.3.1 and 6.3.2, the relation between Wt-o and W'emp is also got. Comparing the two relations, when the error between initial gross empty mass and breakdown empty mass is zero, the final mass is got. After several times updates, the optimized mass is gained and shown in Table VI-3; the final mass breakdown is shown in Table VI-4.

Table VI-3 Optimized Mass

	Mass (kg)	**Percentage of Wto**
Take-off	58900	
Empty	32997	56.1%
Fuel	13743	23.3%
Payload	12160	20.6%

Table VI-4 Mass Breakdown

Part	Mass (kg)	Percentage of Wto
Wing	5299.7	9.0%
Fuselage	5954.8	10.1%
Tail	1274.5	2.2%
Undercarriage	2238.2	3.8%
Powerplant relate	2714	4.6%
Powerplant	4200	7.1%
Fuel System	327.4	0.6%
FCS	720.3	1.2%
Hydraulic System	776.6	1.3%
Electrical system	1177.7	2.0%
Accessory Drives	176.7	0.3%
APU	350	0.6%
ECS	881.1	1.5%
Instrument	170	0.3%
Radio	160	0.3%
Fire Precaution	176.7	0.3%
External paint	49	0.1%
Furnishing	5760	9.8%

VI.4 Centre of Gravity Calculation

After the mass breakdown and update, the mass of each part of the aircraft is confirmed; the next stage is centre of gravity calculation.

According to the Cranfield Notes, aircraft can be divided into two parts: the structure and systems related to fuselage, whose location is fixed; the structure and systems related to wing, whose location can be changed with wing to match the requirements of CG range and static margin.

VI.4.1 Fuselage Related Components Centre of Gravity

The structure and systems fixed on the fuselage include horizontal tail, vertical tail, fuselage, instruments, electrical except generators, electronics, furnishing, environment control system, APU, fire precaution, external, crew and payload. According to the Cranfield Notes, the CG of each part are calculated and shown in Table VI-5.

Table VI-5 Fuselage Related Components CG

Part	Maximum Take-off		Empty	
	Mass (kg)	**CG (m)**	**Mass (kg)**	**CG (m)**
Horizontal tail	734.5	31.17	734.5	31.17
Vertical tail	540	30.94	540	30.94
Fuselage	5954.8	15.16	5954.8	15.16
Instruments	170	2.70	170	2.70
Electrical	736.1	13.99	736.1	13.99
Electronics	160	2.58	160	2.58
Furnishing	5760	16.32	5760	16.32
ECS	551.8	11.69	551.8	11.69
APU	350	32.48	350	32.48
Fire	176.7	28.43	176.7	28.43
External	49	16.7	49	16.7
Crew	570	16.7	570	16.7
Payload	12160	16.43	0	0
Total	**28136.6**	**16.69**	**15976.6**	**16.88**

VI.4.2 Wing Related Components Centre of Gravity

Except the structure and systems fixed on the fuselage, the location of the other structure and systems relate to the location of wing, including wing, engines, nacelle, fuel and fuel system, flight control system, hydraulic system, anti-icing system, electrical power system, accessory drive and landing gear. Different from the centre of gravity of the structure and systems related fuselage, whose origin is the front point of the fuselage, the origin of the wing relate structure and systems' centre of gravity is the front point of the wing crossing fuselage. When the wing location is added to it, the real centre of gravity location is got. According to the Cranfield Notes, the CG of each part based on the temple origin are calculated and shown in Table VI-6.

Table VI-6 Wing Related Components CG

Part	Maximum Take-off		Empty	
	Mass (kg)	CG (m)	Mass (kg)	CG (m)
Wing	5299.7	4.28	5299.7	4.28
Engines	4200	1.85	4200	1.85
Nacelle	2714	3.05	2714	3.05
Fuel and fuel system	14070.1	4.26	327.4	4.26
Flight control system	720.3	5.91	720.3	5.91
Hydraulic system	776.6	3.48	776.6	3.48
Anti-icing system	349.3	2.24	349.3	2.24
Electrical power system	441.6	3.61	441.6	3.61
Accessory drive	176.7	1.75	176.7	1.75
Nose landing gear	223.82	-8.335	223.82	-8.335
Main landing gear	2014.4	5.203	2014.4	5.203
Total	**30986.5**	**3.86**	**17235.5**	**3.54**

Since the location of wing is 12.55m, the CG location of the structure and systems related to wing is 16.41m and 16.09m for the take-off and empty respectively.

VI.4.3 Overall Centre of Gravity

The CG and mass of structure and systems related to both fuselage and wing are available now. The CG of the whole aircraft can be therefore calculated by the following formula:

$$L_{t-o} = \frac{W_{fuselagerelate\_t-o} \times L_{fuselagerelate\_t-o} + W_{wingrelate\_t-o} \times L_{wingrelate\_t-o}}{W_{fuselagerelate\_t-o} + W_{wingrelate\_t-o}} = 16.54m$$

$$L_{emp} = \frac{W_{fuselagerelate\_emp} \times L_{fuselagerelate\_emp} + W_{wingrelate\_emp} \times L_{wingrelate\_emp}}{W_{fuselagerelate\_emp} + W_{wingrelate\_emp}} = 16.47m$$

The MAC (mean aerodynamic chord) of wing is 3.523m, the front point of MAC from the front of aircraft is 15.82m. Thus the CG range for the take-off and empty is:

$$CG_{t-o} = \frac{L_{t-o} - L_{MAClocation}}{L_{MAC}} = 20\%$$

$$CG_{emp} = \frac{L_{emp} - L_{MAClocation}}{L_{MAC}} = 18\%$$

Considering only half of the passengers taking the aircraft and all of them sit in the front of the aircraft, using the same method, the most forward CG location and CG range is calculated:

$$L_{front} = 15.97m$$

$$CG_{front} = 4\%$$

Considering only half of the passengers taking the aircraft and all of them sit in the rear of the aircraft, using the same method, the most rearward CG location and CG range is calculated:

$$L_{rear} = 17.13m$$

$$CG_{rear} = 37\%$$

To sum up, the CG location is 15.97m~17.13m, while the CG range is 4%~37%.

VII Centre of Gravity Calculation, Fuel Tank Layout and System Requirements

VII.1Task

In the former stage, the single aisle conventional configuration and the twin aisles configuration were further developed and assessed. As a result, the two configurations were combined and the final configuration was got.

The task in the last stage is: further develop the concept of the final configuration, give more detailed parameters and freeze the concept at the end of this phase, the specifications of the aircraft should be finished.

As a team member of the configuration and mass sub-team, the author was with responsibility of the CG range recalculation and checking. Meanwhile, as the coordinator of the structure, powerplant and systems sub-team, the author was in charge of the fuel tank layout and system requirements analysis.

VII.2Centre of Gravity Calculation

Since the final configuration of the aircraft is the combination of the single aisle conventional configuration and the twin aisles configuration, the total mass of the aircraft is changed to 64,982kg, and the mass of each component and system are calculated again, as shown in Table VII-1.

Based on the new 3-view drawing and Cranfield methods, the CG of each component and system in take-off and empty condition are calculated again, as presented in Table VII-2 and VII-3.

Table VII-1 Components and Systems Mass

Part	Mass (kg)
Wing	5904.6
Fuselage	8484.7
Tail	1382.8
Undercarriage	2500
Powerplant relate	960
Powerplant	6480
Fuel System	987
FCS	779.2
Hydraulic System	815.7
Electrical system	1257.9
APU	200
ECS	975.8
Instrument	374.5
Radio	352.4
Fire Precaution	194.9
External paint	53.5
Furnishing	5246.1

Table VII-2 Fuselage Related Components CG (Final Configuration)

Part	Maximum Take-off		Empty	
	Mass (kg)	CG (m)	Mass (kg)	CG (m)
Horizontal tail	827.7	32.04	827.7	32.04
Vertical tail	555	31.27	555	31.27
Fuselage	8484.7	15.35	8484.7	15.35
Instruments	374.5	11.49	374.5	11.49
Electrical	786.1	15.92	786.1	15.92
Electronics	352.4	6	352.4	6
Furnishing	5246.1	16.5	5246.1	16.5
ECS	601.6	11.69	601.6	11.69
APU	200	32.91	200	32.91
Fire	194.9	17	194.9	17
External	53.5	17	53.5	17
Crew	570	11.37	570	11.37
Payload	12160	17	0	0
Total	30656.6	16.70	18496.6	16.50

Table VII-3 Wing Related Components CG (Final Configuration)

Part	Maximum Take-off		Empty	
	Mass (kg)	CG (m)	Mass (kg)	CG (m)
Wing	5904.6	5.79	5904.6	5.79
Engines	6480	1.51	6480	1.51
Nacelle	960	2.71	960	2.71
Fuel and fuel system	15964.7	5.11	987	5.11
Flight control system	779.2	11.65	779.2	11.65
Hydraulic system	815.7	5	815.7	5
Anti-icing system	374.2	2.09	374.2	2.09
Electrical power system	471.7	3.61	471.7	3.61
Nose landing gear	250	-6.96	250	-6.96
Main landing gear	2250	5.64	2250	5.64
Total	34000.0	4.60	18959.1	4.20

The location of wing is 11.96m; therefore, the CG location of the structure and systems related to wing is 16.56m and 16.16m for the take-off and empty respectively.

The CG of whole aircraft in take-off and empty is:

$$L_{t-o} = \frac{W_{fuselagerelate\_t-o} \times L_{fuselagerelate\_t-o} + W_{wingrelate\_t-o} \times L_{wingrelate\_t-o}}{W_{fuselagerelate\_t-o} + W_{wingrelate\_t-o}} = 16.63m$$

$$L_{emp} = \frac{W_{fuselagerelate\_emp} \times L_{fuselagerelate\_emp} + W_{wingrelate\_emp} \times L_{wingrelate\_emp}}{W_{fuselagerelate\_emp} + W_{wingrelate\_emp}} = 16.33m$$

The MAC of wing is 3.865m; the distance from the front point of MAC to the front of aircraft is 15.555m. Thus the CG range for the take-off and empty is:

$$CG_{t-o} = \frac{L_{t-o} - L_{MAClocation}}{L_{MAC}} = 28\%$$

$$CG_{emp} = \frac{L_{emp} - L_{MAClocation}}{L_{MAC}} = 20\%$$

For the most forward CG location, considering only half of the passengers taking the aircraft and all of them sit in the front of the aircraft, the payload is 6,080kg and the CG of payload is 11.5m. Using the same method, the most forward CG location and CG range is calculated:

$$L_{front} = 16.02m$$

$$CG_{front} = 12\%$$

For the most rearward CG location, considering only half of the passengers taking the aircraft and all of them sit in the rear of the aircraft, the payload is 6,080kg and the CG of payload is 20.5m. Using the same method, the most rearward CG location and CG range is calculated:

$$L_{rear} = 16.90m$$

$$CG_{rear} = 35\%$$

Generally, the CG location of the aircraft is 16.02m~16.90m, while the CG range is 12%~35%.

VII.3Fuel Tank Layout

During this stage, the major structures of the aircraft are designed. Therefore, the conditions for fuel tank layout are available. As the baseline of the aircraft, fuel is considered to be stored in the wing tank firstly; if the wing tank can not take so much, the central tank should be then considered.

VII.3.1 Initial Wing Tank Layout

According to the design of wing structure, the front spar of wing is at 15% of chord, the rear spar is at 65%, the rib pitch is 900mm.

Considering from shortening the time of refuelling, the wing tank of civil aircraft is always divided into two parts, the inboard wing tank and the outboard wing tank, and the capacity of each tank should be close to ensure the refuelling time close. In the first step,

the MAC of wing is selected as the boundary of inboard wing tank and outboard wing tank. The distance between outboard wing tank boundary to the wing tip is chosen as 1500mm. The two wing tanks layout is illustrated in Figure Ⅶ-1.

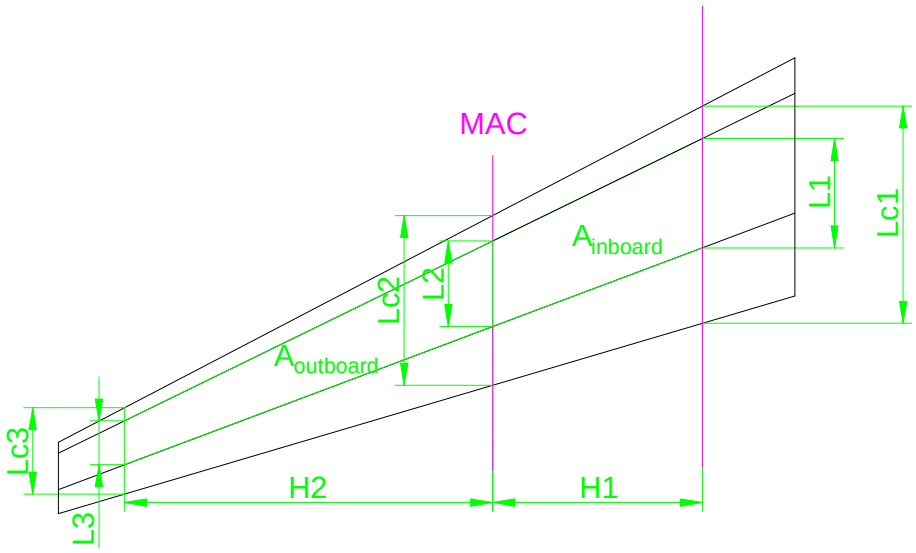

Figure VII-1 Initial Wing Tank Layout

The area of each tank can be calculated as;

$$A_{inboard} = \frac{(L1+L2)}{2} \times H1 = 10.57m^2$$

$$A_{outboard} = \frac{(L2+L3)}{2} \times H2 = 12.34m^2$$

In terms of the thickness of each tank, from the aerodynamic sub-team, it is known that the thickness/chord ratio is 0.15 and 0.1 at root and tip respectively. Since the central wing box is a cube, the thickness/chord ratio at inside boundary of inboard wing tank is 0.15. The thickness/chord ratio at outside boundary of inboard wing tank can be calculated as 0.135. The thickness/chord ratio at outside boundary of outboard wing tank can be calculated as 0.105. Considering the thickness/chord ratio takes the maximum of each boundary, a 0.8 coefficient should be taken when calculating the average of the thickness. Then the average thickness of each boundary can be calculated:

$$T_{L1} = L_{c1} \times TC_{L1} \times 0.8 = 0.76m$$

$$T_{L2} = L_{c2} \times TC_{L2} \times 0.8 = 0.42m$$

$$T_{L3} = L_{c3} \times TC_{L3} \times 0.8 = 0.17m$$

Considering the structures inside the tank, a coefficient of 0.85 according to Roskam's Airplane Design is taken when calculating the pure volume of each fuel tank:

$$V_{inboard} = A_{inboard} \times \frac{(T_{L1} + T_{L2})}{2} \times 0.85 = 5.30m^3$$

$$V_{outboard} = A_{outboard} \times \frac{(T_{L2} + T_{L3})}{2} \times 0.85 = 3.06m^3$$

Since the Flying Crane is in conceptual design phase, the fuel density is taken as the minimum which is $750\,kg/m^3$. Thus the fuel capacity of each tank is:

$$W_{inboard} = V_{inboard} \times \rho = 3978kg$$

$$W_{outboard} = V_{outboard} \times \rho = 2293kg$$

Then the fuel can be contained by the wing tanks is:

$$W_{wingfuel} = 2 \times W_{inboard} + 2 \times W_{outboard} = 12542kg$$

The total fuel for the aircraft is given by the configuration and mass sub-team, 14,980kg, which is 2,438kg more than the fuel can be taken by the wing tanks. It means that the central tank should be considered. In addition, the fuel capacity difference between the inboard wing tank and the outboard wing tank is 1,685kg, which is too large, therefore, the boundary between the inboard wing tank and the outboard wing tank should be moved inside.

VII.3.2 Final Fuel Tank Layout

The new configuration of the fuel tanks, as can be seen in Figure VII-2, includes 5 separate tanks: one central tank, two inboard wing tanks and two outboard wing tanks. The boundary between the inboard wing tank and the outboard wing tank is the No.5 rib of each wing, the distance between outboard wing tank boundary to the wing tip is taken as 3 rib pitches (2,700mm).

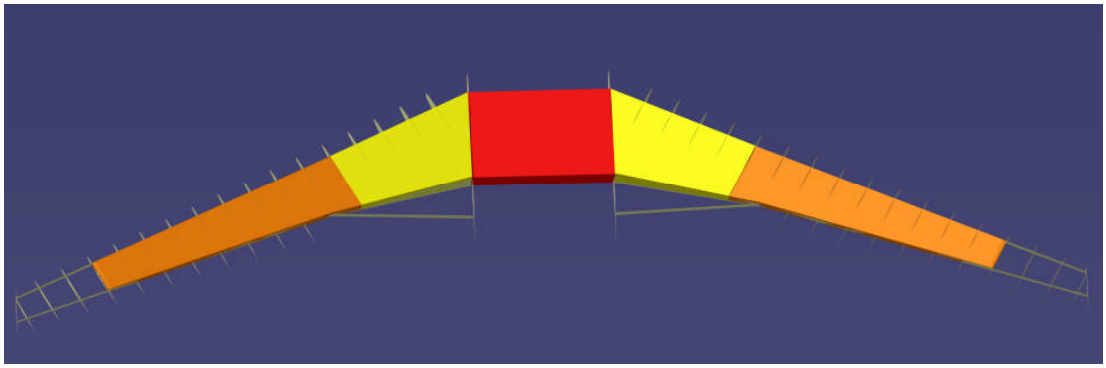

Figure VII-2 Final Fuel Tank Layout

Using the same method introduced before, the capacity of each wing tank can be calculated:

$$W_{inboard} = 3360kg$$

$$W_{outboard} = 2880kg$$

The fuel capacity difference between the inboard wing tank and the outboard wing tank is 580kg, which is reasonable. The fuel can be contained by the wing tanks is 12,480kg, for the total fuel 14,980kg, there are still 2,500kg need to be contained by the central tank.

For the central wing tank, the area is:

$$A_{central} = L_0 \times H_0 = 10.45m^2$$

The thickness is:

$$T_0 = T_{L1} = 0.76m$$

Then the volume is:

$$V_{central} = A_{central} \times T_0 \times 0.85 = 6.77m^3$$

The fuel capacity of central tank is:

$$W_{central} = V_{centrral} \times \rho = 5080kg$$

Since the capacity of central tank is 5,080kg, which is larger than the requirement, 2,500kg, and the fuel capacity difference between the inboard wing tank and the outboard wing tank is reasonable, the final configuration of the fuel tanks is feasible.

The result of fuel tank configuration is shown in Table Ⅶ-4.

Table VII-4 Fuel Tank Layout

	Design Point (kg)	Maximum (kg)
Central Tank	2500	5080
Inboard Wing Tank	2×3360	2×3360
Outboard Wing Tank	2×2880	2×2880
Total Fuel	14980	17560

VII.4System Requirements

VII.4.1 System Technologies Analysis

During the conceptual design phase, the system details are not necessary to be studied. However, the technologies intended to be used on the airframe systems should be analysed, because system technologies have influences on the configuration of the aircraft and the mass of each system.

For the flight control system, advanced technology, for example, the fly-by-wire FCS, can make the aircraft easier to be operated. It can adjust the balance of control surfaces according to different conditions and increases the control stability. In addition, using FBW system, the fuel consumption could be reduced. Regarding the more advanced technology, fly-by-light technology or PBW technology, it is not suitable considering from the risk control. As a result, digital fly-by-wire technology is selected to be used for the flight control system on the Flying Crane.

For the environment control system (including de-icing system), the traditional ECS uses intake air of engines to cool the electrics, to pressurize the cabin and to eliminate the ice

of leading edge and entrance of engines. This kind of system is low efficient and reduces the efficiency of engine significantly. According to Fabienne Couaillac's *Environment Control Systems for the All-Electric Aircraft*, using all electric ECS, the fuel consumption can be reduced by 3%. Moreover, it can produce huge benefit to the aircraft. Therefore, the all electric ECS is selected to be applied on the Flying Crane.

During the life circle of an aircraft, the cost of maintenance takes a large percentage of the cost of the whole aircraft. To reduce the maintenance cost, the prognostic and health management system is a good choice. By online test and diagnose, this system can detect the failure of the aircraft and realise condition-based maintenance. Then the maintenance time and logistic scale is reduced, and the usability of the aircraft is increased. In addition, this system can realise the online failure isolation and increase the safety of the aircraft.

Besides digital fly-by-wire flight control system, all electric environment control system and prognostic and health management system which can produce huge influences on the whole aircraft, the other technologies on sub-systems, such as distributed load management on electrical power system, high pressure on hydraulic system, can also benefit for the aircraft. These technologies will be analysed and confirmed in the preliminary design phase.

VII.4.2 System Mass Sizing

Based on the mass estimation and breakdown of whole aircraft, the gross mass of each system is given, as presented in Table VII-5.

Compared with the similar current aircraft, such as the Airbus A319 and the Boeing 737-700, the mass of each system can be checked and adjusted. For example, according to *Electrically Power Control Surface Actuation* by Nicolas Bataille, the mass of hydraulic system on the A319 is estimated about 882kg, while the A319 is the shorten version of

the A320 and the control surfaces of the A319 are larger than that of the Flying Crane, 815kg for the hydraulic system of the Flying Crane is reasonable.

Table VII-5 Systems Gross Mass

System	Gross Mass (kg)
Fuel	990
Electrical Power	1250
Environment Control	970
Hydraulic	815
Flight Control	780
Avionics	725
APU	200
Total	5730

However, the mass breakdown of the whole aircraft depends on empirical formula, and does not consider the changes brought by the advanced technologies. In adition, the optimization compared with the A319 and the Boeing 737-700 is also lack of considering the advanced technologies' influence. The mass should be updated according to the technologies intended to be used on the systems.

According to 7.4.1 System Technologies Analysis, there are three main technologies intended to be applied on the Flying Crane. The digital fly-by-wire has been considered in the mass of flight control system. The all electric environment control system will make the mass of ECS increase about 30% [Personal conversion with Cheng Jie, environment control system engineer of AVIC I GDP, Cranfield, 6th August 2008]. Thus the mass of ECS should be:

$$W_{ECS} = W_{ECS0} \times (1 + 0.3) = 1260kg$$

By using PHM, some sensors should be added, the system mass will be increased. However, with the integration of mechanic and electrical systems, the computers and wire are reduced, and the mass will be reduced at the same time. As a result, the influence of PHM and mechanic and electric integration are both neglected. In terms of the

hydraulic system, high pressure of 5,000psi is intended to be used. Compared with the traditional hydraulic system whose pressure is only 3,000psi, 20% mass of hydraulic system can be saved, the mass of hydraulic system is :

$$W_{HyS} = W_{HyS0} \times (1 - 0.2) = 650kg$$

The influences of the other systems' technologies are not considered during this phase. The final result of the systems mass sizing is shown in Table Ⅶ-6.

Table VII-6 Systems Mass

System	Gross Mass (kg)
Fuel	990
Electrical Power	1250
Environment Control	1260
Hydraulic	650
Flight Control	780
Avionics	725
APU	200
Total	5855

Ⅶ.4.3 System Centre of Gravity Location Arrangement

After sizing the mass of each system, the work needed to be done for systems during the conceptual design phase is arranging the location of each system. Only the rough positions of the systems are required to be arranged based on the CG range of whole aircraft. Meanwhile, the arrangement of the positions of systems should consider the systems' working area and the origin.

For the ECS, the power comes from the engines, the working area exists all over the cabin, the middle of the aircraft is the best point to simple the system and save mass. Regarding the hydraulic system, the actuation components are located in the wing, tail unit and landing gear, while the pumps are near the engines. As a result, the hydraulic

system is divided into two parts, one part near the engines, which presents the power sources and actuators in the wing and undercarriage, the other part near the control surface of tail unit and presents the actuators in there. In terms of the electrical power systems, it is in the front of fuselage and near the engines, while the avionics is between the nose landing gear and front cargo. The fuel system is near the centre of wing. The flight control system is near the rear edge of wing and the APU in the rear of the fuselage. All the locations of systems are shown in Figure Ⅶ-3.

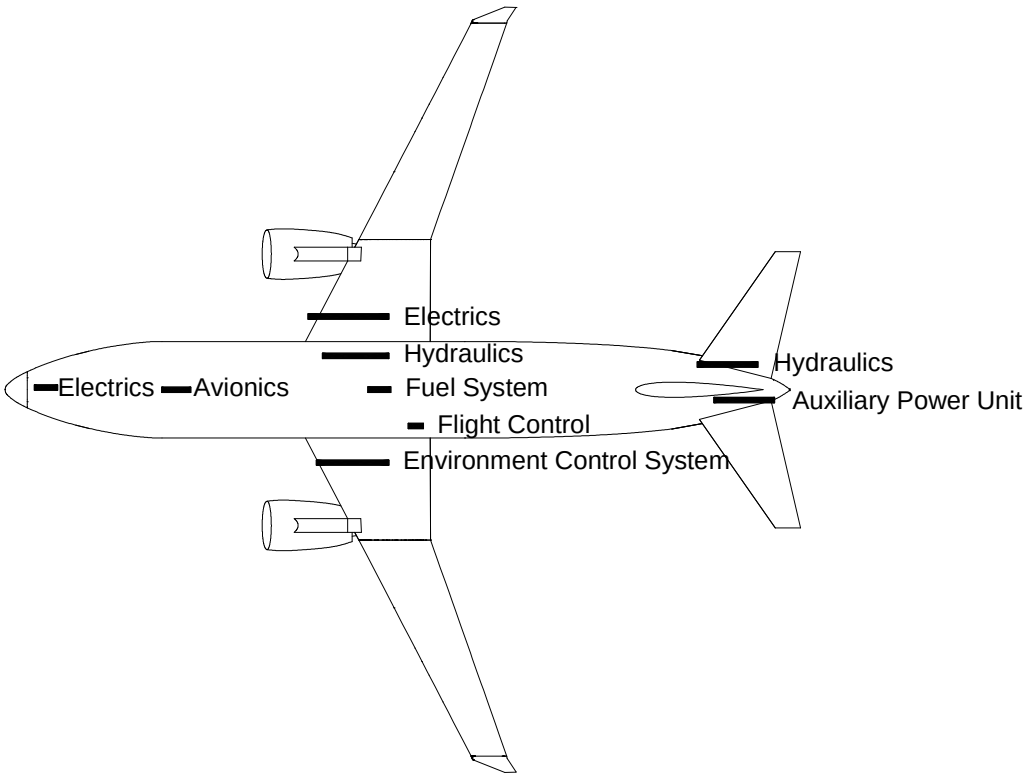

Figure VII-3 Systems CG Location

VIII Conclusion

Supported by the staffs and cooperating with the whole AVIC I group students, the conceptual design of a 130-Seat Civil Airliner Flying Crane is completed. After several times' assessments and updates, the final configuration is developed and frozen.

During the six months' work in group design project, the author experienced every stage of the conceptual design of the Flying Crane. From market survey to analysis of requirements, from four different configurations primary conceptual design to assessments, from two configurations further development to the combination to the final configuration. Although the author was in charge of different works in different stages, the whole process was experienced.

The author made the manufacturer survey and analysed the performance requirements during the derivation requirements phase; designed the cabin layout, assessed the performance of different configurations, estimated the mass and calculated the centre of gravity during the conceptual design and evaluation phase. He calculated the centre of gravity, designed the fuel tank and analysed the systems requirements in the consolation and review phase.

For the future work, the Flying Crane could go to the preliminary deign phase.

REFERENCES

A.1. Aerospaceweb Website, available at: http://www.aerospaceweb.org/

A.2. Airbus. Official Website, available at: http://www.airbus.com

A.3. AVD 0608-*The Aircraft Design Process*, Cranfield College of Aeronautics, Cranfield, UK.

A.4. AVD 0609-*Conceptual Design – Civil Aircraft Fuselage Layout*, Cranfield College of Aeronautics, Cranfield.

A.5. Bataille, N. (2006). *Electrically Power Control Surface Actuation*. Cranfield University, Cranfield, UK.

A.6. Boeing. Official Website, available at: http://www.boeing.com

A.7. CivilAviation Website, available at: http://www.civilaviation.eu

A.8. Couaillac, F. (2007). *Environment Control Systems for the All-Electric Aircraft*. Cranfield University, Cranfield, UK.

A.9. DAeT 9218-*Aircraft Mass Prediction- Powerplants, Systems and Equipments*, Cranfield College of Aeronautics, Cranfield, UK.

A.10. DAeT 9317-*Aircraft Mass Prediction- Structural Components*, Cranfield College of Aeronautics, Cranfield, UK.

A.11. European Aviation Safety Agency (2005/06), *Certification Specifications For Large Aeroplanes*, CS-25, European Aviation Safety Agency (EASA)

A.12. Federal Aviation Administration, *Federal Aviation Regulation*, FAR, Federal Aviation Administration (FAA), Washington.

A.13. Li Shitu. (2008). *Conceptual Design of a 130-Seat Civil Airliner Flying Crane- Mass, Aerodynamics and Performance Analysis*. Cranfield University, Cranfield, UK.

A.14. Liu Huping. (2008). *Conceptual Design of a 130-Seat Civil Airliner Flying Crane- Individual Final Report of GDP*. Cranfield University, Cranfield, UK.

A.15. JANE'S ALL THE WORLD'S AIRCRAFT, available at: http://java.janes.com/public/jawa/index.shtml

A.16. Raymer, Daniel. P. (1992). *Aircraft Design: A Conceptual Approach*. American Institute of Aeronautic and Astronautics, Washington, U.S

A.17. Roskam, J. (1985). *Airplane Design*. Roskam Aviation and Engineering Cooperation, Ottawa, Kansas.

A.18. Torenbeek, E. (1982). *Synthesis of Subsonic Airplane Design*. Delft University Press. Delft, Holland.

A.19. Wang Bin. (2008). *Conceptual Design of a 130-Seat Civil Airliner Flying Crane- Market Analysis*. Cranfield University, Cranfield, UK.

A.20. Wang Yinhu. (2008). *Conceptual Design of a 130-Seat Civil Airliner Flying Crane- Aerodynamics, Configuration, Stability and Control*. Cranfield University, Cranfield, UK.

A.21. Wikipedia Website, available at: http://en.wikipedia.org/

A.22. Zhang Zhigang. (2008). *Conceptual Design of a 130-Seat Civil Airliner Flying Crane- Geometrical Investigation, Evaluation Criteria, Weight and Performance Estimation*. Cranfield University, Cranfield, UK.

Appendix B - Actuator Performance Requirements Estimation

B.1 Stall Load and Stroke Estimation

Using the method described in Section 4.2.1 and the available parameters of the Airbus A320 and the Flying Crane listed in Table 3-1, 3-2 and 3-3, the stall load and stroke of elevators and rudder of the Flying Crane are estimated.

For elevators, according to the parameters presented in Table 3-2 and 3-3, the elevator area ratio (2D) of the Flying Crane to the Airbus A320 is:

$$R_{2D-elevator} = \frac{A_{elevator-FC}}{A_{elevator-A320}} = \frac{13.2}{15.5} = 0.85$$

Therefore the elevator linear geometric ratio (1D) of the Flying Crane to the Airbus A320 is:

$$R_{1D-elevator} = \sqrt{R_{2D-elevator}} = \sqrt{0.85} = 0.92$$

Thus the stall load of the Flying Crane elevators can be calculated:

$$F_{a-elevator-FC} = \frac{F_{s-elevator-FC} \times L_{s-elevator-FC}}{L_{a-elevator-FC}} = \frac{F_{s-elevator-A320} \times R_{2D} \times L_{s-elevator-A320} \times R_{1D}}{L_{a-elevator-A320} \times R_{1D}}$$
$$= \frac{F_{a-elevator-A320} \times L_{a-elevator-A320} \times R_{2D} \times R_{1D}}{L_{a-elevator-A320} \times R_{1D}} = F_{a-elevator-A320} \times R_{2D} = 27.7 \times 0.85$$
$$= 23.5kN$$

Since the maximum deflection angle of control surface refers to the maximum stroke of actuator, the arm of actuator force can be calculated based on the deflection angle of control surface and stroke of actuator. For the arm of elevator actuator force of the A320:

$$L_{a-elevator} = \frac{\frac{1}{2} S_{t-elevator}}{\sin(\frac{D_{u-elevator} + D_{d-elevator}}{2})} = 75.3mm$$

Where $S_{t-elevator}$ is the stroke of elevator actuator, $D_{u-elevator}$ and $D_{d-elevator}$ are the up deflection angle and down deflection angle of elevator respectively.

Therefore the arm of elevator actuator load of the Flying Crane is:

$$L_{a-elevator-FC} = L_{a-elevator-A320} \times R_{1D-elevator} = 69.4mm$$

The stroke of the Flying Crane elevator actuator is:

$$S_{t-elevator-Fc} = 2 \times L_{a-elevator-FC} \times \sin(\frac{D_{u-elevator-FC} + D_{d-elevator-Fc}}{2}) = 2 \times 69.4 \times \sin(\frac{25+25}{2}) = 58.6mm$$

Similar to elevator, the load and stroke of rudder are estimated, the results are illustrated in Table B-1.

B.2 No Load Rate and Power Estimation

As described in Section 4.2.2, the minimum actuation time of elevators and rudder of the Flying Crane is 1s, thus the maximum rate (no load rate) of elevators and can be calculated:

$$V_{NLR-elevator} = \frac{S_{t-elevator}}{1} = 58.6mm/s$$

$$V_{NLR-rudder} = \frac{S_{t-rudder}}{1} = 92.4mm/s$$

According to the typical actuator performance curves shown in the researches of J. Charriar [4], Montero Yanez [19] and J. Pointon [9], the peak power of each actuator can be estimated using the following expression:

$$P_p = 0.57 \times V_{NLR} \times F_{st}$$

The peak power of the elevators and rudder of A320 and Flying Crane are then estimated, as illustrated in Table B-1.

Table B-1 Airbus A320 and Flying Crane Elevators and Rudder

		A320	Flying Crane	Unit	Ratio		
					1D	2D	Reference
General							
	T-O Weight	73500	64582	kg			0.88
	Overall Length	37.57	34.04	m			0.91
Elevator							
	Area	15.5	13.2	m^2	0.92	0.85	0.85
	Deflection(up)	30	25	°			0.83
	Deflection(down)	17	25	°			1.47
	Actuator Stroke	60	58.6	mm			0.98
	No Load rate	60	58.6	mm/s			0.98
	Stall Load	27.7	23.5	kN			0.85
	Arm	75.3	69.4	mm			0.92
	Moment	2085.0	1632.3	N·m			0.78
	Peak Power	943.4	782.8	W			0.83
Rudder							
	Area	21.5	23.2	m^2	1.04	1.08	1.08
	Deflection(up)	25	20	°			0.8
	Deflection(down)	25	20	°			0.8
	Actuator Stroke	110	92.4	mm			0.84
	No Load rate	110	92.4	mm/s			0.84
	Stall Load	44.3	47.7	kN			1.08
	Arm	130.2	135.2	mm			1.04
	Moment	5768.0	6452.9	N·m			1.12
	Peak Power	2766.1	2504.4	W			0.90

B.3 Discussion

It is a little surprising to find that the stall load of the Flying Crane rudder is larger than that of the A320; the reason is that the Flying Crane has a larger fin than the A320, while the maximum deflection of rudder on the former aircraft is smaller.

It should be noticed that the peak power estimation in this study uses the ratio 0.57 which is smaller than the ratio used in J. Pointon's research [9], which is 0.7. However, both ratios are analysed from the typical actuator performance curve shown in the research of J. Charriar [4], J. Pointon used the simplified actuator performance curve while this study uses the more accurate one. In addition, J. Pointon also mentioned that there might be overestimate in his case study.

Furthermore, from Table B-1, it can be seen that, the peak power ratio between the Flying Crane and the Airbus A320 is 0.83 for elevators and 0.90 for rudder respectively; compared with the take-off weight ratio 0.88, the results are acceptable.

Appendix C – Electrohydrostatic Actuation System Reliability Estimation

C.1 Introduction

The level of failure rate is an important factor of the reliability of a system, fault dependency diagrams give a means of rapidly assessing the failure rate to be achieved from a given system function architecture [41]. A more thorough assessment of reliability can be achieved using Fault Tree Analysis (FAT) and Failure Modes and Effects Analysis (FMEA). However, it is felt that these methods are not necessary or appropriate for such a study. Fault dependency diagrams are therefore applied to estimate the system reliability.

C.2 Control Surface Function Architecture

To draw the fault dependency diagram, the function architecture should be analysed firstly. Because elevators are responsible for pitch control of aircraft, while rudder is for yaw control, the EHA system for the Flying Crane tail unit is divided into two individual parts, elevators and rudder. Both of them need to satisfy the safety requirements which means the failure rate should be no more than 10^{-9}/FH.

A typical single control surface function architecture of the F-35 which using the EHA developed by the Parker Aerospace for military application is shown in Figure C-1[28]. Since this kind of EHA architectures is for military application, they use one dual-redundant EHA for one control surface section, and three control channels from flight control computer to control electronics.

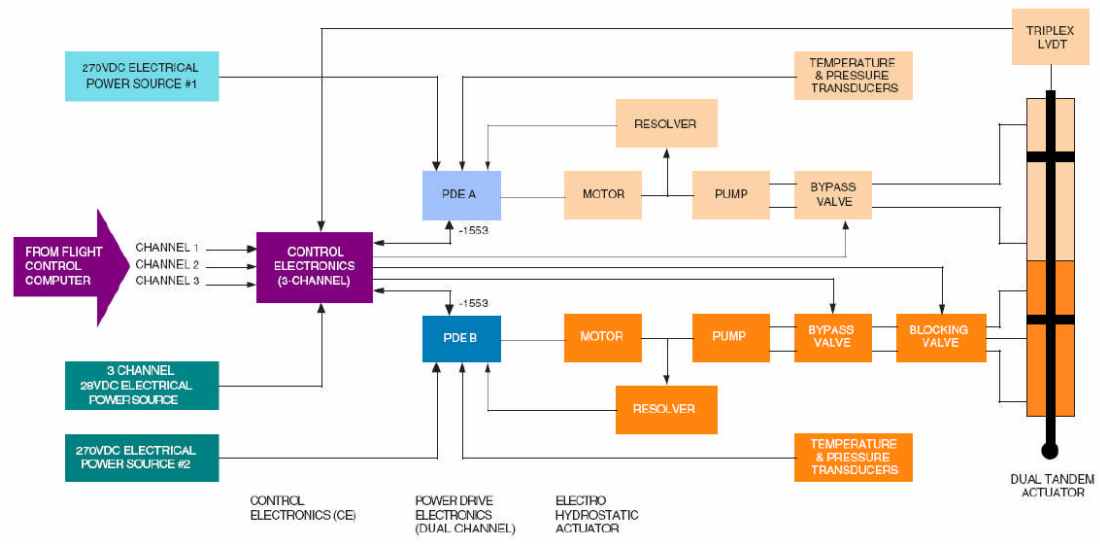

Figure C-1 Redundant EHA Architecture of F-35

In terms of the EHA system for the Flying Crane tail unit, as described in Chapter 5, it uses two individual simplex EHAs for each elevator and three for rudder. Regarding the flight control signal channels, the A320 has two Elevator/Aileron Computers (ELACs) and three Spoiler/Elevator Computers (SECs). It uses EALC 1 and 2, SEC 1 and 2 to control the two actuators of each elevator, while uses mechanic means to control the actuators of rudder. On the A340, there are three Flight Control Primary Computers (FCPCs) and two Flight Control Secondary Computers (FCSCs). It uses FCPCs for the pitch control and FCSCs as backup, while yaw control is still provided by mechanic means. For the MEA A380, it has the same flight control computer configuration with the A340, while both pitch and yaw control are provided by flight control computers (FCPCs and FCSCs) [11]. As one kind of MEA actuation system, the EHA system for both elevators and rudder of the Flying Crane are designed to be controlled by flight control computers. For the computer numbers, similar to the A320, two FCPCs and two FCSCs are used for elevators (pitch control), while three FCPCs for rudder (yaw control).

Associated with the EHA system architecture shown in Figure 5-2, the EHA system control surface function architecture can be drawn. A typical one, left elevator, is shown in Figure C-2.

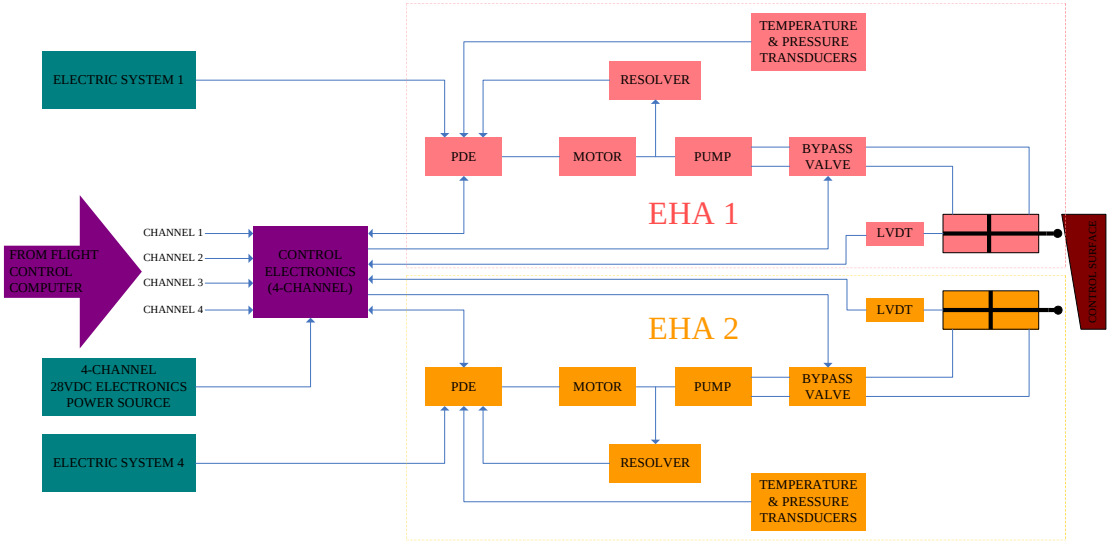

Figure C-2 EHA System Control Surface Function Architecture

Symmetry with the left elevator, the right elevator has the similar function architecture except power sources. Regarding rudder's function architecture, it is also similar to the elevators, while there are three individual simplex EHAs and controlled by three FCPCs.

C.3 Elevator Reliability Estimation

Based on the function architecture, the fault dependency diagram of each section is analysed. Figure C-3 is the fault dependency diagram for a single elevator section (left elevator).

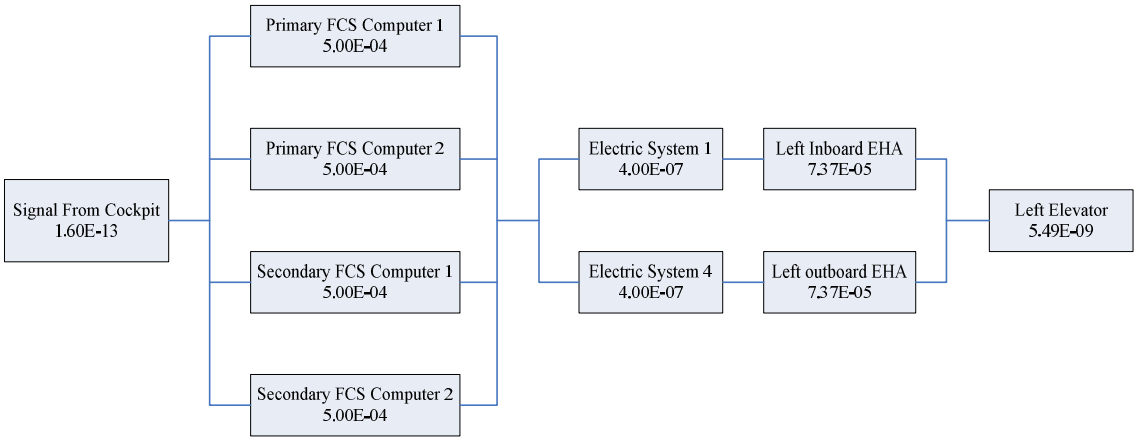

Figure C-3 Left Elevator Fault Dependency Diagram

In Figure C-3, the failure rate of control command signal is 1.60×10^{-13}/ FH [31], the failure rate of flight control computer is 5.00×10^{-4} / FH [42], the failure rate of electrical system is 4.00×10^{-7} / FH [41], and the failure rate of EHA is 7.37×10^{-5} / FH [19]. Then the failure rate of left elevator is calculated as 5.49×10^{-9} /FH ($P_{L-elevator}$).

The probability of a fault occurring on the whole elevator is therefore:

$$P_{r-elevator} = 1-(1-P_{L-elevator})\times(1-P_{R-elevator}) = 1-(1-P_{L-elevator})^2 = 1.10\times10^{-8}/\text{FH}$$

which can not satisfy the safety requirements ($\leq 10^{-9}$ / FH).

The reliability of the EHA system can be improved by adding EHA channels. However, adding channel means increase mass and cost. In addition, in Figure C-3, the failure rate of the EHA came from Yanez's research, which was nearly 20 years ago. As analyzed in Chapter 5, with the development of EHA technology and engineering application on the F-35 and the A380, the technology level of EHA has been improved a lot. It is expected that the failure rate of EHA in the near future can research the technology level to be no more than 2.2×10^{-5} / FH, which means that the reliability of EHA needs to be improved by nearly two and a half times than it in Yanez's research. Based on this hypothesis, the

failure rate of elevators is calculated again and the result is 1.00×10^{-9} / FH, which can just fulfill the requirement 10^{-9} /FH. Thus the probability of failure of the EHA system for the Flying Crane elevators is ‘extremely improbable’.

C.4 Rudder Reliability Estimation

Similar to the elevator, the fault dependency diagram of the rudder is also analysed, as shown in Figure C-4.

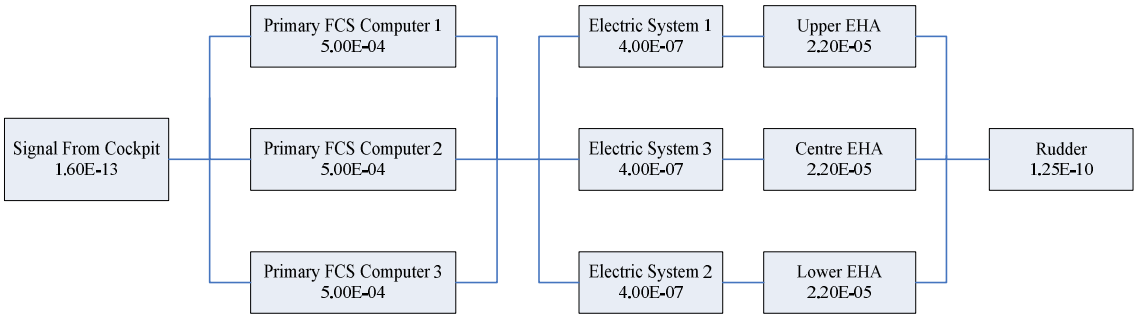

Figure C-4 Rudder Fault Dependency Diagram

According to Figure C-4, the failure rate of the EHA system for the Flying Crane rudder is 1.25×10^{-10} / FH, which is smaller than10^{-9} /FH. Therefore, the EHA system designed for the Flying Crane rudder can satisfy the safety requirement.

Appendix D – Variable Area Actuation System Reliability Estimation

D.1 Control Surface Function Architecture

As described in Appendix C, the level of failure rate can represent the reliability of a system, and fault dependency diagrams are suitable means to estimate the failure rate. In addition, similar to the EHA system, the variable area actuation system can also be divided into two parts according to different functions, elevators for pitch control while rudder for yaw control.

To use the fault dependency diagrams, function architecture needs to be analysed. Based on the variable area actuation system architecture illustrated in Figure 6-1, a typical control surface function architecture, left elevator, is analysed and shown in Figure D-1.

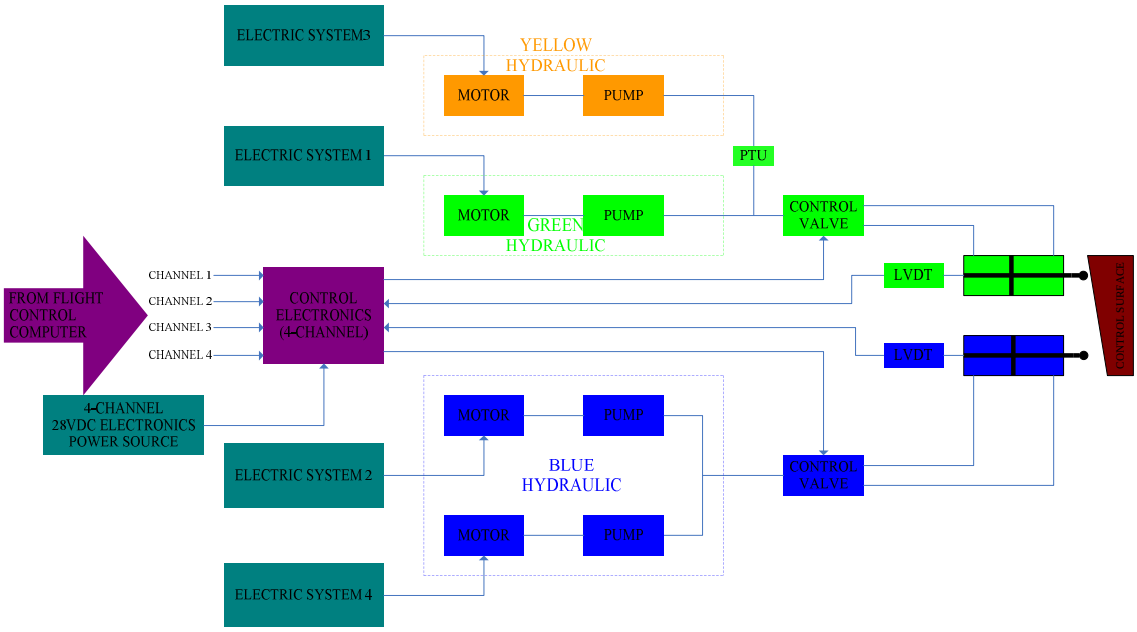

Figure D-1 Variable Area Actuation System Control Surface Function Architecture

In Figure D-1, the control channels for elevators (pitch control) are selected as four channels using two FCPCs and two FCSCs, which are same with the EHA system and similar to the Airbus aircraft.

Figure D-1 illustrates the function architecture of the left elevator. For the right elevator which is symmetry with the left elevator, it has the similar function architecture except the green hydraulic system and the yellow hydraulic system are replaced by each other. In terms of the rudder's function architecture, it is similar to elevators while there are three individual actuators powered by three hydraulic systems, and they are controlled by three FCPCs.

D.2 Elevator Reliability Estimation

According to the function architecture, the fault dependency diagram is analysed. Figure D-2 shows the fault dependency diagram for a single elevator section (left elevator).

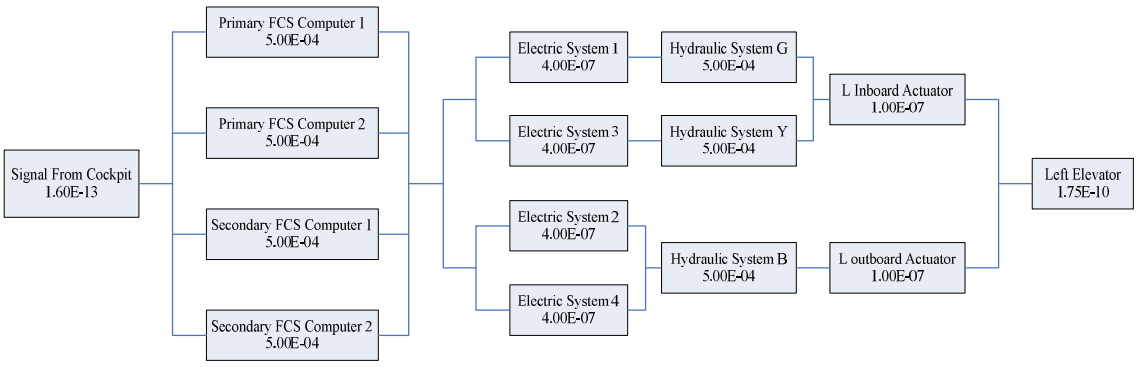

Figure D-2 Left Elevator Fault Dependency Diagram

In Figure D-2, the failure rate of control command signal is 1.60×10^{-13} / FH [31], the failure rate of flight control computer is 5.00×10^{-4} / FH [42], the failure rate of electrical system is 4.00×10^{-7} / FH [41], while the failure rate of hydraulic system and actuator are 5.00×10^{-5} / FH and 1.00×10^{-7} / FH respectively [41], then the failure rate of left elevator can be estimated as 1.75×10^{-10} /FH ($P_{L-elevator}$).

The probability of a fault occurring on the whole elevator is therefore:

$$P_{r-elevator} = 1-(1-P_{L-elevator})\times(1-P_{R-elevator}) = 1-(1-P_{L-elevator})^2 = 3.51\times10^{-10}\,/\mathrm{FH}$$

Which can satisfy the safety requirement ($\leq 10^{-9}$/FH) .

D.3 Rudder Reliability Estimation

Similar to the elevators, the fault dependency diagram of rudder is analysed and illustrated in Figure D-3.

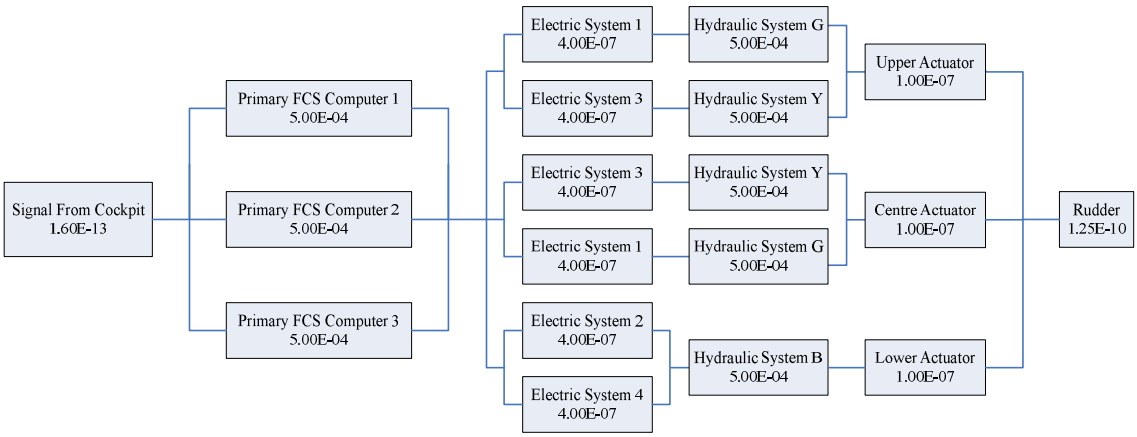

Figure D-3 Rudder Fault Dependency Diagram

According to Figure D-3, the failure rate of variable area actuation system for the Flying Crane yaw control (rudder) is 1.25×10^{-10} / FH, which is smaller than 10^{-9} /FH. Therefore, the probability of failure of the variable area actuation system for the Flying Crane rudder is 'extremely improbable'.

Appendix E – Conventional Fly-By-Wire Actuation System Sizing

E.1 Power Estimation

E.1.1 Design Power Estimation

As described in Chapter 2 and Chapter 6, a conventional FBW actuator needs to be sized based on the corner point of the performance requirement curve, which aims to satisfy the large load requirement in high speed flight condition and high actuation velocity requirement in low speed flight condition.

According to the performance requirement curves analysed in Chapter 4, the corner point of elevators and rudder can be calculated:

$$P_{c-elevator} = F_{\max-elevator} \times V_{\max-elevator} = 23.5 \times 58.6 = 1377.1W$$

$$P_{c-rudder} = F_{\max-rudder} \times V_{\max-rudder} = 47.7 \times 92.4 = 4407.5W$$

For the conventional FBW actuation system architecture, as illustrated in Figure 3-2, the A320 gives a typical example. According to Figure 3-2 and the description in Chapter 3, the power requirement of each centralised hydraulic system is estimated, as presented in Table E-1.

Similar to the EHA system and the variable area actuation system, a +10% error is taken into account as the sensitivity consideration. Thus the design point of each centralised hydraulic system is:

$$P_{dp-G} = 1.1 \times P_{p-G} = 1.1 \times 5784.6 = 6363.0W$$

$$P_{dp-B} = 1.1 \times P_{p-B} = 1.1 \times 4407.5 = 4848.2W$$

$$P_{dp-Y} = 1.1 \times P_{p-Y} = 1.1 \times 5784.6 = 6363.0W$$

Table E-1 Centralised Hydraulic System Power

Power source	Actuator			System Power (W)	
	Name	Mode	Power(W)	Required	Designed
Green system	L inboard elevator	Active	1377.1	5784.6	6363.0
	Upper rudder	Active	4407.5		
Blue system	R outboard elevator	Stand-by	0/1377.1	4407.5	4848.2
	Lower rudder	Active	4407.5		
	L outboard elevator	Stand-by	0/1377.1		
Yellow system	R inboard elevator	Active	1377.1	5784.6	6363.0
	Centre rudder	Active	4407.5		
Total	/	/	/	15976.6	17574.3

E.1.2 Average Power Estimation

Hydraulic pump in the conventional centralised hydraulic system is variable displacement piston pump, and its displacement is variable according to the load (power requirement). Therefore, the hydraulic systems can be regarded as working on demand systems. As described in Chapter 6, the duty cycle of '80/20 Rule' is suitable to estimate the average power of system:

$$P_{a-G} = 0.2 \times P_{dp-G} + 0.8 \times 0.2 \times P_{dp-G} = 2290.7W$$

$$P_{a-B} = 0.2 \times P_{dp-B} + 0.8 \times 0.2 \times P_{dp-B} = 1745.4W$$

$$P_{a-Y} = 0.2 \times P_{dp-Y} + 0.8 \times 0.2 \times P_{dp-Y} = 2290.7W$$

E.1.3 Power Consumption Estimation

The efficiency of hydraulic system mainly depends on the efficiency of hydraulic pump and power loss in pipes and components. As analysed in Chapter 6, the efficiency of hydraulic system is estimated as 70.5% based on the current technology. Then the maximum power consumption of each hydraulic system is:

$$P_{mcon-G} = P_{dp-G} / \eta_{VAA} = 6363.0 / 0.705 = 9020.8W$$

$$P_{mcon-B} = P_{dp-B} / \eta_{VAA} = 4848.2 / 0.705 = 6873.3W$$

$$P_{mcon-Y} = P_{dp-Y} / \eta_{VAA} = 6363.0 / 0.705 = 9020.8W$$

Since the hydraulic systems can be regarded as working on demand system, the average power consumption of each hydraulic system is calculated based on the average system power:

$$P_{acon-G} = P_{a-G} / \eta_{VAA} = 2290.7 / 0.705 = 3247.5W$$

$$P_{acon-B} = P_{a-B} / \eta_{VAA} = 1745.4 / 0.705 = 2474.4W$$

$$P_{acon-Y} = P_{a-Y} / \eta_{VAA} = 2290.7 / 0.705 = 3247.5W$$

Therefore, the total average power consumption of the conventional FBW actuation system is 8969.3W.

E.2 Mass Estimation

In terms of system mass, the specific power (power/mass ratio) of 5000 psi hydraulic system has been estimated as 206.7 W/kg in Chapter 6 Section 6.6. Then the mass of each system can be calculated as below:

$$M_G = \frac{P_{dp-G}}{R'_{PM}} = \frac{6363.0}{206.7} = 30.8kg$$

$$M_B = \frac{P_{dp-B}}{R'_{PM}} = \frac{4848.2}{206.7} = 23.4kg$$

$$M_Y = \frac{P_{dp-Y}}{R'_{PM}} = \frac{6363.0}{206.7} = 30.8kg$$

The total mass of the conventional FBW actuation system is 85.0kg.

E.3 Thermal Management

TMS using fuel as heat sinks is more efficient than those using cooling air. In addition, using the exist system, fuel TMS does not increase cost. Furthermore, centralised hydraulic systems are always located near the fuel tanks. As a result, fuel is used as the heat sink to absorb the heat power of the convention FBW actuation system, rather than the cooling air which is used for the EHA system and the variable area actuation system.

It should be noticed that, sometimes, at the end of mission, the temperature of fuel is quiet high due to not having enough fuel to absorb the heat power of hydraulic system; cooling air is required in this condition. However, this kind of situations only happens occasionally and can be avoided. Therefore, it is neglected in this case study.

Appendix F – System Fuel Penalties Calculation

F.1 Introduction

As discussed in Chapter 7, the cost of power, mass and drag of a system can be represented as fuel penalties. This Appendix addresses the fuel penalties calculation of the EHA system, the variable area actuation system and the conventional FBW actuation system designed in Chapter 5, 6 and Appendix E respectively.

According to AVD 0503 [35], the fuel penalties of systems in terms of power, mass and drag for a single flight phase can be calculated by the following equations:

$$(\Delta W_{FO})_{\Delta f_p} = \frac{r}{c}\Delta f_p (e^{ctg/r} - 1)$$

$$(\Delta W_{FO})_{\Delta W_A} = \Delta W_A (e^{ctg/r} - 1)$$

$$(\Delta W_{FO})_{\Delta D} = r\Delta D (e^{ctg/r} - 1)$$

Where ΔW_{FO} is the extra weight of fuel used to fly range, R, due to system;

Δf_p is the rate of fuel used due to system power off-take;

ΔW_A is the system weight;

ΔD is the system direct drag increase;

r is the Lift/Drag ratio;

c is the thrust specific fuel consumption (sfc);

t is the time taken to fly range, R;

g is the gravitational constant of acceleration, 9.81m/s²;

Since there are several phases of flight, such as take-off, climb, cruise, landing and so on, to calculate all the phases is a huge work. However, cruise is the longest phase of the flight, and most fuel is burned in this phase. Therefore, it is selected as the typical phase to be analysed.

F.2 Aircraft Parameters

The parameters of the Flying Crane are shown in Table F-1 [1].

Table F-1 Flying Crane Parameters

		Notation	Parameters	Unit
All up mass		AUM	64,582	kg
Design fuel mass		DFM	14,978	kg
Range		R	3,704	km
Wing area		A	118	m²
Cruise	**Height**	/	11,887	m
	Mach number	M	0.78	/
	Thrust per engine	/	200,000	N
	Thrust specific fuel consumption	c	1.5×10^{-5}	kg/sN

According to AVD 0504 [43], the 'Average' Aircraft Mass (AAM) of cruise phase is assumed as 60% DFM remaining, thus the AAM is:

$$AAM=AUM-0.4\times DFM=64582-0.4\times14978=58590.8kg$$

For the air data in cruise phase, the density of atmosphere at 11,887m is 0.3164kg/m^{-3}, while the speed of sound is 295.1m/s [44], then the aircraft speed is:

$$V=M\times a=0.78\times295.1=230.15m/s$$

The lift coefficient is:

$$C_L=\frac{\frac{W}{A}}{\frac{1}{2}\times\rho\times V^2}=\frac{\frac{58590.8\times9.81}{118}}{0.5\times0.3164\times230.15^2}=0.5812$$

According to the Flying Crane specification [1], the drag coefficient can be calculated:

$$C_D=0.01911+0.04441\times C_L{}^2=0.01911+0.04441\times0.5812=0.0341$$

Thus the lift/drag ratio is:

$$r = \frac{C_L}{C_D} = \frac{0.5812}{0.0341} = 17.0$$

And the time of cruise phase is:

$$t = \frac{R}{V} = \frac{3704 \times 10^3}{230.15} = 16093.4s$$

Therefore, the $(e^{ctg/r} - 1)$ is:

$$(e^{ctg/r} - 1) = e^{0.000015 \times 16102.1 \times 9.81/17.0} - 1 = 0.15$$

F.3 Electrohydrostatic Actuation System

The average power consumption of the EHA system is 4842.0W. As described in Chapter 5, the EHA system is powered by electrical systems. Assuming the efficiency of electrical system as 70% [43], the shaft power off-take of the EHA system is:

$$\Delta P_{EHA} = \frac{P_{acon-EHA}}{\eta_{EPS}} = \frac{4842.0}{0.7} = 6917.1W$$

Then the percentage increase in sfc due to power off-take is:

$$\Delta c = 0.175 \times \frac{\Delta P_{EHA}}{Thrust} = 0.175 \times \frac{6917.1}{2 \times 200000} = 0.03\%$$

The rate of fuel used due to system power off-take is:

$$\Delta f_p = sfc \times \Delta c \times thrust = 1.5 \times 10^{-5} \times \frac{0.03}{100} \times 200000 = 9.08 \times 10^{-5} kg/s$$

The fuel penalty due to the EHA system power off-take is:

$$(\Delta W_{FO})_{\Delta f_p} = \frac{r}{c} \Delta f_p (e^{ctg/r} - 1) = \frac{17.0}{1.5 \times 10^{-5}} \times 9.08 \times 10^{-5} \times 0.15 = 15.4N$$

The fuel penalty due to the EHA system mass is:

$$(\Delta W_{FO})_{\Delta W_A} = \Delta W_A (e^{ctg/r} - 1) = 62.9 \times 9.81 \times 0.15 = 92.0N$$

The cooling air flow requirement of the EHA system is 101.2g/s, thus the EHA system direct drag increase is:

$$\Delta D = coolingairflow \times V = 101.2 \times 10^{-3} \times 230.15 = 23.29N$$

Then the fuel penalty due to the EHA system direct drag increase is:

$$(\Delta W_{FO})_{\Delta D} = r\Delta D(e^{ctg/r} - 1) = 17.0 \times 23.29 \times 0.15 = 59.2N$$

Therefore, the total fuel penalty due to the EHA system is 166.6N.

F.4 Variable Area Actuation System

The variable area actuation system is powered by the localised hydraulic systems, while the hydraulic systems are powered by electrical systems. Similar to the EHA system, the shaft power off-take of the variable area actuation system can be calculated based on the 70% electrical system efficiency:

$$\Delta P_{VAA} = \frac{P_{acon-VAA}}{\eta_{EPS}} = \frac{6387.7}{0.7} = 9125.3W$$

Then percentage increase in sfc due to power off-take is:

$$\Delta c = 0.175 \times \frac{\Delta P_{VAA}}{Thrust} = 0.175 \times \frac{9125.3}{2 \times 200000} = 0.04\%$$

The rate of fuel used due to system power off-take is:

$$\Delta f_p = sfc \times \Delta c \times thrust = 1.5 \times 10^{-5} \times \frac{0.04}{100} \times 200000 = 1.20 \times 10^{-4} kg/s$$

The fuel penalty due to the variable area actuation system power off-take is:

$$(\Delta W_{FO})_{\Delta f_p} = \frac{r}{c}\Delta f_p(e^{ctg/r} - 1) = \frac{17.0}{1.5 \times 10^{-5}} \times 1.20 \times 10^{-4} \times 0.15 = 20.3N$$

The fuel penalty due to the variable area actuation system mass is:

$$(\Delta W_{FO})_{\Delta W_A} = \Delta W_A (e^{ctg/r} - 1) = 60.5 \times 9.81 \times 0.15 = 88.5N$$

The cooling air flow requirement of the variable area actuation system is 152.8g/s, thus the system direct drag increase is:

$$\Delta D = coolingairflow \times V = 152.8 \times 10^{-3} \times 230.15 = 35.17N$$

Then the fuel penalty due to the variable area actuation system direct drag increase is:

$$(\Delta W_{FO})_{\Delta D} = r\Delta D(e^{ctg/r} - 1) = 17.0 \times 35.17 \times 0.15 = 89.3N$$

Therefore, the total fuel penalty due to the variable area actuation system is 198.1N.

F.5 Conventional Fly-By-Wire Actuation System

The convention FBW actuation system is different from the other two systems. Firstly, it is powered by the centralised hydraulic systems which take shaft power directly from engines rather than via electrical systems, thus the power consumption of the conventional FBW actuation system is the shaft power off-take. Secondly, as described in Appendix E, there is no cooling air flow requirement in the conventional FBW actuation system because it is cooled by fuel. It means that the fuel penalty due to system direct drag increase is zero.

According to the conventional FBW actuation system parameters estimated in Appendix E, the percentage increase in sfc due to system power off-take is:

$$\Delta c = 0.175 \times \frac{\Delta P_{FBW}}{Thrust} = 0.175 \times \frac{8969.3}{2 \times 200000} = 0.039\%$$

The rate of fuel used due to system power off-take is:

$$\Delta f_p = sfc \times \Delta c \times thrust = 1.5 \times 10^{-5} \times \frac{0.039}{100} \times 200000 = 1.17 \times 10^{-4} kg/s$$

The fuel penalty due to the conventional FBW actuation system power off-take is:

$$(\Delta W_{FO})_{\Delta f_p} = \frac{r}{c}\Delta f_p (e^{ctg/r} - 1) = \frac{17.0}{1.5\times 10^{-5}} \times 1.17 \times 10^{-4} \times 0.15 = 19.9N$$

The fuel penalty due to the conventional FBW actuation system mass is:

$$(\Delta W_{FO})_{\Delta W_A} = \Delta W_A (e^{ctg/r} - 1) = 85.0 \times 9.81 \times 0.15 = 124.3N$$

Therefore, the total fuel penalty due to the conventional FBW actuation system is 144.3N.